

University of Denver

Digital Commons @ DU

---

Electronic Theses and Dissertations

Graduate Studies

---

1-1-2016

## Cost-Effective Prosthetic Hand Controlled by EMG

Mohammad Yahya Almuhanha  
*University of Denver*

Follow this and additional works at: <https://digitalcommons.du.edu/etd>



Part of the [Biomedical Engineering and Bioengineering Commons](#)

---

### Recommended Citation

Almuhanha, Mohammad Yahya, "Cost-Effective Prosthetic Hand Controlled by EMG" (2016). *Electronic Theses and Dissertations*. 1200.

<https://digitalcommons.du.edu/etd/1200>

This Thesis is brought to you for free and open access by the Graduate Studies at Digital Commons @ DU. It has been accepted for inclusion in Electronic Theses and Dissertations by an authorized administrator of Digital Commons @ DU. For more information, please contact [jennifer.cox@du.edu](mailto:jennifer.cox@du.edu), [dig-commons@du.edu](mailto:dig-commons@du.edu).

---

# Cost-Effective Prosthetic Hand Controlled by EMG

## Abstract

A cost-effective five-finger prosthetic hand is designed from aluminum, modeled and controlled using surface Electromyography (EMG) signals, which are obtained from the human body. Force sensors are used to control required forces needed to grasp and pick objects. A prototype hand is developed and it is experimentally tested to reproduce a wide spectrum of human hand motions. The size of the five-finger hand is similar to an adult male human hand, and it is capable of reproducing most of movements. Each finger has the same number of links as the real/human hand. Each finger also has a force sensor used to sense applied forces to the fingertip, subsequently dictating to the amputee to take specific actions. By using a vibration motor, the amputee knows if any 'object' is in touch with the prosthetic hand. Compared to other existing (and more expensive hands that include biotic sensors and smart motors), it is shown and it is experimentally validated that this cost-effective prosthetic five-finger hand is durable, strong, and capable of reproducing hand motions.

## Document Type

Thesis

## Degree Name

M.S.

## Department

Mechatronics Systems Engineering

## First Advisor

Kimon P. Valavanis, Ph.D.

## Second Advisor

Matthew Rutherford

## Third Advisor

Michael Keables

## Keywords

Electromyography, Vibration motor, Prosthetic hand

## Subject Categories

Biomedical Engineering and Bioengineering

## Publication Statement

Copyright is held by the author. User is responsible for all copyright compliance.

Cost-Effective Prosthetic Hand Controlled by EMG

---

A Thesis

Presented to

Faculty of the Daniel Felix Ritchie School of

Engineering and Computer Science

University of Denver

---

In Partial Fulfillment

Of the Requirements for the Degree

Master of Science

---

By

Mohammad Al-Muhanna

August 2016

Advisor: Dr. Kimon P. Valavanis

Author: Mohammad Al-Muhanna  
Title: Cost-Effective Prosthetic Hand Controlled by EMG  
Advisor: Dr. Kimon P. Valavanis  
Degree Date: August 2016

## **Abstract**

A cost-effective five-finger prosthetic hand is designed from aluminum, modelled and controlled using surface Electromyography (EMG) signals, which are obtained from the human body. Force sensors are used to control required forces needed to grasp and pick objects. A prototype hand is developed and it is experimentally tested to reproduce a wide spectrum of human hand motions.

The size of the five-finger hand is similar to an adult male human hand, and it is capable of reproducing most of movements. Each finger has the same number of links as the real/human hand. Each finger also has a force sensor used to sense applied forces to the fingertip, subsequently dictating to the amputee to take specific actions. By using a vibration motor, the amputee knows if any 'object' is in touch with the prosthetic hand.

Compared to other existing (and more expensive hands that include biotic sensors and smart motors), it is shown and it is experimentally validated that this cost-effective prosthetic five-finger hand is durable, strong, and capable of reproducing hand motions.

## **Acknowledgments**

I would like to express my sincere thanks to my advisor, Dr. Kimon P. Valavanis for his guidance, help and encouragement throughout my studies. I also wish to thank Dr. Brad Davidson for his valuable advice. Thanks go to my committee members for their feedback and support. I like to acknowledge Mr. J. Buckley for helping me build the prototype hand, and Mr. J. Edelstein for allowing me to use all required equipment and sensors for the experimental studies.

Last, but not least, my thanks go to my family for their support and warm love.

## Table of Contents

Abstract .....	ii
Acknowledgments.....	iii
Table of Contents .....	iv
Table of Figures .....	vii
Nomenclature .....	ix
Chapter 1 : Introduction .....	1
1.1 Motivation and Rationale .....	1
1.2 Thesis Objective.....	2
1.3 Thesis Outline .....	4
Chapter 2 : Related Work .....	6
2.1 Literature Review .....	6
2.2 Remarks.....	18
Chapter 3 : Problem Statement and Proposed Solution .....	19
3.1 Problem Statement .....	19
3.2 Proposed Cost-effective Prosthetic Hand.....	20
Chapter 4 : Design Structure.....	25
4.1 Introduction .....	25
4.2 Forward Kinematics Equations of the Fingertip. ....	29
4.2.1 Homogenous Transformation Matrix A .....	29
4.2.2 Basic Forms of Homogenous Transformation.....	29
4.3 Denavit – Hartenberg (DH) Convention .....	31
4.4 Determining DH Parameters. ....	32
4.5 Velocity Kinematic .....	36
4.5.1 Skew Symmetric Matrix.....	37
4.5.2 Properties of Skew Symmetric Matrix .....	38
4.5.3 Jacobian Matrix .....	38
4.6 Singularity Configuration.....	43

Chapter 5 : Dynamic Equations .....	44
5.1 Introduction .....	44
5.2 Kinematic Energy (K) and Potential Energy (P).....	46
5.2.1 The Kinematic Energy (K) .....	46
5.2.2 The Potential Energy (p).....	51
Chapter 6 : EMG Signal Processing .....	64
6.1 Introduction .....	64
6.2 EMG and the Muscle Contraction.....	64
6.3 Surface EMG.....	67
6.4 Noise in the EMG Signal .....	68
6.5 EMG Signal Detecting and Processing .....	69
6.6 Common-mode Rejection Ratio CMRR. ....	70
6.7 Instrumentational Amplifier.....	71
6.8 AD620 Instrumentational Amplifier. ....	74
6.9 Pre-Amplifier Stage.....	76
6.10 Filtering Stages.....	77
6.10.1 Sallen-Key Filter.....	79
6.10.2 Transfer Function Calculation of the Sallen-key Filter .....	79
6.10.3 Low-pass and High-pass Filter Sallen-Key .....	81
6.11 Amplifying Stage .....	83
Chapter 7 : Prosthetic Hand Control.....	86
7.1 Introduction .....	86
7.2 Hardware Connection.....	86
7.3 Muscle Training and Signal Reading.....	87
7.4 Programming the Arduino.....	88
7.5 Simulink Model of the Hand's Design.....	90
7.6 Design Details .....	91
7.7 Feedback Signal .....	92
Chapter 8 : Results .....	94

8.1 Hand Results .....	94
8.2 Signal Results .....	99
Chapter 9 : Conclusion and Future Work .....	105
9.1 Conclusion.....	105
9.2 Future Work and Recommendations.....	106
References.....	108



## Table of Figures

Figure 1.1 BeBionic hand of a female human [1].....	2
Figure 1.2 Five-finger prosthetic hand structure.....	3
Figure 2.1 Developed three fingered robotic hand [4].....	7
Figure 2.2 EMG prosthetic hand with two motors [6].....	9
Figure 2.3 Divided strength space of FDS and FDP muscles; x-axis is normalized hand position, and y- axis is normalized force [7].....	10
Figure 2.4 Graph of FDS and FDP muscles [7].....	10
Figure 2.5 Components of each finger unit [9].....	12
Figure 2.6 Mechanical structure of the hand [10].....	14
Figure 2.7 Three fingers prosthetic hand [2]. ....	16
Figure 2.8 Touch hand [13]. ....	16
Figure 2.9 Structure of the finger [14].....	17
Figure 3.1 (a) Is an active electrode [21], and (b) is a twisted cables.....	21
Figure 3.2 The Arduino board. ....	22
Figure 3.3 Fingers with the force sensor.....	23
Figure 3.4 Final hand design.....	24
Figure 4.1 prismatic and revolute joints [37].....	26
Figure 4.2 RRP and RRR manipulator [36].....	26
Figure 4.3 The links in thumb and other fingers.....	26
Figure 4.4 Left is three links manipulator [24], right is two rotated frames. ....	27
Figure 4.5 Two rotated frames [25]. ....	32
Figure 4.6 Shows DH parameters [25]. ....	33
Figure 5.1 The one degree of freedom system [25].....	45
Figure 5.2 The finger's link. ....	48
Figure 5.3 The two links manipulator [25].....	53
Figure 6.1 Motor unit [26]. ....	65
Figure 6.2 a, b, c, and d: Shows the mechanism of the muscle [28].....	66
Figure 6.3 (a) Is invasive electrode [29], [30] and (b) is non-invasive electrode [31]. ....	67
Figure 6.4 The differential amp for two electrode signals [32]. ....	69
Figure 6.5 The entire circuit of the instrumentation amplifier.....	72
Figure 6.6 (a) Is the pinout of AD620 and (b) Is the circuit diagram of AD620.....	75
Figure 6.7 The LM324 operation amplifier. ....	76
Figure 6.8 The LM324 schematic. ....	76
Figure 6.9 Left is high pass filter, right is low pass filter. ....	78
Figure 6.10 The generic unity-gain Sallen-key filter.....	80
Figure 6.11 The low pass filter Sallen-key. ....	81
Figure 6.12 The high pass filter Sallen-key. ....	83
Figure 6.13 The operation amplifier. ....	84
Figure 7.1 The diagram of the circuit. ....	87
Figure 7.2 Shows the design of link and finger in V-rep program. ....	91
Figure 7.3 Left is the vibration motor, right is the feedback circuit. ....	93
Figure 8.1 The movements of middle finger.....	97
Figure 8.2 The movements of index finger.....	97

Figure 8.3 The movements of pinky finger. ....	97
Figure 8.4 The movements of ring finger. ....	97
Figure 8.5 Show the hand when holding a tennis ball in different situations. ....	97
Figure 8.6 Precision open. ....	98
Figure 8.7 Tripod grip. ....	98
Figure 8.8 Hook grip. ....	98
Figure 8.9 Mouse grip. ....	98
Figure 8.10 Relaxed grip. ....	98
Figure 8.11 Power grip. ....	98
Figure 8.12 Show different gripping patterns. ....	98
Figure 8.13 Signal when the muscle at contraction ....	99
Figure 8.14 Signal when the muscle at rest. ....	99
Figure 8.15 Two short contractions. ....	100
Figure 8.16 Muscle at contraction. ....	100
Figure 8.17 Long contraction. ....	100
Figure 8.18 Muscle at rest. ....	100
Figure 8.19 Signal after cutting the negative part. ....	101
Figure 8.20 EMG signal of pinky finger. ....	101
Figure 8.21 EMG signal of ring finger. ....	101
Figure 8.22 EMG signal for middle finger. ....	101
Figure 8.23 EMG signal of the index finger. ....	102
Figure 8.24 EMG of thumb. ....	102

## Nomenclature

RRR Manipulator: Revolute, revolute, revolute joint manipulator

PPP Manipulator: Prismatic, prismatic, prismatic joint manipulator

Configuration (q): Set of joints variables

$\theta_n$ : Rotational angle of joint n

$L_n$ : Length of link n

{n}: Frame number n

$x_n, y_n, z_n$ : x, y, and z positions of frame n

$x_n^m$ : x position of frame n with respect to frame m

$y_n^m$ : y position of frame n with respect to frame m

$R_n^m$ : Rotation matrix from frame n to frame m

$R_n^{\prime m}$ : Derivative of  $R_n^m$

$O_n^m$ : Translation matrix from frame n to frame m

$O_n^{\prime m}$ : Derivative of  $O_n^m$

$R_n, \theta$ : Rotation about axis n by angle  $\theta$

$A_i$ : Homogenous transformation matrix of joint i

$A_n^m$ : Homogenous transformation matrix from frame n to frame m

$c_{nm}$ :  $\cos(n + m)$

$Trans_{n,m}$ : Translation matrix along axis n by m

$Rot_{n,m}$ : Rotation matrix about axis n by angle m

$a_i$ : Length of link i

$\alpha_i$ : Link i twist

$d_i$ : Link  $i$  offset

$S$ : Skew symmetric matrix

$v_n^m$  : Linear velocity of frame  $n$  to frame  $m$

$w_3^0$  : Angular velocity of frame 3 to frame 0

$J_v$ : Jacobian for linear velocity

$J_w$ : Jacobian for angular velocity

$\xi$ : Vector of linear and angular velocities

$I$ : Inertia tensor

$I_n^m$  : Inertia tensor of link  $m$  with respect to  $n$  axis

$v_{cm}$ : Common-mode voltage

$A_{cm}$ : Common-mode gain

$A_d$ : Differential gain

## **Chapter 1 : Introduction**

### **1.1 Motivation and Rationale**

Approximately 1 in every 200 people in the U.S. has undergone an amputation. Annually, in the U.S., approximately 156,000 people go through an amputation operation, and, there are currently over 1.7 million people in the U.S. with an amputated limb. Amputations (because of trauma) have been declining over recent years, as have amputations from cancer. However, amputations due to vascular diseases, such as diabetes, are increasing.

Artificial hand designs and existing prototypes aim to basically satisfy amputee needs. Costs range from \$1,500 to \$36,000 depending on functionality and different features. Regardless, prosthetic hands may be divided in two groups considering price, size, feedback sensing, and strength of force for gripping, weight, and movement capabilities. The first group includes the most expensive hands that are similar to a natural human hand size and replicate natural hand movements. Such designs look like a natural hand, they have good sensing and feedback mechanisms and they are strong enough for daily life activities. A representative design of this group is the Steeper's BeBionic hand [1], which costs \$36,000.00; it has the ability to grip following 14 different patterns, finger sensing to help the user sense, a rear magnet to improve hand strength and speed of gripping. Its weight is 390 gr and its configuration is shown in Figure 1.1. The second group of hands varies in size reaching the size close to the normal human hand; however, designs in this

group have limited strength and limited gripping patterns. Furthermore, some inexpensive hands do not have feedback sensing, like 3D printed hands [2].



Figure 1.1 BeBionic hand of a female human [1].

## 1.2 Thesis Objective

This thesis is motivated by the challenge to develop a prosthetic hand that is not heavy, it is very cost-effective (to be affordable by almost every amputee), with effective and efficient feedback sensing mechanisms and capable of reproducing most of a human hand's movement and gripping patterns. The prosthetic hand should be strong enough to hold different object shapes and weight, and its size should be comparable to a human hand.

As such, the thesis focuses on designing a cost-effective five-finger prosthetic hand. Aluminum is chosen as the building material. Each finger is actuated separately by controlling the angle of a corresponding servo motor. The five fingers combined, account

for 14 DOF. Each finger except the thumb, has three links, one base and three joints. The thumb has two links, one base and two joints. The hand design is shown in Figure 1.2.

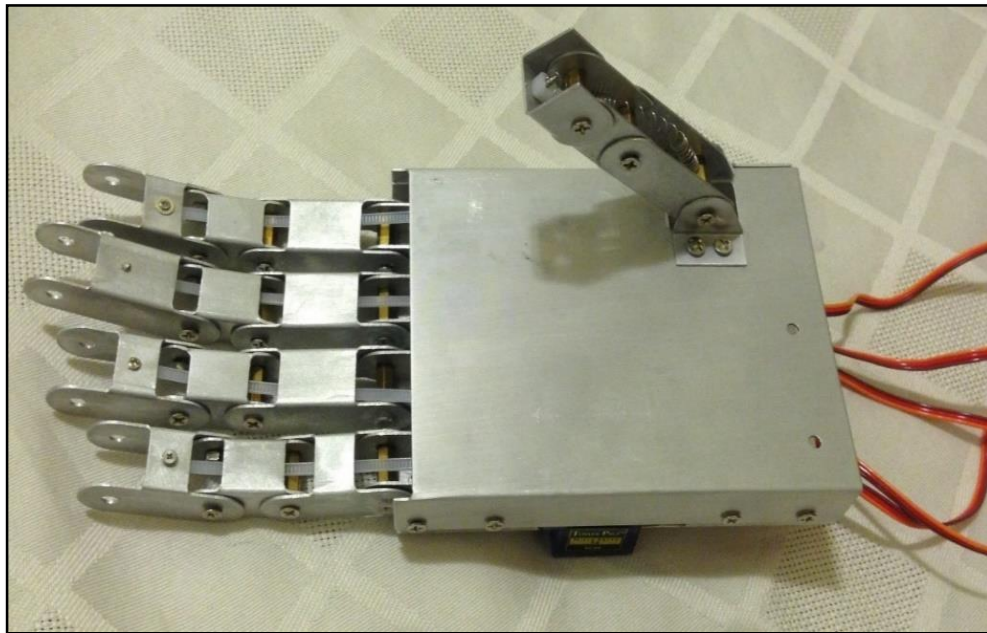


Figure 1.2 Five-finger prosthetic hand structure.

Each finger uses a force sensor to sense objects (in touch with the finger) and returns a feedback signal. The prosthetic hand is controlled by surface EMG signals obtained from surface electrodes that are connected to the arm muscle(s). Obtained signals from the electrodes go through a controller to generate specific finger/hand motions, and also provide the necessary feedback. For the proposed design, five muscles are used to reproduce hand motions.

The most challenging task of designing the prosthetic hand is EMG signal detection and processing. It starts with connecting (three) multi-useable electrodes, positive, negative and ground, to the skin/surface covering the muscle, in order to detect muscle movement. Five muscles are used to detect the EMG (one per finger) using a total of 11 electrodes,

one serving as the common ground. The ground electrode is connected close to any bone; the positive/negative electrodes of each muscle are connected to the top and bottom end or to the middle of the muscle.

The EMG signal passing through the electrode wires may be affected by electromagnetic fields close to the wires [3], and this may generate undesirable noise in the EMG signal. Twisting the electrode wires (see Figure 3.1b) prevents interference and reduces noise as electromagnetic fields in opposite direction cancel each other. After EMG signal detection, EMG signal processing follows, which includes differential, pre-amplifier, filtering and amplifier stages. The five fingers are controlled by an Arduino UNO depending on the received EMG signal(s). A force sensor is attached to each fingertip to sense any object in touch with a finger. These force sensors turn on and off vibration motors connected to the amputee's arm, informing the amputee if there is anything in touch with the fingertip.

Note that the proposed EMG signal detection, processing and control approach is dependable and reliable, accurate, repeatable and cost-effective, while the corresponding circuit size is really small.

### **1.3 Thesis Outline**

Chapter 1 motivates the thesis, while Chapter 2 presents related work, focusing on similar designs. Chapter 3 presents the problem statement followed by the proposed solution. Chapters 4 and 5 discuss the design structure and components of the prosthetic hand. Chapter 6 details the steps for EMG signal detection and processing. Chapter 7



presents the control scheme for the prosthetic hand and includes simulation results. Chapter 8 focuses on experimental studies and results, while Chapter 9 concludes the thesis.

## **Chapter 2 : Related Work**

### **2.1 Literature Review**

Considerable research has been published on this subject.

In [4] the authors present development of a low cost three finger robotic hand with six degrees of freedom. The hand has three actuators and it can grasp different shapes such as oval, cuboid, circular and cylindrical as shown in Figure 2.1. The grasping command depends on the EMG signals coming from three surface electrodes. By using a fuzzy classifier, the grasp planner can recognize a shoulder's abduction or adduction movement based on the root mean square value of the EMG signal. A proportional controller associated with position touch sensors has been used to provide feedback signals. The raw EMG signals from electrodes go to the EMG preprocessing unit. This unit consists of a differential amplifier, which subtracts the two signals that come from the muscle; the first signal comes from the electrode that is connected to the middle of the muscle and the second signal comes from the electrode connected to the end of muscle. This step is used to 'stabilize' the signal.

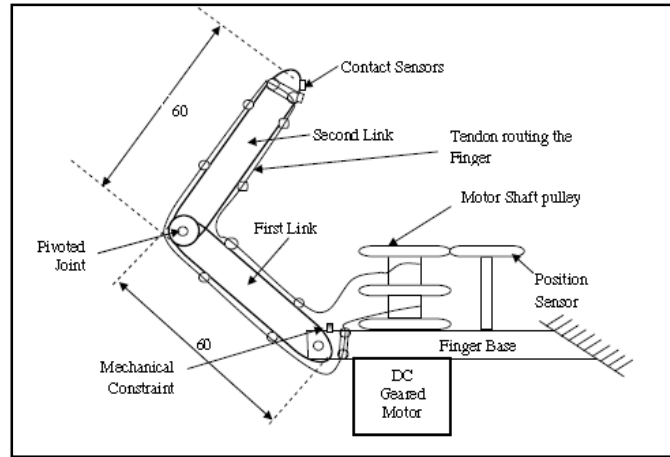


Figure 2.1 Developed three fingered robotic hand [4].

Then, the signal passes into a fuzzy classifier to recognize the abduction or adduction movement of the shoulder to open or close the hand. The skeleton of this hand is made from nylon and each finger has two equal-length links. Each finger is actuated by a DC motor for flexing and extension movements. There is a pulley with tendons wrapped around it. In order to transmit the force from the DC motor to the pulley, a nylon thread is used to extend and flex the links of each finger. There are limitations to this design. The first limitation is that there are just two links in each finger so the fingers cannot reach very many points in the working area. Also, the hand cannot catch other shapes like a triangle. In addition, during the filtering stage the designer used a notch filter to remove noise, which removes frequencies that are between 50-60 HZ. This may make the EMG signal lose much of the signal powered data.

In [5], research has been done to evaluate recognition of various patterns, and to study real-time implantation. A surface EMG signal is used to allow for the prosthetic hand the ability to evaluate six different hand motions. There are three electrodes connected to

each muscle, two electrodes which measure the differential voltage in two different points in the muscle and the third electrode that serves as ground. Signals from the electrodes pass through a protection circuit (for the subject's safety) followed by the differentiation stage, which makes the signal more stable by using a differential amplifier (in this case, an instrumentational amplifier). Any unwanted signal that has high and low frequencies is removed using a RC bandpass filter. The signal, then, amplifies to be readable by the controller. Much focus has been given to getting data from training the six hand motions to imitate such motions. Stored data are processed in two to three stages depending on the computational complexity of the data, feature reduction, and classification.

Fingers have been designed using CAD software. Components were built by using rapid prototyping techniques with polypropylene. Each finger has two revolute hinge joints and three degrees of freedom. The reason behind having this simple structure is that abduction/adduction movements of the metacarpophalangeal joint have been ignored. There are holes made on phalanges to route the drive string through all the phalanges. Using the DC motor, nut, and bolt mechanisms, the string can be pulled/ pushed so the finger will be closed or opened, depending on the motor's direction of rotation, which is decided by the order coming from the EMG's signals.

Research in [6] focused on development of high performance, low degrees of freedom EMG prosthetic hand, which uses two motors to realize various motions. One of these motors is connected to the thumb to generate rotary motion from 0 to 90 degrees. The second motor is connected to the other four fingers. To increase contact area and static friction, soft material has been used to cover the fingers. Also, nails added to the end of

each finger assist in helping fingers catch small objects. This design has a protection device to optimize its mechanical structure, keeping the design safe from the impact caused by a sudden external shock or an overload current. In addition, the design has a spring parallel to the plane of the palm. During a sudden shock, the springs bend laterally alongside it. The limitations of this hand are that there is no feedback, and all four fingers move together; it is also not strong enough. The hand configuration is shown in Figure 2.2.

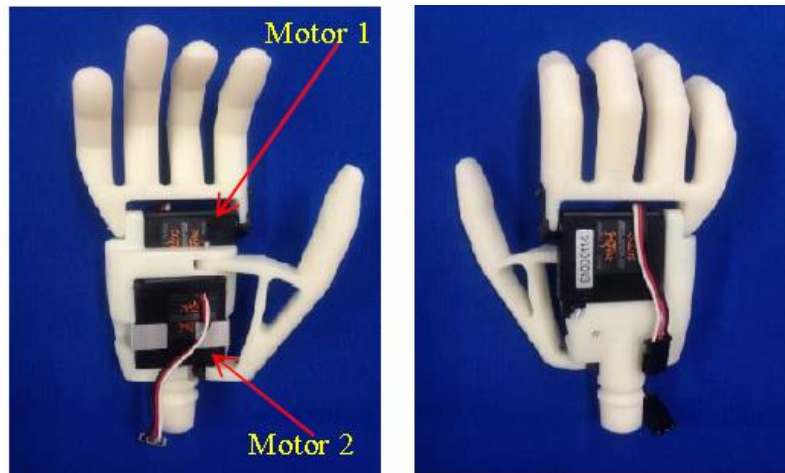


Figure 2.2 EMG prosthetic hand with two motors [6].

Research in [7] focuses on a biologically inspired parallel actuation system that attempts to control the actuators of the prosthetic hand using the Flexor Digitorum Profundus (FDP) and Flexor Digitorum Superficialis (FDS) muscles. By looking at Figures 2.3 and 2.4, one may observe that Region 1 represents the more frequently dexterous tasks, while Region 2 represents the less frequent movements determining movements that need more force.

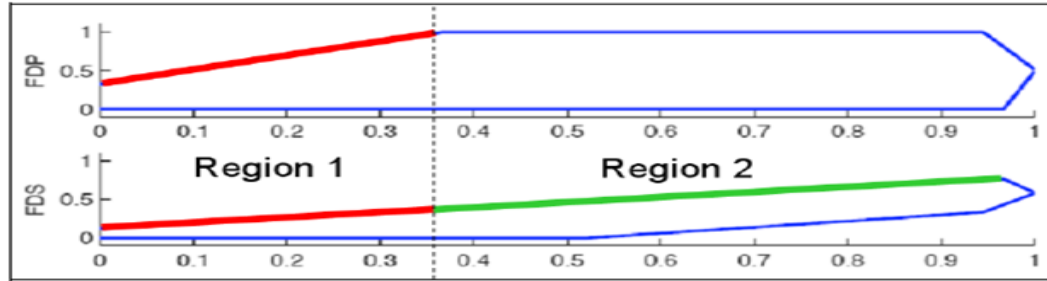


Figure 2.3 Divided strength space of FDS and FDP muscles; x-axis is normalized hand position, and y- axis is normalized force [7].

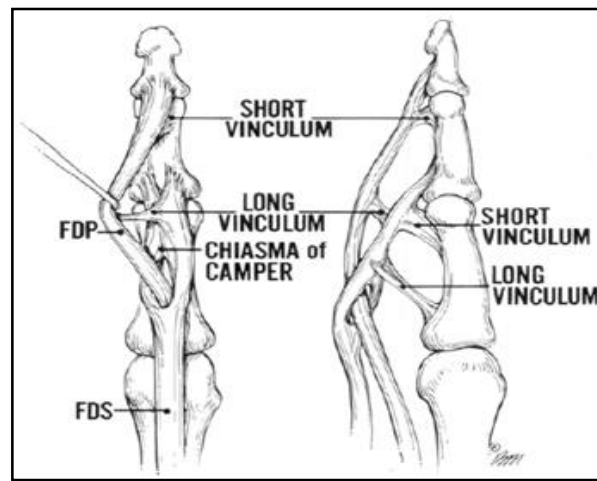


Figure 2.4 Graph of FDS and FDP muscles [7].

The design [7] mimics a male's human hand size with the same degrees of freedom. It couples both the DIP with PIP joints of the fingers, and the IP with MCP joints of the thumb. This is done by using a single actuator for both the PIP and DIP joints. There are two DC motors, the first one connected to the metacarpal phalange of the finger to actuate the horizontal degree of freedom of the MCP joint, while the second one is connected to the base of the thumb to actuate the CMC joint to obtain an approximation of the

abduction/adduction motion. The limitation of this design is that there are no feedback sensors.

The goal of [8] is to develop a cost-effective robotic hand controlled by EMG signals collected from surface skin electrodes. There are two ways to obtain signals from muscles. The first way is invasive (surgery or implantation required); the second way is non-invasive (external sensing). Each method has advantages and disadvantages. The invasive way allows for very readable signals but, sometimes, there may be some side effects, like infection or body rejection to electrodes. The hand's design consists of motorized digits, which are either extended or contracted depending on the EMG signal that comes from the muscle. Each digit is driven by a DC motor and gearbox. There is sensing feedback to determine the amount of torque that should be applied to the object by the hand to avoid hand fatigue.

EMG signals from the electrodes pass through three processing steps. In the first step, an instrumentational amplifier is used to amplify the differential between signals coming from the two electrodes. In the second step, the signal from the first step passes through a 25 - 400 HZ band pass filter to remove unwanted low and high frequencies. Finally, to make the signal slower and suitable for a microcontroller to read, the raw EMG signals are converted to the mean average voltage signal MAV. Depending on the EMG signals' values, the microcontroller receives varying voltages from the MAV to control the motorized hand.

This hand has motorized digits, which can be spread out, and can contract depending on the EMG signals. There is a DC motor in each digit to actuate it. Also, there

is a current sensor to measure the maximum current to prevent the motor from having any damage. Limitations of this design are: there are no feedback sensors; the used filter does not account for the signals with 50 HZ (which is the electricity waves).

Research in [9] focuses on designing a cable-driven anthropomorphic robotic hand that has 20 degrees of freedom. The main body of the hand is made using a 3D printer, where the hand has five fingers. Each finger has three joints, namely, the metacarpophalangeal (MCP), proximal interphalangeal (PIP), and distal interphalangeal (DIP) joints. There is one degree of freedom for each DIP and PIP joints. Two degrees of freedom result from the MCP joint. The first degree of freedom is to achieve the flexion-extension motion; the second degree is used to achieve the abduction-adduction finger motion. The three joints in the thumb are: Carpometacarpal (CMC), Metacarpophalangeal (MCP), and Interphalangeal (IP) joints. The thumb's IP and MCP joints are used to process one degree of freedom in the flexion-extension direction, respectively, while the CMC joint has two degrees of freedom, as shown in Figure 2.5.

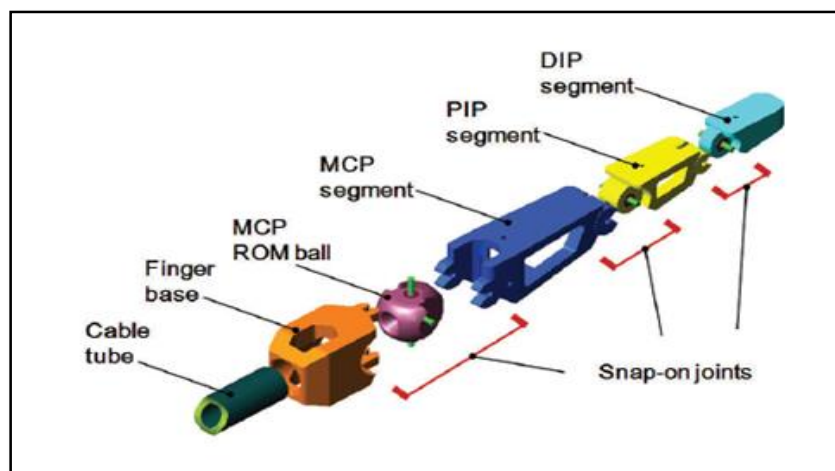


Figure 2.5 Components of each finger unit [9].



An objective of this design is on reducing cost, by depending on 3D printing to design the hand's parts. The LEGO-Style snap - on joint was used in each joint connection between two finger segments. The mechanism of snap - on joint on one side consists of 3D printed parts with a C- shape clip. There is a steel shaft in the center of the other side of the joint. The snap - on joint is formed when the steel shaft is closed by friction engagements, and by snapping on of the clip. For each finger there are four pairs of antagonistic tendons to control the finger's DOF. Also, in the sensing field, there are three layers in each 16 independent skin pads that exist in the hand. These three layers include: Velcro that is embedded in artificial skin, a tactile sensing element, and a 3D printed frame. The artificial skin is made from a silicon rubber which is cleanable, and is resistant to water and oil, and also an anti-smudge to any adhesive. The second layer has the ability to identify the magnitude and the amount of pressure points on the hand because it has sent an array from a five fingers grip system, to determine the position of the pressure. There is a flexible paper-thin, and this paper will bind with the Velcro's surface and the sensor layer will carefully have wrapped onto the 3D printed frame.

Research in [10] discusses the design of a low-cost prosthetic hand controlled by EMG. This hand has been designed with three fingers and one degree of freedom to grasp objects. These three fingers are controlled by one DC motor. The design is shown in Figure 2.6. The microcontroller depends on incoming data from EMG to decide about the PWM required for the DC motor to complete required tasks. The microcontroller monitors the amount of current required by the DC motor to prevent it from any damage. To get the EMG signals, electrodes made from silver/silver chloride were used. The EMG signal that

comes from the electrodes is between 20 microvolts to 2 millivolts, and it passes through three stages to be readable by the microcontroller.

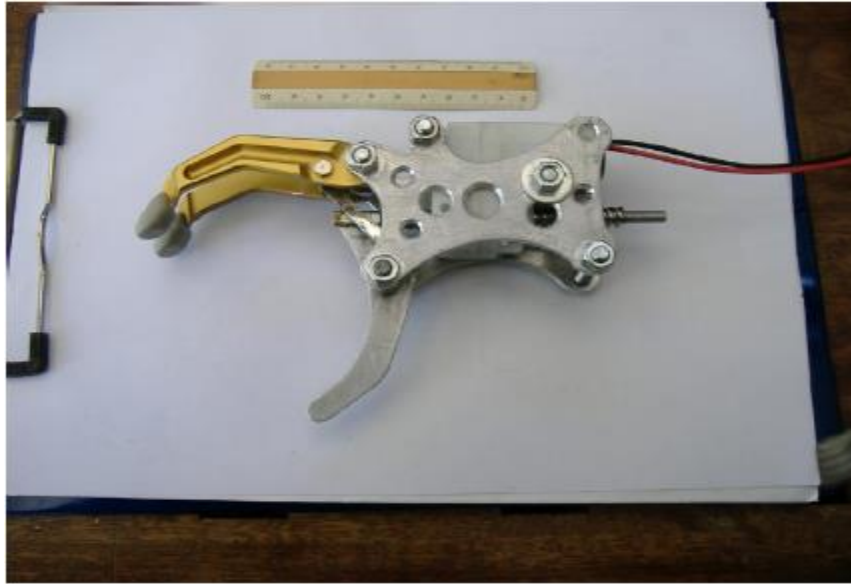


Figure 2.6 Mechanical structure of the hand [10].

The first stage in EMG processing is the pre-amplifier stage that uses the INA129 instrumentational amplifier. In this stage, the difference between the two signals coming from the electrodes (connected to the middle and end of the muscle) is found. The amplifier gain in this step is about 10 - it is not that high because the signal has noise that should not be amplified. In the second stage, the signal passes through the RC high pass filter followed by a TL082 low pass filter operational amplifier. The gain for this step is 200, and frequencies that pass are between 20 HZ and 400HZ. Finally, the signal converts to a digital signal by using an A/D converter, so the controller can easily deal with it. The limitation with this hand is that there is no feedback, and the design has low degrees of freedom.

In [11] a simplified 3D printed EMG prosthetic hand was developed. The design is actuated by two motors and controlled by an EMG signal. This prosthetic hand has been

covered by a highly stretchable cosmetic glove that has the human color, and its fingers look like the human fingers. After detecting the signal from the electrodes, the signal is processed by using a 32-bit microprocessor for pattern recognition and controlling of the motors. The design has two motors. The first motor is connected to the thumb to create a rotary motion ranging from 0 to 90 degrees. The second motor is connected to the other four fingers to create the opening and closing motions. These two motors are embedded inside the palm. Also, the wearable electrodes have been designed to detect the EMG signal. Limitations with this design are that there is no feedback signal that helps the amputee to sense his/her environment, and the design has low degrees of freedom.

In [12] a low degree of freedom prosthetic hand is designed for child amputees. Two small servo motors are used to keep the design small and not heavy. A wire-driven mechanism is used to actuate the fingers. During the age of 0 to 8 years, children learn most of their hand's functions and movements. Therefore, the amputee children learn how to use their muscles (at least) for several movements. The limitations in this design are the low degrees of freedom, and lack of feedback signal in the design.

In [2] a prosthetic hand was developed having 10 joints including 4 active joints. This hand was built according to the intuition of the phantom-hand motion. There are four motors that are embedded into the palm and wrist to actuate the fingers. This hand has three fingers with 10 degrees of freedom as shown in Figure 2.7. The thumb has two active joints. This design has low degrees of freedom and there is no feedback signal.

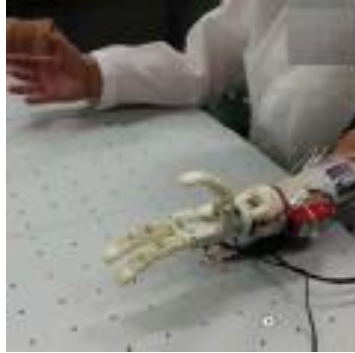


Figure 2.7 Three fingers prosthetic hand [2].

In [13] a low-cost electrically powered prosthetic hand was developed. The supplement of the amputee-prosthetic EMG control of this hand is the novel haptic user interface (HUI). The skeleton of this hand is made by using 3D printed material to be light, as shown in Figure 2.8.

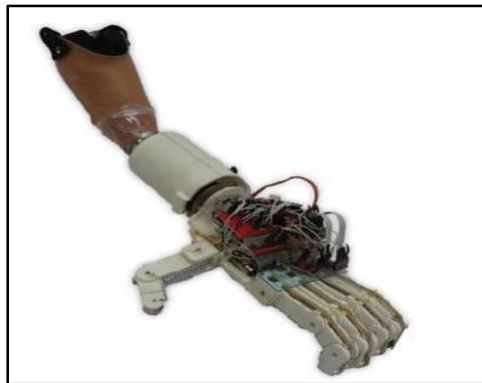


Figure 2.8 Touch hand [13].

The designer used HUI to create a communication between the prosthetic hand and the amputee. The HUI uses a haptic medium (vibrotactile motors) to display the information to the amputee, instead of using the vision display. This design uses flex sensors as position sensors in each finger to give feedback to the microcontroller to control

the motors. The microcontroller checks the flex sensor for the finger's position. When the sensor value shows that the finger is fully opened or fully closed, the microcontroller turns off the motor. The limitation of this design is that there is no feedback signal to inform the amputee if the finger touches an object or not, and whether the touch was soft or hard.

In [14] a three fingers robotic hand with four degrees of freedom is designed. The hand has palm, thumb, index finger, and middle finger. These fingers are tendon-driven. Each finger (except the thumb) consists of three parts; distal phalange (DP), a proximal phalange (PP), the middle phalange (MP), and metacarpal bone (MB). The thumb does not have a middle phalange MP. The process of actuating the fingers begins from the proximal phalange. The proximal phalange will be actuated by pulling the wire using a DC motor. Then, the distal-middle phalange will be actuated synchronously by a link mechanism. The design steps start with designing a single phalange called a distal-middle phalange (DMP). Here the DMP phalange connects to the DP and the MP. The second step will be done by using a link mechanism between the MCP joint (which is the joint that connects the MP and the PP) and the PIP joint (which is the joint that connects the PP with the MP). In the final step a spring will be used as an extension muscle. The design is shown in Figure 2.9. The limitations in this design are; there is no feedback signal, and there are few fingers so this hand cannot imitate many of the human hand movements.

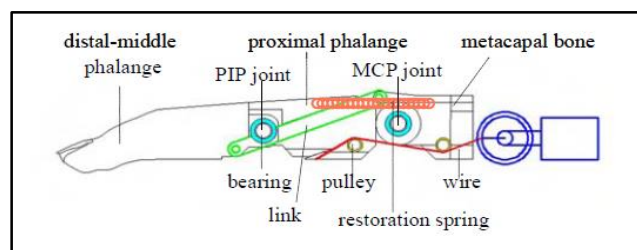


Figure 2.9 The structure of the finger [14].

## **2.2 Remarks**

Looking at the literature, it is obvious that there is a long list of design considerations to design, develop and control a cost-effective EMG prosthetic hand. In this thesis, priority is given to size, weight, complexity, cost effectiveness, as well as efficient functionality. Many of previous designs address some of these attributes, but it appears that there is no cost-effective design that addresses all of them, in unison, for a single prosthetic arm – and this has motivated the proposed design.

## **Chapter 3 : Problem Statement and Proposed Solution**

### **3.1 Problem Statement**

The human body is amazing. Each part of the body has a specific function, yet when combined with all the other parts working together, the body is a magnificent machine. Just as with other machines, when parts of the machine/body break down, some human parts can be transferred from one person to another; some human parts can be replaced with man-made parts; and when some human parts no longer work, and the body cannot be 'repaired', it will stop working altogether. One of the most important parts of the human body is the hand. The hand movements help the body perform such actions as pushing, pulling and/or grasping objects; feeding one's self, writing, etc.

The hand is structured to handle objects of different sizes, shapes, and weight. It is covered by skin with nerve endings to sense the external world through touch. Use of the arms and hands assists in balancing the person's body in space, either while being still, as on a tightrope, or while moving, as in running.

Living without a hand or hands becomes very challenging for the amputee. Many attempts have been made towards resolving problems for amputees to help them live a more normal life. History reports that an early surgery, done between 950 – 710 B.C., discovered on a mummified Egyptian corpse, attempted to create a solution for the loss of a big toe by using a piece of wood to replace a big toe [15]. The first documentation of the use of an artificial hand occurred between 218-201 B.C., for Marcus Sergius [16], a Roman

general who lost his right hand during a battle. Sergius used an iron hand to hold his shield and went back to the battle to fight again [17].

Since then, the field of creating / developing artificial hands has continued to grow. The first study of EMG was done by Francesco Redi in 1666 [18], followed by the first record of EMG signals by Jules Marey in 1890 [19]. Marey was also the first person to use the term “electromyography”. Great progress in the field of artificial hands occurred when the EMG signal was discovered to be able to control the prosthetic hand. Researchers continued to try to design a prosthetic hand which could satisfy the needs of the amputees. The best designs found to be useful to amputees are those that can mimic the actual movements of the human hand, have good sensory feedback, and create enough force to handle objects with smooth movements and have very good EMG signal detection and processing. A prosthetic hand that includes all these requirements in one prosthetic device would make it cost prohibitive for most amputees. This research has focused on the creation of an affordable prosthetic hand that functions ‘well enough’ to make it available and useful for amputees.

### **3.2 Proposed Cost-effective Prosthetic Hand**

Creating an inexpensive prosthetic hand requires many steps, beginning with a way for the prosthesis to detect the EMG signal. A major concern was to determine which kind of electrodes should be used. If regular electrodes were used, this would require changing the electrodes frequently, which would increase cost over time. Instead, it was determined and decided to use multiuse electrodes for / during the EMG detection process.



The next decision was to determine the sequence of steps (process) to best transfer the detected signal(s) from the electrodes without ‘transferring’ the noise, which results from the electromagnetic field coming from other nearby electrical devices. There are two ways to minimize such noise. The first one is to use active electrodes [20], i.e., use very short wires to connect the electrodes with the circuit, as shown in Figure 3.1a. The second is to twist the wires that transfer the signal, as shown in Figure 3.1b. By twisting the wires, the space between the wires is divided into many small areas. In this way, the electromagnetic field resulting from one small area is cancelled by the electromagnetic field that results from the next area. Both of these methods can be used, depending upon the situation and the length of the resting arm. Sometimes long twisted wires are needed to connect the electrodes, and sometimes the use of active electrodes is better.

A high-quality, low-price instrumentational amplifier will be used to subtract the two incoming signals from the two electrodes that connect to the muscle. This subtraction process will eliminate the noise that results from reading signals from more than one muscle. The pre-amplifier stage will begin to make the detecting signal large enough to process by the use of low and high pass active filters. This filtered signal is amplified to be readable by the Arduino. The LM324 operation amplifier is used in the following four

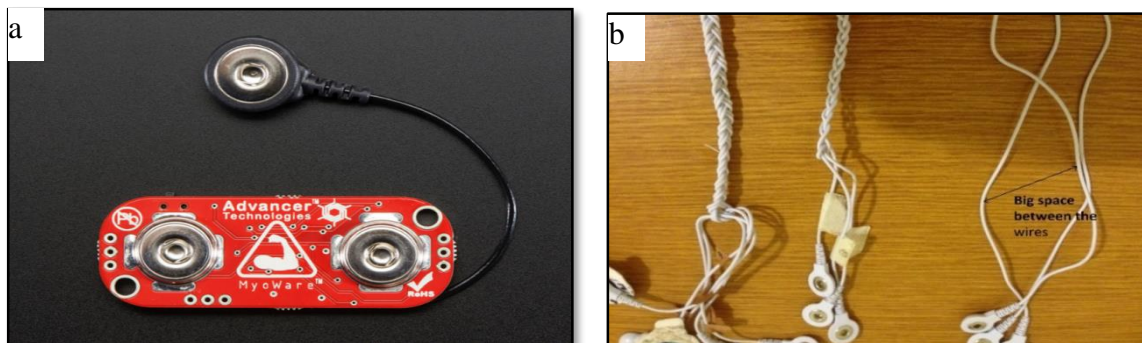


Figure 3.1 (a) An active electrode [21], and (b) twisted cable.

stages: (1) the pre-amplifier stage (2) the low pass active filter (3) the high pass active filter, and (4) last amplifier stage. The LM324 has four amplifiers so that each one could be used as a separate amplifier [22].

This circuit reads each muscle's activities as an electrical signal and sends it to the controller to create an action. This circuit has a lightweight, low price, and small size, and produces reliable results. Therefore, it can be used in many applications, such as to aid with a prosthetic limb or other EMG controlled projects.

After reading the EMG signal by the Arduino, the Arduino makes a decision to control the finger or fingers of the hand, depending upon the EMG signal. There are many functions in the Arduino, which make it perfect to use. The Arduino has six analog pins (from A0 to A5) that can be used for inputting or outputting analog signals. It also has fourteen digital pins to use as input or output digital signals, as shown in Figure 3.2 below. In addition, the total price of the Arduino and its cable is less than four dollars.

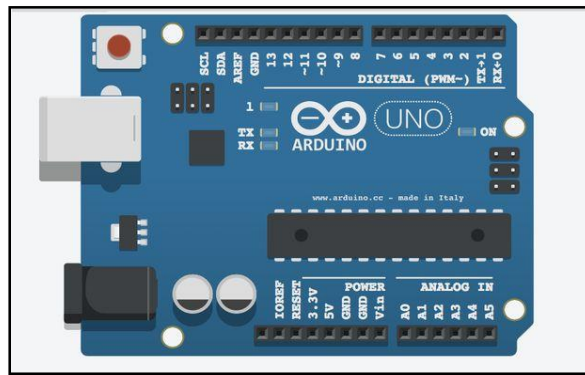


Figure 3.2 The Arduino board.

Once the EMG signal is completed, the signal becomes readable by the Arduino, and the Arduino may then control the prosthetic hand. The biggest challenge now is to design a lightweight, human-sized hand, with good feedback and strong enough to

complete the activities of a human hand. One design could be completed by using a 1 mm thick piece of Aluminum sheet, which is light in weight, yet strong enough to hold a load of several pounds. This load will come from the different activities of the prosthetic, such as grasping or carrying objects. The prosthetic hand will need five fingers, four of which have three links, one base and three joints. The thumb will need two links; one base and two joints. Each finger will actuate separately by a servo motor, and each finger can create the closing and opening movements of a human finger.

Each finger will need one force sensor resistor (FSR) [23] attached to the fingertip as shown in Figure 3.3 below. These sensors are used to give feedback information in the event a finger touched by an object or surface. Each of these force sensors will send a signal to the rest of the arm, and can tell the amputee about the strength of the contact between the object/surface and the finger, allowing the amputee to decide what amount of force he/she needs to use with this object and what action to initiate.

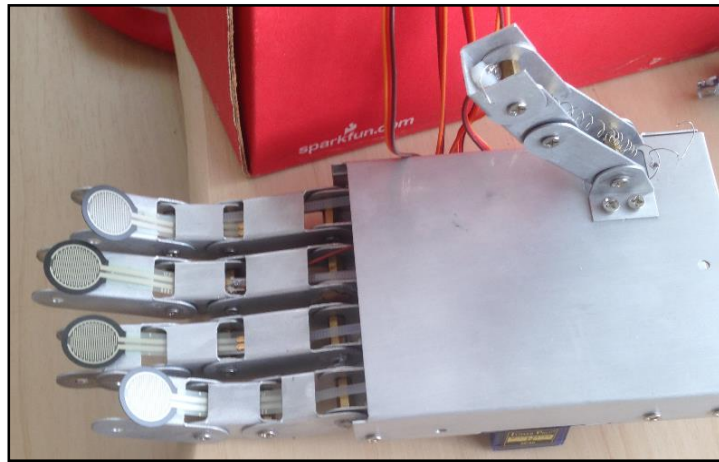


Figure 3.3 Fingers with the force sensor.

The force sensor must tell the amputee if there is an object/surface touching the finger, and what amount of force is being created. The simplest, most economical way to determine this information is by the use of a vibration motor connected to the upper arm. When the signal comes from the sensor connected at the fingertip, the signal will turn on a 2N2222A transistor, which works as a switch. The transistor will turn on the motor with a voltage which is proportional with the strength of the signal coming from this sensor. Once the sensors have been placed in the fingers of the hand, the inner side of the hand should be covered with something which will create a good amount of friction in order to be able to touch, pick up or catch the object/surface in a safe way and with the least amount of force. The most effective and economical way to do this is by using a rubber substance which is not heavy, yet strong enough to not become easily damaged, has good friction, and is inexpensive. The final design of the project is shown in Figure 3.4 below.



Figure 3.4 Final hand design.

## **Chapter 4 : Design Structure**

### **4.1 Introduction**

This chapter discusses the structure of the prosthetic hand's design with the five fingers; pinky, ring, middle, index and thumb. Each finger has three degrees of freedom and the thumb has two. By considering each finger as a serial manipulator the forward kinematics equations and equations of motion may be derived. In general, robotic manipulators may be serial or parallel. A serial manipulator starts with a base link, then a series of links, and ends with one end link. The parallel manipulator consists of two bases, a series of links and ends with two end points.

A robotic manipulator is a series of links and joints, in which the joint  $i$  connects link  $i$  with link  $i+1$ . Robotic manipulators have several types of joints, i.e. ball, revolution, prismatic, and socket. The two most popular types of joints are the revolute joint R and the prismatic joint P. The links in the revolute joint R can move in rotational movement. The links in the prismatic joint P can move in linear movement as show in Figure 4.1.

Each manipulator is named by the sequence of the joints that make up the manipulator. For example, if the manipulator contains three revolute joints, it will be described as an RRR manipulator. If the manipulator consists of two revolute joints and the third joint is a prismatic joint, it is called an RRP manipulator, and so on, as shown in Figure 4.2. The finger is designed with only revolute joints, so the finger will be considered to be a series RRR manipulator and the thumb will be a series RR manipulator.

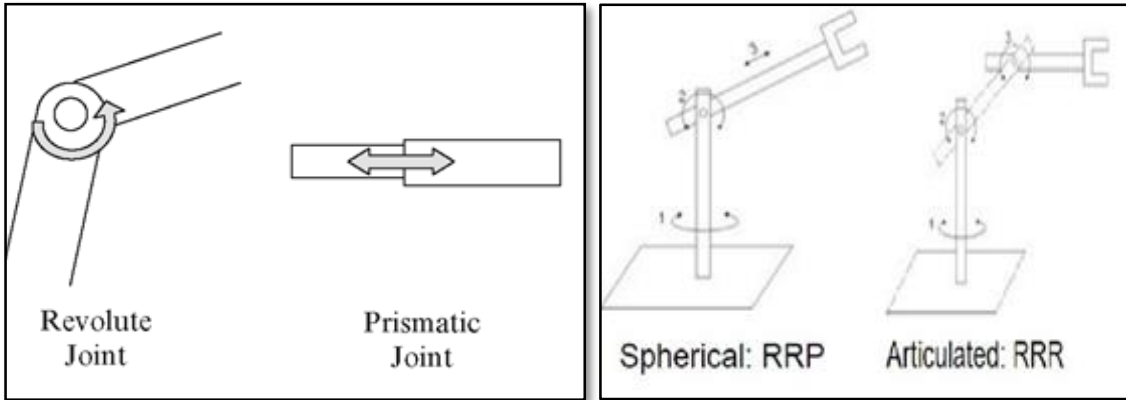


Figure 4.1 prismatic and revolute joints [37]. Figure 4.2 RRP and RRR manipulator [36].

Each finger has three links, three revolute joints, and one base fixed to the palm.

The thumb has one base fixed to the palm, and two revolute joints as shown in Figure 4.3.

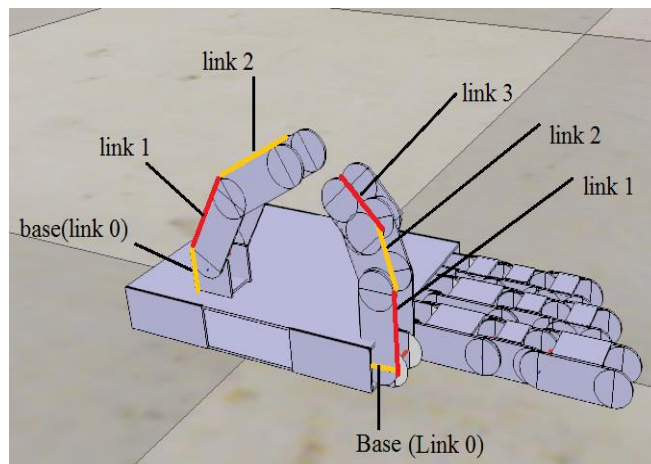


Figure 4.3 The links in thumb and other fingers.

This chapter will discuss how to derive the forward kinematic equations to find the position of the fingertip by addressing the frame for each revolute joint. We presume that the rotation of the joint will be around the Z axis and each finger will have a configuration  $(q)$ , where  $q$  is a set of joint variables, which, in this case, is the angle of rotation around the Z axis.

$$q = \{\theta_1, \theta_2, \theta_3\}$$

Where  $\theta_1, \theta_2, \theta_3$  are the rotational angles of first, second, and third joint respectively, and the  $x, y$  coordinates of the fingertip in Figure 4.4 can be obtained by:

$$x = L_1 \cos \theta_1 + L_2 \cos (\theta_1 + \theta_2) + L_3 \cos (\theta_1 + \theta_2 + \theta_3) \quad (4.1)$$

$$y = L_1 \sin \theta_1 + L_2 \sin (\theta_1 + \theta_2) + L_3 \sin (\theta_1 + \theta_2 + \theta_3) \quad (4.2)$$

$L_1, L_2,$  and  $L_3$  are the lengths of the link one, two and link three respectively.

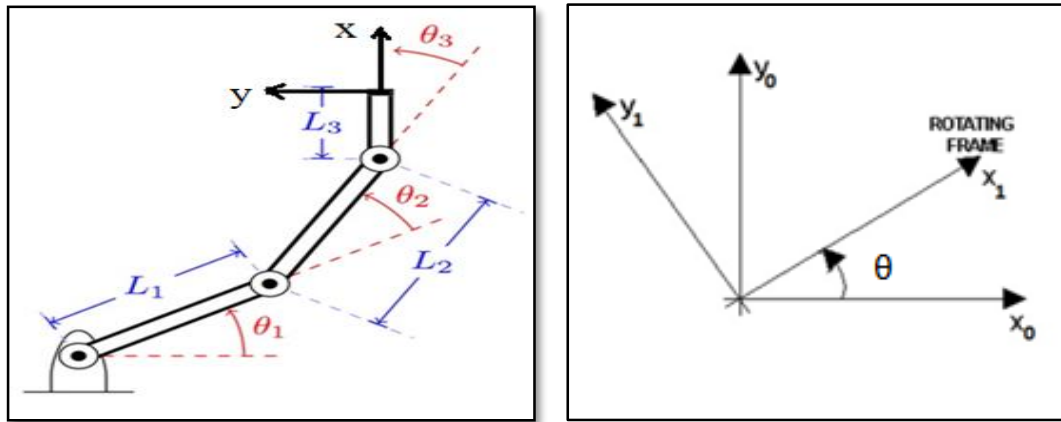


Figure 4.4 Left is three links manipulator [24], right is two rotated frames.

In which, each joint has an axis of rotation and frame attached to this joint, when the joint moves the frame of the joint will change with respect to other frames in the same finger. It is possible to find the position of the fingertip to the finger's base by finding the relationship between the current frame (fingertip) to the previous frame and so on until we get the base frame. The following relations can be used to find the position of frame one  $\{1\}$  with respect to frame zero  $\{0\}$  in Figure 4.4.

$$x_1^0 = \begin{bmatrix} \cos \theta \\ \sin \theta \end{bmatrix} \quad (4.3)$$

$$y_1^0 = \begin{bmatrix} -\sin \theta \\ \cos \theta \end{bmatrix} \quad (4.4)$$

Where,

$x_1^0$  Represents the x position of the frame one with respect to frame zero.

$y_1^0$  Represents the y position of the frame one with respect to frame zero.

From (4.3) and (4.4), the rotation matrix from frame one to frame zero  $R_1^0$  will be:

$$R_1^0 = \begin{bmatrix} x_1^0 & y_1^0 \end{bmatrix} = \begin{bmatrix} \cos \theta & -\sin \theta \\ \sin \theta & \cos \theta \end{bmatrix} \quad (4.5)$$

OR

$$R_1^0 = \begin{bmatrix} x_1^0 & y_1^0 \end{bmatrix} = \begin{bmatrix} x1.x0 & y1.x0 \\ x1.y0 & y1.y0 \end{bmatrix} \quad (4.6)$$

We can conclude that the rotation matrix for three dimensions will be:

$$R_1^0 = \begin{bmatrix} x1.x0 & y1.x0 & z1.x0 \\ x1.y0 & y1.y0 & z1.y0 \\ x1.z0 & y1.z0 & z1.z0 \end{bmatrix} \quad (4.7)$$

So, if the frame rotates about x-axis by  $\theta$ , about y-axis by  $\theta$ , or about z-axis by  $\theta$  the rotation matrix  $R_x, \theta$ ,  $R_y, \theta$ , and  $R_z, \theta$  will be as follow:

$$R_x, \theta = \begin{bmatrix} 1 & 0 & 0 \\ 0 & \cos \theta & -\sin \theta \\ 0 & \sin \theta & \cos \theta \end{bmatrix} \quad (4.8)$$

$$R_z, \theta = \begin{bmatrix} \cos \theta & -\sin \theta & 0 \\ \sin \theta & \cos \theta & 0 \\ 0 & 0 & 1 \end{bmatrix} \quad (4.9)$$

$$R_y, \theta = \begin{bmatrix} \cos \theta & 0 & \sin \theta \\ 0 & 1 & 0 \\ -\sin \theta & 0 & \cos \theta \end{bmatrix} \quad (4.10)$$



## 4.2 Forward Kinematics Equations of the Fingertip.

A homogenous transformation matrix should be introduced to derive the forward kinematic equations for the hand's fingers. This is used to represent the position and orientation of the current frame to the other frame.

### 4.2.1 Homogenous Transformation Matrix A

The homogenous transformation matrix of the frame  $\{i\}$  ( $A_i$ ) is a matrix that represents the position and orientation of the frame  $\{i\}$  relative to frame  $\{i-1\}$ . It is a very important concept in manipulator calculations.

$$A_i = \begin{bmatrix} R_i^{i-1} & O_i^{i-1} \\ 0 & 1 \end{bmatrix} \quad (4.11)$$

Where  $A_i$  is a function of a single joint variable,  $R_i^{i-1}$  and  $O_i^{i-1}$  are the rotation and translation matrices of frame  $i$  with respect to the frame  $i-1$  respectively.

$$A_i = A_i(q_i)$$

And  $q_i$  is the variable associated with joint  $i$  (in revolute joint it is  $\theta_i$ ). The finger's design has two or three links. Therefore, there is a need to calculate  $A$  for each link, and the following equation gives the position and orientation of the three links fingertip.

$$A_3^0 = \begin{bmatrix} R_3^0 & O_3^0 \\ 0 & 1 \end{bmatrix} \quad (4.12)$$

### 4.2.2 Basic Forms of Homogenous Transformation

There are six basic forms of homogenous transformation matrices according to the type of movement and about which axis. For simplicity we referred to cos as  $c$  and for sin as  $s$ , and  $\cos(Q_1 + Q_2)$  as  $C_{12}$  and so on.

$$\text{Trans}_{x,a} = \begin{bmatrix} 1 & 0 & 0 & a \\ 0 & 1 & 0 & 0 \\ 0 & 0 & 1 & 0 \\ 0 & 0 & 0 & 1 \end{bmatrix} \quad (4.13)$$

$$\text{Rot}_{x,\alpha} = \begin{bmatrix} 1 & 0 & 0 & 0 \\ 0 & C\alpha & -S\alpha & 0 \\ 0 & S\alpha & C\alpha & 0 \\ 0 & 0 & 0 & 1 \end{bmatrix} \quad (4.14)$$

$$\text{Trans}_{Y,b} = \begin{bmatrix} 1 & 0 & 0 & 0 \\ 0 & 1 & 0 & b \\ 0 & 0 & 1 & 0 \\ 0 & 0 & 0 & 1 \end{bmatrix} \quad (4.15)$$

$$\text{Rot}_{y,\theta} = \begin{bmatrix} C\theta & 0 & S\theta & 0 \\ 0 & 1 & 0 & 0 \\ -S\theta & 0 & C\theta & 0 \\ 0 & 0 & 0 & 1 \end{bmatrix} \quad (4.16)$$

$$\text{Trans}_{Z,c} = \begin{bmatrix} 1 & 0 & 0 & 0 \\ 0 & 1 & 0 & 0 \\ 0 & 0 & 1 & c \\ 0 & 0 & 0 & 1 \end{bmatrix} \quad (4.17)$$

$$\text{Rot}_{z,\beta} = \begin{bmatrix} C\beta & -S\beta & 0 & 0 \\ S\beta & C\beta & 0 & 0 \\ 0 & 0 & 1 & 0 \\ 0 & 0 & 0 & 1 \end{bmatrix} \quad (4.18)$$

Where,

$\text{Trans}_{x,a}$ ,  $\text{Trans}_{Y,b}$ ,  $\text{Trans}_{Z,c}$  are the matrices of translations above x, y, and z axis by a, b, and c respectively.

$\text{Rot}_{x,\alpha}$ ,  $\text{Rot}_{y,\theta}$ ,  $\text{Rot}_{z,\beta}$  are the matrices of rotation about x, y, and z by  $\alpha$ ,  $\theta$ ,  $\beta$  respectively.

### 4.3 Denavit – Hartenberg (DH) Convention

In forward kinematic calculations there is a need to calculate  $A_i$  for each joint, and this process could be a very complex process for the manipulator which has many links.

To simplify this process there are many conventions that can be used such as DH (Denavit –Hartenberg ) convention.

There are two assumptions which should be satisfied for the DH convention, DH1 and DH2. First (DH1), the axis  $x_{n+1}$  is perpendicular to the axis  $z_n$ . Second (DH2), the axis  $x_{n+1}$  intersects the axis  $z_n$ . DH convention comes from the product of four matrices, in which the movement will be rotation about the z-axis by  $\theta_i$  then translation about z-axis by distance  $d_i$  follows by translation about x-axis by  $a_i$  distance. Finally, it will rotate about x-axis by  $\alpha_i$ .

$$A_i = \text{Rot}_{z,\theta_i} \cdot \text{Trans}_{z,d_i} \cdot \text{Trans}_{x,a_i} \cdot \text{Rot}_{x,\alpha_i} \quad (4.19)$$

$$A_i = \begin{bmatrix} C\theta_i & -s\theta_i & 0 & 0 \\ S\theta_i & C\theta_i & 0 & 0 \\ 0 & 0 & 1 & 0 \\ 0 & 0 & 0 & 1 \end{bmatrix} * \begin{bmatrix} 1 & 0 & 0 & 0 \\ 0 & 1 & 0 & 0 \\ 0 & 0 & 1 & d_i \\ 0 & 0 & 0 & 1 \end{bmatrix} * \begin{bmatrix} 1 & 0 & 0 & a_i \\ 0 & 1 & 0 & 0 \\ 0 & 0 & 1 & 0 \\ 0 & 0 & 0 & 1 \end{bmatrix} *$$

$$\begin{bmatrix} 1 & 0 & 0 & 0 \\ 0 & C\alpha_i & -S\alpha_i & 0 \\ 0 & S\alpha_i & C\alpha_i & 0 \\ 0 & 0 & 0 & 1 \end{bmatrix}$$

$$A_i = \begin{bmatrix} c\theta_i & -s\theta_i * c\alpha_i & s\theta_i * s\alpha_i & a_i * c\theta_i \\ s\theta_i & c\theta_i * c\alpha_i & -c\theta_i * s\alpha_i & a_i * s\theta_i \\ 0 & s\alpha_i & c\alpha_i & d_i \\ 0 & 0 & 0 & 1 \end{bmatrix} \quad (4.20)$$

Where,  $a_i, \alpha_i, d_i, \theta_i$  are the parameters of the joint  $i$  and link  $i$  and they defined as follows:

$O_i$  represents the origin of the frame  $\{i\}$ .

$a_i$  represents the link's length (the distance from the intersection of  $x_{i+1}$  and  $z_i$  to  $O_{i+1}$  along  $x_{i+1}$ ).

$\alpha_i$  represents the link twist (angle from  $z_i$  to  $z_{i+1}$  about  $x_i$ )

$d_i$  represents the link offset (the distance from intersection of  $x_{i+1}$  and  $z_i$  to  $O_i$  along  $z_i$ )

$\theta_i$  represents the joint angle (the angle from  $x_i$  to  $x_{i+1}$  about  $z_i$ )

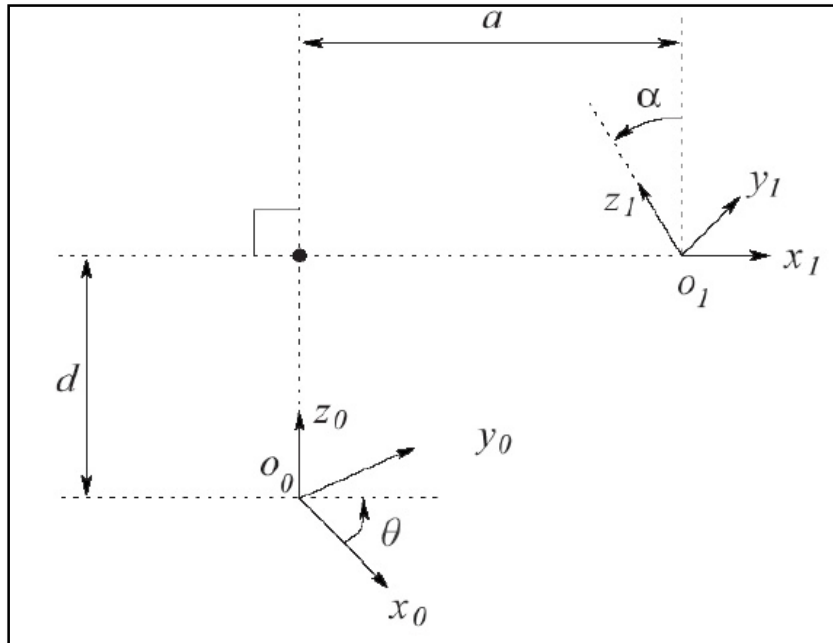


Figure 4.5 Two rotated frames [25].

#### 4.4 Determining DH Parameters.

There are several steps that should be followed to determine the DH parameters.

- 1- Assign  $z_{i1}$  to be the axis of actuation for joint  $i+1$ .
- 2- Choose the origin of frame zero  $\{0\}$  anywhere along  $z_0$  axis.
- 3- Choose  $x_0, y_0$  to satisfy right- hand rule.

There are three cases can effect on choosing  $Z_i$  depending on  $Z_{i-1}$ :

- 1)  $Z_i$  and  $Z_{i-1}$  are not coplanar.
- 2)  $Z_i$  and  $Z_{i-1}$  are intersecting.
- 3)  $Z_i$  and  $Z_{i-1}$  are parallel.

Frames need to be specified and DH parameters need to be determined for each case. When  $Z_i$  and  $Z_{i-1}$  are not coplanar, there is the shortest line between both axis and perpendicular on both. This line should be chosen as  $X_i$ , and  $O_i$  will be the intersection between  $Z_i$  and  $X_i$ .  $Y_i$  will be chosen depending on right hand rule as shown in Figures 4.5 and 4.6.

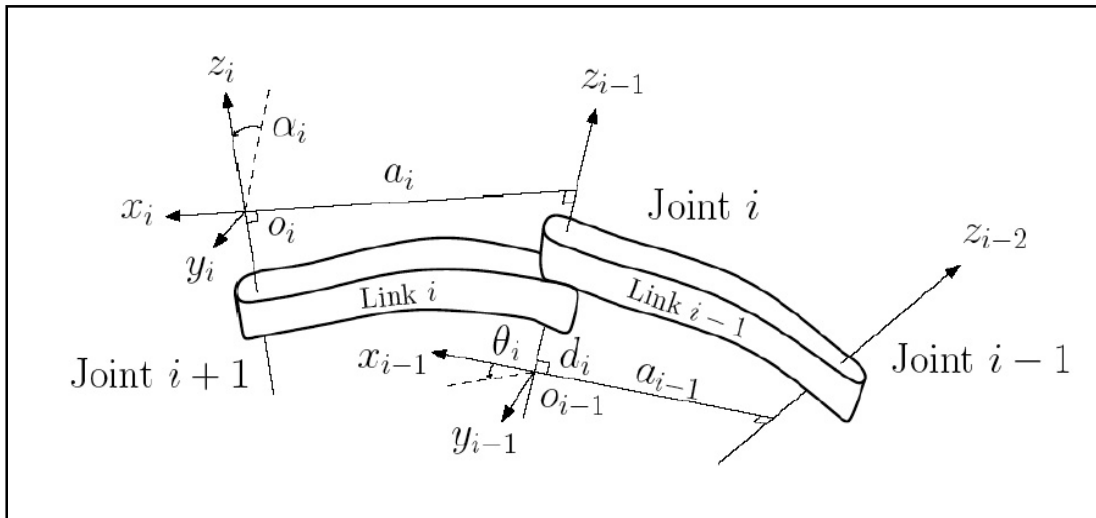


Figure 4.6 Shows DH parameters [25].

In the case when the  $Z_i$  and  $Z_{i-1}$  are intersecting,  $X_i$  will be normal to the plane formed by  $Z_{i-1}$  and  $Z_i$  in any direction. The intersection point between  $Z_i$  and  $Z_{i-1}$  will be  $O_i$ , and  $y_i$  should be chosen in a way that satisfies the right hand rule.

In the case when the  $Z_i$  and  $Z_{i-1}$  are in the parallel, the easier way to deal with that is by choosing the intersection point of  $X_i$  and  $Z_{i-1}$  at  $O_{i-1}$  to make  $d_i$  equal to zero, and  $O_i$  will be anywhere along  $Z_i$ . According to the project's finger design,  $Z_i$  and  $Z_{i-1}$  are

paralleled. Therefore, the last procedure can be applied in this design. First, frame zero  $\{0\}$  should be chosen at the base of the finger, and finger's rotation will be around Z-axis. Next, the intersect line between  $Z_0$  and  $Z_1$  will be  $X_1$ , and Y will be chosen so as to satisfy the right hand rule. By repeating these steps for all other joints, the design will have a frame for each joint as shown in Figure 4.6, and the DH parameters will be as shown in table 4.1 below:

Link #	$L_i$	$\alpha_i$	$d_i$	$\theta_i$
1	L1	0	0	$\theta_1$
2	L2	0	0	$\theta_2$
3	L3	0	0	$\theta_3$

Table 4.1: Shows DH parameters for each finger.

Now, applying DH parameters in equation (4.20) to get the transformation matrices as follow:

$$A_1 = \begin{bmatrix} c\theta_1 & -s\theta_1 & 0 & l_1 * c\theta_1 \\ s\theta_1 & c\theta_1 & 0 & l_1 * s\theta_1 \\ 0 & 0 & 1 & 0 \\ 0 & 0 & 0 & 1 \end{bmatrix} \quad (4.21)$$

$$A_2 = \begin{bmatrix} c\theta_2 & -s\theta_2 & 0 & l_2 * c\theta_2 \\ s\theta_2 & c\theta_2 & 0 & l_2 * s\theta_2 \\ 0 & 0 & 1 & 0 \\ 0 & 0 & 0 & 1 \end{bmatrix} \quad (4.22)$$

$$A_3 = \begin{bmatrix} c\theta_3 & -s\theta_3 & 0 & l_3 * c\theta_3 \\ s\theta_3 & c\theta_3 & 0 & l_3 * s\theta_3 \\ 0 & 0 & 1 & 0 \\ 0 & 0 & 0 & 1 \end{bmatrix} \quad (4.23)$$

The homogenous transformation matrix from the fingertip to the finger's base can be obtained by:

$$A_2^0 = A_1 * A_2$$

this is for thumb

$$A_2^0 = \begin{bmatrix} c\theta_{12} & -s\theta_{12} & 0 & l_2 * C\theta_{12} + l_1 * C\theta_1 \\ s\theta_{12} & c\theta_{12} & 0 & l_2 * S\theta_{12} + l_1 * S\theta_1 \\ 0 & 0 & 1 & 0 \\ 0 & 0 & 0 & 1 \end{bmatrix} \quad (4.24)$$

For all other fingers:

$$A_3^0 = A_1 * A_2 * A_3$$

$$= \begin{bmatrix} C\theta_{123} & -S\theta_{123} & 0 & l_3 * C\theta_{123} + l_2 * C\theta_{12} + l_1 * C\theta_1 \\ S\theta_{123} & C\theta_{123} & 0 & l_3 * S\theta_{123} + l_2 * S\theta_{12} + l_1 * S\theta_1 \\ 0 & 0 & 1 & 0 \\ 0 & 0 & 0 & 1 \end{bmatrix} \quad (4.25)$$

The first element of the last column is the x position of the fingertip, the second element is the y position, and the third element is the z position, and it is equal to zero because the rotation will be around it.

Here we are substituting the values of the links' lengths of each finger in the above matrix, to get the fingertip position for any joints variables.

1) The pinky finger's links' lengths are:

Base = 2 cm, link 1 = 2.5cm, link 2 = 2cm, link 3 = 2.5cm.

2) The ring finger's links lengths are:

Base = 2 cm, link 1 = 3.5cm, link 2 = 2cm, link 3 = 2.5cm.

3) The Middle finger's links lengths are:

Base = 2 cm, link 1 = 3.5cm, link 2 = 2cm, link 3 = 3.5cm.

4) The index finger's links lengths are:

Base = 2 cm, link 1 = 3.5cm, link 2 = 2cm, link 3 = 2.5cm.

5) The thumb's links lengths are:

Base = 2 cm, link 1 = 3.5cm, link 2 = 3.3cm.

Thus, the homogenous transformation matrix for each finger will be:

$$T_{\text{pink}} = \begin{bmatrix} C\theta_{123} & -S\theta_{123} & 0 & 2.5 * C\theta_{123} + 2 * C\theta_{12} + 2.5 * C\theta_1 \\ S\theta_{123} & C\theta_{123} & 0 & 2.5 * S\theta_{123} + 2 * S\theta_{12} + 2.5 * S\theta_1 \\ 0 & 0 & 1 & 0 \\ 0 & 0 & 0 & 1 \end{bmatrix} \quad (4.26)$$

$$T_{\text{Ring}} = \begin{bmatrix} C\theta_{123} & -S\theta_{123} & 0 & 2.5 * C\theta_{123} + 2 * C\theta_{12} + 3.5 * C\theta_1 \\ S\theta_{123} & C\theta_{123} & 0 & 2.5 * S\theta_{123} + 2 * S\theta_{12} + 3.5 * S\theta_1 \\ 0 & 0 & 1 & 0 \\ 0 & 0 & 0 & 1 \end{bmatrix} \quad (4.27)$$

$$T_{\text{Middle}} = \begin{bmatrix} C\theta_{123} & -S\theta_{123} & 0 & 3.5 * C\theta_{123} + 2 * C\theta_{12} + 3.5 * C\theta_1 \\ S\theta_{123} & C\theta_{123} & 0 & 3.5 * S\theta_{123} + 2 * S\theta_{12} + 3.5 * S\theta_1 \\ 0 & 0 & 1 & 0 \\ 0 & 0 & 0 & 1 \end{bmatrix} \quad (4.28)$$

$$T_{\text{Index}} = \begin{bmatrix} C\theta_{123} & -S\theta_{123} & 0 & 2.5 * C\theta_{123} + 2 * C\theta_{12} + 3.5 * C\theta_1 \\ S\theta_{123} & C\theta_{123} & 0 & 2.5 * S\theta_{123} + 2 * S\theta_{12} + 3.5 * S\theta_1 \\ 0 & 0 & 1 & 0 \\ 0 & 0 & 0 & 1 \end{bmatrix} \quad (4.29)$$

$$T_{\text{Thumb}} = \begin{bmatrix} c\theta_{12} & -s\theta_{12} & 0 & 3.3 * C\theta_{12} + 3.5 * C\theta_1 \\ s\theta_{12} & c\theta_{12} & 0 & 3.3 * S\theta_{12} + 3.5 * S\theta_1 \\ 0 & 0 & 1 & 0 \\ 0 & 0 & 0 & 1 \end{bmatrix} \quad (4.30)$$

#### 4.5 Velocity Kinematic

In the previous section, the forward kinematic of each finger has been determined to be the relationship between the fingertip position and orientation with respect to the joints position and orientation. This section will discuss the velocity kinematic as it relates to the linear and angular velocities of the fingertip to the linear and angular velocities of the finger's joints. To determine the velocity kinematic, the Jacobian of the forward



kinematic and the skew symmetric matrix should be explained. The singularity of the finger will be found, which is the configuration that causes the loss in degrees of freedom.

#### 4.5.1 Skew Symmetric Matrix

Before discussing the force, torque, and velocity calculations, the skew symmetric matrix and Jacobian matrix should be explained and calculated. A skew symmetric matrix  $S$  is a matrix which is used to simplify many of computational operations such as the relative velocity between coordinate frames. The square matrix  $S$  is said to be a skew matrix if and only if:

$$S^T + S = 0 \quad (4.31)$$

Where for any  $i, j = 1, 2, 3$

$$S_{i,j} + S_{j,i} = 0 \quad (4.32)$$

From equation 4.32 it is clear that every  $S_{i,i}$  or  $S_{j,j}$  is equal to zero. Therefore, the skew symmetric matrix for the vector  $S = [S_1, S_2, S_3]$  will have the following form:

$$S = \begin{bmatrix} 0 & -S_3 & S_2 \\ S_3 & 0 & -S_1 \\ -S_2 & S_1 & 0 \end{bmatrix} \quad (4.33)$$

For example, by considering the following vectors:

$$A = \begin{bmatrix} 1 \\ 0 \\ 0 \end{bmatrix}, B = \begin{bmatrix} 1 \\ 1 \\ 0 \end{bmatrix}, C = \begin{bmatrix} 0 \\ 1 \\ 2 \end{bmatrix}$$

The skew matrices for the previous vectors are:

$$S(A) = \begin{bmatrix} 0 & 0 & 0 \\ 0 & 0 & -1 \\ 0 & 1 & 0 \end{bmatrix}, S(B) = \begin{bmatrix} 0 & 0 & 1 \\ 0 & 0 & -1 \\ -1 & 1 & 0 \end{bmatrix}, S(C) = \begin{bmatrix} 0 & -2 & 1 \\ 2 & 0 & 0 \\ -1 & 0 & 0 \end{bmatrix}$$

### 4.5.2 Properties of Skew Symmetric Matrix

1- The operator  $S$  is linear.

$$S(ax + by) = a S(x) + b S(y) \quad (4.34)$$

Where,  $x$  and  $y$  are vectors, and  $a$  and  $b$  are scalars.

2- For any two vectors  $x$  and  $y$ , the inner product of the skew matrix of the first vector and the second vector are equal to the cross product of the first vector and second vector.

$$S(x)y = x \times y \quad (4.35)$$

3- For any two vectors  $x$  and  $y$ , and orthogonal  $R$ :

$$R(x \times y) = R(x) \times R(y) \quad (4.36)$$

4-  $R S(x) R^T = S(Rx)$  (4.37)

### 4.5.3 Jacobian Matrix

The jacobian matrix  $J$  is a very important quantity in many of the robotic analysis such as force, velocity, and torque. It consists of two parts, linear velocity  $J_v$  and angular velocity  $J_w$ . The linear velocity for the three links fingertip  $v_3^0$  is given by:

$$v_3^0 = o_3^{\prime 0} \quad (4.38)$$

Where,  $o_3^{\prime 0}$  is the derivative of the linear part in homogenous transformation matrix equation (4.12).

The angular velocity of the three links fingertip  $w_3^0$  is given by:

$$S(w_3^0) = R_3^{\prime 0} (R_3^0)^T \quad (4.39)$$

Now, let  $\xi$  be the vector of linear and angular velocities:

$$\dot{\mathbf{x}} = \begin{bmatrix} \dot{v}_3^0 \\ \dot{w}_3^0 \end{bmatrix} \quad (4.40)$$

$$\dot{\mathbf{x}} = \mathbf{J} \cdot \mathbf{P}' \quad (4.41)$$

Then,  $\mathbf{P}'$  is the derivative of the manipulator variables, and  $\mathbf{J}$  is the Jacobian matrix

$$\mathbf{J} = \begin{bmatrix} \mathbf{J}_V \\ \mathbf{J}_w \end{bmatrix} \quad (4.42)$$

$$\mathbf{J}_{vi} = \mathbf{z}_{i-1} \times (\mathbf{o}_3 - \mathbf{o}_{i-1}) \quad (4.43)$$

$$\mathbf{J}_{wi} = \mathbf{z}_{i-1} \quad (4.44)$$

Therefore, equation 4.42 will be:

$$\mathbf{J} = \begin{bmatrix} \mathbf{z}_0 \times (\mathbf{o}_3 - \mathbf{o}_0) & \mathbf{z}_1 \times (\mathbf{o}_3 - \mathbf{o}_1) & \mathbf{z}_2 \times (\mathbf{o}_3 - \mathbf{o}_2) \\ \mathbf{z}_0 & \mathbf{z}_1 & \mathbf{z}_2 \end{bmatrix}$$

The first step to finding the Jacobian matrix is to find  $\mathbf{o}_i$  and  $\mathbf{z}_i$  for all joints  $i=0, 1, 2, 3$  for three links fingers, and  $i=0, 1, 2$  for the thumb.

$$\mathbf{o}_0 = \begin{bmatrix} 0 \\ 0 \\ 0 \end{bmatrix}, \mathbf{o}_1 = \begin{bmatrix} l_1 c_1 \\ l_1 s_1 \\ 0 \end{bmatrix}, \mathbf{o}_2 = \begin{bmatrix} l_1 c_1 + l_2 c_{12} \\ l_1 s_1 + l_2 s_{12} \\ 0 \end{bmatrix}, \mathbf{o}_3 = \begin{bmatrix} l_1 c_1 + l_2 c_{12} + l_3 c_{123} \\ l_1 s_1 + l_2 s_{12} + l_3 s_{123} \\ 0 \end{bmatrix}$$

$$\mathbf{z}_0 = \mathbf{z}_1 = \mathbf{z}_2 = \begin{bmatrix} 0 \\ 0 \\ 1 \end{bmatrix}$$

$$\mathbf{J} = \begin{bmatrix} -(l_3 s_{123} + l_2 s_{12} + l_1 s_1) & -(l_3 s_{123} + l_2 s_{12}) & -l_3 s_{123} \\ l_3 c_{123} + l_2 c_{12} + l_1 c_1 & l_3 c_{123} + l_2 c_{12} & l_3 c_{123} \\ 0 & 0 & 0 \\ 0 & 0 & 0 \\ 0 & 0 & 0 \\ 1 & 1 & 1 \end{bmatrix} \quad (4.45)$$

From the above matrix, we can note that the first two rows represent the linear velocity of the origin of frame 3 ( $\mathbf{o}_3$ ) with respect to the base. The third row of this matrix

is the linear velocity of the frame 3, relative to the z axis, and it is zero. The last three rows represent the rotation of the last frame about the vertical axis.

$$J = \begin{bmatrix} z_0 \times (o_2 - o_0) & z_1 \times (o_2 - o_1) \\ z_0 & z_1 \end{bmatrix} \text{ this is for thub}$$

$$J = \begin{bmatrix} -(l_2 s_{12} + l_1 s_1) & -l_2 s_{12} \\ l_2 c_{12} + l_1 c_1 & l_2 c_{12} \\ 0 & 0 \\ 0 & 0 \\ 0 & 0 \\ 1 & 1 \end{bmatrix} \quad (4.46)$$

Here, the first two rows represent the linear velocity of the origin of frame 2 ( $o_2$ ) with respect to the base. The third row of this matrix is the linear velocity of the frame 2 relative to z axis, and it is zero. The last three rows represent the rotation of the last frame about the vertical axis.

Now, equation (4.41) can be written as the following form:

For the three links fingers:

$$\mathfrak{f} = \begin{bmatrix} v_x \\ v_y \\ v_z \\ w_x \\ w_y \\ w_z \end{bmatrix} = \begin{bmatrix} -(l_3 s_{123} + l_2 s_{12} + l_1 s_1) & -(l_3 s_{123} + l_2 s_{12}) & -l_3 s_{123} \\ l_3 c_{123} + l_2 c_{12} + l_1 c_1 & l_3 c_{123} + l_2 c_{12} & l_3 c_{123} \\ 0 & 0 & 0 \\ 0 & 0 & 0 \\ 0 & 0 & 0 \\ 1 & 1 & 1 \end{bmatrix} \cdot \begin{bmatrix} \theta'_1 \\ \theta'_2 \\ \theta'_3 \end{bmatrix} \quad (4.47)$$

For the thumb:

$$\mathfrak{f} = \begin{bmatrix} v_x \\ v_y \\ v_z \\ w_x \\ w_y \\ w_z \end{bmatrix} = \begin{bmatrix} -(l_2 s_{12} + l_1 s_1) & -l_2 s_{12} \\ l_2 c_{12} + l_1 c_1 & l_2 c_{12} \\ 0 & 0 \\ 0 & 0 \\ 0 & 0 \\ 1 & 1 \end{bmatrix} \cdot \begin{bmatrix} \theta'_1 \\ \theta'_2 \end{bmatrix} \quad (4.48)$$

Whereas,  $v_x$ ,  $v_y$ ,  $v_z$ ,  $w_x$ ,  $w_y$ , and  $w_z$  represent the linear and angular velocities of the fingertip respectively.

By substituting the lengths of each finger's links to equation 4.47 and 4.48, the results will

be:

1) The pinky finger:

$$\mathbf{f} = \begin{bmatrix} v_x \\ v_y \\ v_z \\ w_x \\ w_y \\ w_z \end{bmatrix} = \begin{bmatrix} -(2.5 * s_{123} + 2 * s_{12} + 2.5 * s_1) & -(2.5 * s_{123} + 2 * s_{12}) & -2.5 * s_{123} \\ 2.5 * c_{123} + 2 * c_{12} + 2.5 * c_1 & 2.5 * c_{123} + 2 * c_{12} & 2.5 * c_{123} \\ 0 & 0 & 0 \\ 0 & 0 & 0 \\ 0 & 0 & 0 \\ 1 & 1 & 1 \end{bmatrix} \cdot \begin{bmatrix} \theta'_1 \\ \theta'_2 \\ \theta'_3 \end{bmatrix}$$

(4.49)

2) The ring finger

$$\mathbf{f} = \begin{bmatrix} v_x \\ v_y \\ v_z \\ w_x \\ w_y \\ w_z \end{bmatrix} = \begin{bmatrix} -(2.5 * s_{123} + 2 * s_{12} + 3.5 * s_1) & -(2.5 * s_{123} + 2 * s_{12}) & -2.5 * s_{123} \\ 2.5 * c_{123} + 2 * c_{12} + 3.5 * c_1 & 2.5 * c_{123} + 2 * c_{12} & 2.5 * c_{123} \\ 0 & 0 & 0 \\ 0 & 0 & 0 \\ 0 & 0 & 0 \\ 1 & 1 & 1 \end{bmatrix} \cdot \begin{bmatrix} \theta'_1 \\ \theta'_2 \\ \theta'_3 \end{bmatrix}$$

(4.50)

3) The middle finger

$$\mathbf{f} = \begin{bmatrix} v_x \\ v_y \\ v_z \\ w_x \\ w_y \\ w_z \end{bmatrix} = \begin{bmatrix} -(3.5 * s_{123} + 2 * s_{12} + 3.5 * s_1) & -(3.5 * s_{123} + 2 * s_{12}) & -3.5 * s_{123} \\ 3.5 * c_{123} + 2 * c_{12} + 3.5 * c_1 & 3.5 * c_{123} + 2 * c_{12} & 3.5 * c_{123} \\ 0 & 0 & 0 \\ 0 & 0 & 0 \\ 0 & 0 & 0 \\ 1 & 1 & 1 \end{bmatrix} \cdot \begin{bmatrix} \theta'_1 \\ \theta'_2 \\ \theta'_3 \end{bmatrix}$$

(4.51)

4) The index finger

$$\mathbf{f} = \begin{bmatrix} v_x \\ v_y \\ v_z \\ w_x \\ w_y \\ w_z \end{bmatrix} = \begin{bmatrix} -(2.5 * s_{123} + 2 * s_{12} + 3.5 * s_1) & -(2.5 * s_{123} + 2 * s_{12}) & -2.5 * s_{123} \\ 2.5 * c_{123} + 2 * c_{12} + 3.5 * c_1 & 2.5 * c_{123} + 2 * c_{12} & 2.5 * c_{123} \\ 0 & 0 & 0 \\ 0 & 0 & 0 \\ 0 & 0 & 0 \\ 1 & 1 & 1 \end{bmatrix} \cdot \begin{bmatrix} \theta'_1 \\ \theta'_2 \\ \theta'_3 \end{bmatrix}$$

(4.52)

5) The thumb

$$\mathbf{f} = \begin{bmatrix} v_x \\ v_y \\ v_z \\ w_x \\ w_y \\ w_z \end{bmatrix} = \begin{bmatrix} -(3.3 * s_{12} + 3.5 * s_1) & -3.3 * s_{12} \\ 3.3 * c_{12} + 3.5 * c_1 & 3.3 * c_{12} \\ 0 & 0 \\ 0 & 0 \\ 0 & 0 \\ 1 & 1 \end{bmatrix} \cdot \begin{bmatrix} \theta'_1 \\ \theta'_2 \end{bmatrix} \quad (4.53)$$

## 4.6 Singularity Configuration

The singularity configuration is the configuration that causes the manipulator to lose one or more of its' degrees of freedom. The configuration is called singularity if the rank of the Jacobian matrix is less than its maximum value. The rank of the matrix is the number of independent rows or columns in this matrix. For example, in the case of the thumb, the dimension of the Jacobian matrix is (6, 2). Therefore, the rank of this Jacobian is  $\leq 2$ , and the maximum value of the Jacobian's rank is 2. Thus, the rank of the manipulator's Jacobian  $j(q)$  depends on the configuration  $(q)$ , and it is not constant. To determine the singularity configuration of the manipulator we need to solve the following equation:

$$\det(J(q)) = 0 \quad (4.49)$$

Now, we will apply equation 4.49 for both Jacobians.

First, for three links finger:

$$\det(J(q)) = \det \begin{pmatrix} -(l_3 s_{123} + l_2 s_{12} + l_1 s_1) & -(l_3 s_{123} + l_2 s_{12}) & -l_3 s_{123} \\ l_3 c_{123} + l_2 c_{12} + l_1 c_1 & l_3 c_{123} + l_2 c_{12} & l_3 c_{123} \\ 0 & 0 & 0 \\ 0 & 0 & 0 \\ 0 & 0 & 0 \\ 1 & 1 & 1 \end{pmatrix} = 0$$

Second, for the two links finger:

$$\det(J(q)) = \det \begin{pmatrix} -(3.3 * s_{12} + 3.5 * s_1) & -3.3 * s_{12} \\ 3.3 * c_{12} + 3.5 * c_1 & 3.3 * c_{12} \\ 0 & 0 \\ 0 & 0 \\ 0 & 0 \\ 1 & 1 \end{pmatrix} = 0$$

## Chapter 5 : Dynamic Equations

### 5.1 Introduction

This chapter will discuss the dynamic of the fingers and how to derive the equations of motion using the Euler-Lagrange equation, and its relationship with the force and torque that caused it. The kinematic equations deal with the motion of joints and links without mentioning the force and torque which caused the motion. Dynamic equations have an important part in many manipulators' analyses, such as the design, simulation, and control algorithms. The Euler-Lagrange equation is a form of dynamic equation which can be introduced by using Newton's second law of motion, using the one degree of freedom system. These equations are coming from the difference between the kinematic energy and the potential energy, which is called the Lagrangian (L) of the system.

The Euler-Lagrange equation is a second order partial differential equation, which uses the difference between kinematic energy (K) and potential energy (p) to solve motion problems without need for accelerations.

$$L = K - P$$

To calculate the Euler-Lagrange equation (L), the kinematic and potential energy should be known.

The general formula of the Euler-Lagrange equation is calculated by using the one dimensional system for a ball of mass (m) moving in a Y direction. There is a force (f) which causes this movement, as shown in Figure 5.1.



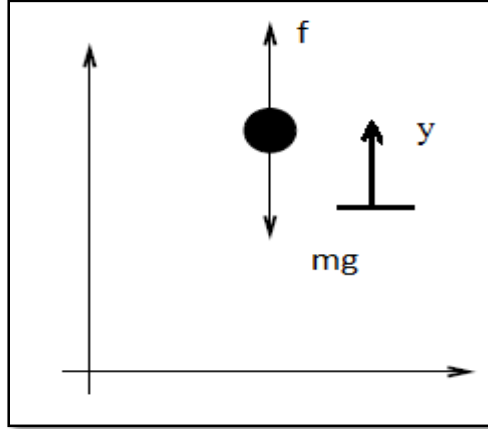


Figure 5.1 The one degree of freedom system [25].

Newton's second law of motion for this system is:

$$m \cdot \ddot{y} = f - mg \quad (5.1)$$

Equation (5.1) can be written as:

$$f = m \cdot \frac{d}{dt}(\dot{y}) + m \cdot g = \frac{d}{dt} \cdot \frac{\partial}{\partial \dot{y}} \left( \frac{1}{2} m \dot{y}^2 \right) + \frac{\partial}{\partial y} (m \cdot g \cdot y) = \frac{d}{dt} \cdot \frac{\partial K}{\partial \dot{y}} - \frac{\partial P}{\partial y}$$

Where, K is the kinematic energy ( $K = \frac{1}{2} m \dot{y}^2$ ), P is the potential energy due to gravity ( $P = mgy$ ).

As mentioned before, The Euler-Lagrange equation (L) can be defined as the difference between the kinematic energy K and the potential energy P.

$$L = K - P = \frac{1}{2} m \dot{y}^2 - mgy$$

$$\frac{\partial L}{\partial \dot{y}} = \frac{\partial K}{\partial \dot{y}} \quad \text{and} \quad \frac{\partial L}{\partial y} = - \frac{\partial P}{\partial y}$$

Therefore, the equation in (5.1) can be written as:

$$\frac{d}{dt} \cdot \frac{\partial L}{\partial \dot{y}} - \frac{\partial L}{\partial y} = f \quad (5.2)$$

Equation (5.2) is called the Euler-Lagrange equation.

## 5.2 Kinematic Energy (K) and Potential Energy (P)

To obtain the Euler-Lagrange equation, there is a need to calculate the kinematic and potential energy for the hand's fingers.

### 5.2.1 The Kinematic Energy (K)

The kinematic energy is the energy that is associated with the motion of the body. It is the work required to move the given mass from rest to stated velocity. There are two types of kinematic energy. First, the translation energy of a moving rigid body which is equal to the product of half of the body's mass by the square of the body's speed. Second, the rotation kinematic energy which depends on the rotation speed of the body about an axis, and it equals the product of half of the body's mass by the square of the rotational speed of the body.

The matrix form of kinematic energy is given by:

$$K = \frac{1}{2} m v^T v + \frac{1}{2} w^T \mathbb{I} w \quad (5.3)$$

Where,  $m$  is the total mass of the object,  $v$  and  $w$  are the linear and angular velocity vectors respectively.  $\mathbb{I}$  is the  $3 \times 3$  symmetric matrix called the inertia tensor. The angular velocity  $w$  can be found from the Skew symmetric matrix as mentioned in chapter four, equation (4.39).

$$S(w) = R' R^T$$

The inertia tensor ( $\mathbb{I}$ ) tells that the angular and linear velocity vectors are stated in an inertial frame. Here,  $R$  in the previous equation (4.39), is the rotation transformation matrix between the frame that attaches to the body and the inertial frame. Therefore, to

determine  $(w^T \mathbf{II} w)$ , the inertia tensor ( $\mathbf{II}$ ) should also show in the inertial frame. By considering that ( $\mathbf{I}$ ) is the inertia tensor with respect to the body frame, then the  $\mathbf{II}$  will be the inertia tensor with respect to frame zero  $\{0\}$ :

$$\mathbf{II} = \mathbf{R} \mathbf{I} \mathbf{R}^T \quad (5.4)$$

This is how to compute the inertia matrix  $\mathbf{II}$ :

The constant inertia matrix ( $\mathbf{II}$ ) does not depend on the object's motion, and it can be found for mass density represented in position  $P(x, y, z)$  by the next expression:

$$\mathbf{II} = \begin{bmatrix} I_{xx} & I_{xy} & I_{xz} \\ I_{yx} & I_{yy} & I_{yz} \\ I_{zx} & I_{zy} & I_{zz} \end{bmatrix} \quad (5.5)$$

Where the components in matrix ( $\mathbf{II}$ ) can be found by the following relations:

$$I_{xx} = \iiint (y^2 + z^2) \cdot P(x, y, z) \, dx \, dy \, dz \quad (5.6)$$

$$I_{yy} = \iiint (x^2 + z^2) \cdot P(x, y, z) \, dx \, dy \, dz \quad (5.7)$$

$$I_{zz} = \iiint (x^2 + y^2) \cdot P(x, y, z) \, dx \, dy \, dz \quad (5.8)$$

$$I_{yx} = I_{xy} = - \iiint xy \cdot P(x, y, z) \, dx \, dy \, dz \quad (5.9)$$

$$I_{zx} = I_{xz} = - \iiint xz \cdot P(x, y, z) \, dx \, dy \, dz \quad (5.10)$$

$$I_{yz} = I_{zy} = - \iiint yz \cdot P(x, y, z) \, dx \, dy \, dz \quad (5.11)$$

The integral limits of the above equations are the dimensions of the link as shown in Figure 5.2 below.

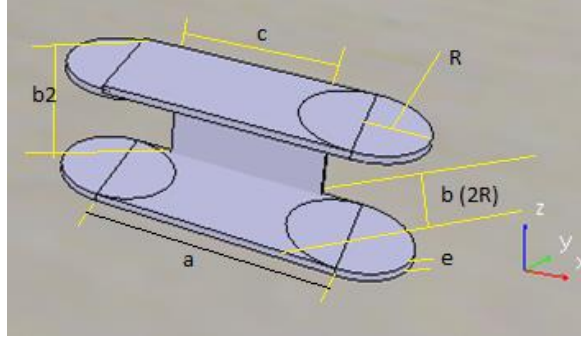


Figure 5.2 The finger's link.

Here,

$$P(x, y, z) = \frac{\text{mass}}{\text{volume}}$$

Now, calculating the inertia tensor matrix elements:

$$I_{xx} = \iiint (y^2 + z^2) \cdot P(x, y, z) dx dy dz$$

$$I_{xx} = [2 * \int_0^a \int_0^b \int_0^e (y^2 + z^2) dx dy dz + 4 * \int_0^R \int_0^R \int_0^e (y^2 + z^2) dx dy dz +$$

$$\int_0^c \int_0^e \int_0^{b/2} (y^2 + z^2) dx dy dz] P(x, y, z)$$

$$= [2 * (\frac{b^3}{3} + \frac{e^3}{3}) a + 4 * (\frac{R^3}{3} + \frac{e^3}{3}) R + (\frac{b^2^3}{3} + \frac{e^3}{3}) c] P(x, y, z) \quad (5.12)$$

$$I_{yy} = \iiint (x^2 + z^2) \cdot P(x, y, z) dx dy dz$$

$$= [2 * \int_0^a \int_0^b \int_0^e (x^2 + z^2) dx dy dz + 4 * \int_0^R \int_0^R \int_0^e (x^2 + z^2) dx dy dz +$$

$$\int_0^c \int_0^e \int_0^{b/2} (x^2 + z^2) dx dy dz] P(x, y, z)$$

$$= [2 * (\frac{a^3}{3} + \frac{e^3}{3}) b + 4 * (\frac{R^3}{3} + \frac{e^3}{3}) R + (\frac{c^3}{3} + \frac{b^2^3}{3}) e] P(x, y, z) \quad (5.13)$$

$$I_{zz} = \iiint (x^2 + y^2) \cdot P(x, y, z) dx dy dz$$

$$\begin{aligned}
&= [2 * \int_0^a \int_0^b \int_0^e (x^2 + y^2) dx dy dz + 4 * \int_0^R \int_0^R \int_0^e (x^2 + y^2) dx dy dz \\
&\quad + \int_0^c \int_0^e \int_0^{b^2} (x^2 + y^2) dx dy dz ] P(x, y, z) \\
&= [2 * (\frac{a^3}{3} + \frac{b^3}{3}) e + 4 * (\frac{R^3}{3} + \frac{R^3}{3}) e + (\frac{c^3}{3} + \frac{b^2^3}{3}) b^2 ] P(x, y, z) \tag{5.14}
\end{aligned}$$

$$\begin{aligned}
I_{yx} = I_{xy} &= - \iiint xy. P(x, y, z) dx dy dz \\
&= - [2 * \int_0^a \int_0^b \int_0^e x. y dx dy dz + 4 * \int_0^R \int_0^R \int_0^e x. y dx dy dz \\
&\quad + \int_0^c \int_0^e \int_0^{b^2} x. y dx dy dz ] P(x, y, z) \\
&= - [(a^2 \frac{b^2}{2}) e + R^4 e + \frac{c^2 e^2}{4} b^2 ] P(x, y, z) \tag{5.15}
\end{aligned}$$

$$\begin{aligned}
I_{zx} = I_{xz} &= - \iiint xz. P(x, y, z) dx dy dz \\
&= - [2 * \int_0^a \int_0^b \int_0^e x. z dx dy dz + 4 * \int_0^R \int_0^R \int_0^e x. z dx dy dz \\
&\quad + \int_0^c \int_0^e \int_0^{b^2} x. z dx dy dz ] P(x, y, z) \\
&= - [(a^2 \frac{e^2}{2}) b + e^2 R^3 + \frac{c^2 b^2^2}{4} e ] P(x, y, z) \tag{5.16}
\end{aligned}$$

$$\begin{aligned}
I_{yz} = I_{zy} &= - \iiint yz. P(x, y, z) dx dy dz \\
&= - [2 * \int_0^a \int_0^b \int_0^e y. z dx dy dz + 4 * \int_0^R \int_0^R \int_0^e y. z dx dy dz \\
&\quad + \int_0^c \int_0^e \int_0^{b^2} y. z dx dy dz ] P(x, y, z) \\
&= - [(b^2 \frac{e^2}{2}) a + e^2 R^3 + \frac{e^2 b^2^2}{4} c ] P(x, y, z) \tag{5.17}
\end{aligned}$$

As mentioned before, there are just three sizes of links. The first link has the following dimensions:  $a = 2$  cm,  $b_2 = 1.4$ cm,  $b = 1.5$ ,  $R = 0.7$  cm,  $c = 1.5$  cm, and  $e = 0.1$  cm. And the mass of this link is 2.3 g.

The second link has the following dimensions:  $a = 2.5$  cm,  $b_2 = 1.5$  cm,  $b = 1.5$ ,  $R = 0.7$  cm,  $c = 2$  cm, and  $e = 0.1$  cm. And the mass of this link is 2.55 g.

Finally, the third link has the following dimensions:  $a = 3.5$  cm,  $b_2 = 1.5$  cm,  $b = 1.5$ ,  $R = 0.7$  cm,  $c = 2$  cm, and  $e = 0.1$  cm. And the mass of this link is 3.52 g.

Now it is possible to calculate the  $I_{ZZ}$  of the inertia tensor matrix for each link in each finger of the design by using equation 5.14 as follows:

$$I_{ZZ}^1 = [2 * (\frac{.02^3}{3} + \frac{.015^3}{3}) .001 + 4 * (\frac{.007^3}{3} + \frac{.007^3}{3}) .001 + (\frac{.015^3}{3} + \frac{.014^3}{3}) .014] \frac{.0023 \text{ kg}}{1.11 * 10^{-6} \text{ m}^3}$$

$$= 7.67 * 10^{-5} \text{ kg.m}$$

$$I_{ZZ}^2 = [2 * (\frac{.025^3}{3} + \frac{.015^3}{3}) .001 + 4 * (\frac{.007^3}{3} + \frac{.007^3}{3}) .001 + (\frac{.02^3}{3} + \frac{.015^3}{3}) .015] \frac{.00255 \text{ kg}}{1.358 * 10^{-6} \text{ m}^3}$$

$$= 1.322 * 10^{-4} \text{ kg.m}$$

$$I_{ZZ}^3 = [2 * (\frac{.035^3}{3} + \frac{.015^3}{3}) .001 + 4 * (\frac{.007^3}{3} + \frac{.007^3}{3}) .001 + (\frac{.02^3}{3} + \frac{.015^3}{3}) .015] \frac{.00352 \text{ kg}}{1.66 * 10^{-6} \text{ m}^3}$$

$$= 1.88 * 10^{-4} \text{ kg.m}$$

Where,  $I_{ZZ}^1$ ,  $I_{ZZ}^2$ , and  $I_{ZZ}^3$  are the inertia tensors about Z axis of link one, link two, and link three respectively.

Now, the kinematic equation will be:

$$K_i = \frac{1}{2} m_i v_i^T v_i + \frac{1}{2} w_i^T I_i w_i$$

$$= \frac{1}{2} m_i (J_{vi}(q)\dot{q})^T J_{vi}(q)\dot{q} + \frac{1}{2} (J_{wi}(q)\dot{q})^T I_i J_{wi}(q)\dot{q}$$

$$= \frac{1}{2} \dot{q}^T [m_i J_{vi}(q)^T J_{vi}(q) + \frac{1}{2} J_{wi}(q)^T I_i J_{wi}(q)] \dot{q}$$

$$= \frac{1}{2} \dot{q}^T [m_i J_{vi}(q)^T J_{vi}(q) + \frac{1}{2} J_{wi}(q)^T R_i(q) I_i R_i^T(q) J_{wi}(q)] \dot{q} \quad (5.18)$$

Let

$$D(q) = \sum_{i=1}^n [m_i J_{vi}(q)^T J_{vi}(q) + J_{wi}(q)^T R_i(q) I_i R_i^T(q) J_{wi}(q)]$$

Therefore, the kinematic energy of an n-link manipulator will be:

$$K = \sum_{i=1}^n k_i = \frac{1}{2} \dot{q}^T D(q) \dot{q} \quad (5.19)$$

### 5.2.2 The Potential Energy (p)

The potential energy P, is the energy which is influenced by a body as a result of its position or some other conditions such as raised weight (gravity), coiled spring, or charged battery (which has the same potential energy as electricity). The potential energy of i-th link in n-link manipulator due to the gravity is given by the following form:

$$P_i = m_i g^T r_{ci} \quad (5.20)$$

Where, g is the gravity vector with respect to the base frame,  $r_{ci}$  is the coordinate of the center of the mass of link i.

Therefore, the potential energy of n-link will be:

$$P = \sum_{i=1}^n p_i = \sum_{i=1}^n m_i g^T r_{ci} \quad (5.21)$$

The equation of motion for the n-link manipulator is:

$$\frac{d}{dt} \left( \frac{\partial L}{\partial \dot{q}_i} \right) - \frac{\partial L}{\partial q_i} = T_i, \quad i=1, 2, 3, \dots, n \quad (5.22)$$

But,

$$L = K - P = \frac{1}{2} \dot{q}^T D(q) \dot{q} - P(q) = \frac{1}{2} \sum_{i,j} d_{i,j}(q) \dot{q}_i \dot{q}_j - P(q)$$

Where,  $d_{i,j}$  is the element of row i and column j of the matrix D (q).

The partial derivative of Lagrangian with respect to joint velocity is:

$$\begin{aligned}\frac{\partial L}{\partial \dot{q}_k} &= \frac{\partial K}{\partial \dot{q}_k} - \frac{\partial P}{\partial \dot{q}_l} = \sum_j d_{kj} \dot{q}_j \\ \frac{d}{dt} \cdot \frac{\partial L}{\partial \dot{q}_k} &= \sum_j d_{k,j} \ddot{q}_j + \sum_j \frac{d}{dt} d_{kj} \dot{q}_j \\ &= \sum_j d_{k,j} \ddot{q}_j + \sum_{i,j} \frac{dd_{kj}}{dq_i} \dot{q}_i \dot{q}_j\end{aligned}$$

$$L = K - P = \frac{1}{2} \dot{q}^T D(q) \dot{q} - P(q) = \frac{1}{2} \sum_{i,j} d_{i,j}(q) \dot{q}_i \dot{q}_j - P(q)$$

The partial derivative of the Lagrangian with respect to the joint velocity is:

$$\frac{\partial L}{\partial \dot{q}_k} = \frac{\partial K}{\partial \dot{q}_k} - \frac{\partial P}{\partial \dot{q}_l} = \frac{1}{2} \sum_{i,j} \frac{\partial d_{i,j}}{\partial q_k} \dot{q}_i \dot{q}_j - \frac{\partial P(q)}{\partial q_k}$$

The Euler-Lagrange equation will be:

$$\frac{d}{dt} \cdot \frac{\partial L}{\partial \dot{q}_k} - \frac{\partial L}{\partial q_k} = T_k, \quad k=1, 2 \dots n \quad (5.23)$$

$$\sum_j d_{kj} \ddot{q}_j + \sum_{i,j} \left\{ \frac{\partial d_{k,j}}{\partial q_i} - \frac{1}{2} \frac{\partial d_{i,j}}{\partial q_k} \right\} \dot{q}_i \dot{q}_j + \frac{\partial P(q)}{\partial q_k} = T_k$$

$$\sum_j d_{kj} \ddot{q}_j + \sum_{i=1}^n \sum_{j=1}^n c_{ijk}(q) \dot{q}_i \dot{q}_j + g_k(q) = T_k$$

$$C_{ijk}(q) = \frac{1}{2} \left\{ \frac{\partial d_{k,j}}{\partial q_i} + \frac{\partial d_{k,i}}{\partial q_j} - \frac{\partial d_{i,j}}{\partial q_k} \right\}$$

$$g_k(q) = \frac{\partial P(q)}{\partial q_k}$$

$$\sum_j d_{kj} \ddot{q}_j + \sum_{i=1}^n \sum_{j=1}^n c_{ijk}(q) \dot{q}_i \dot{q}_j + g_k(q) = T_k$$

In matrix form :

$$D(q) \ddot{q} + C(q, \dot{q}) \dot{q} + g(q) = T \quad (5.24)$$

$$D(q) = \sum_{i=1}^n [m_i J_{vi}(q)^T J_{vi}(q) + J_{wi}(q)^T R_i(q) I_i R_i^T(q) J_{wi}(q)] \quad (5.25)$$

$$C(q, \dot{q}) = [C_{kj}] \text{ where, } C_{kj} = \sum_{i=1}^n C_{ikj}(q) \dot{q}_i = \frac{1}{2} \left\{ \frac{\partial d_{k,j}}{\partial q_i} + \frac{\partial d_{k,i}}{\partial q_j} - \frac{\partial d_{i,j}}{\partial q_k} \right\} \dot{q}_i \quad (5.26)$$



$$g(q) = \left[ \frac{\partial P(q)}{\partial q_1} \quad \frac{\partial P(q)}{\partial q_2} \quad \frac{\partial P(q)}{\partial q_3} \quad \frac{\partial P(q)}{\partial q_n} \right]^T \quad (5.27)$$

Now is the time to calculate  $D(q)$ ,  $C(q, \dot{q})$ , and  $g(q)$  for each finger, by starting with the thumb which has just two links as shown in Figure 5.3 below:

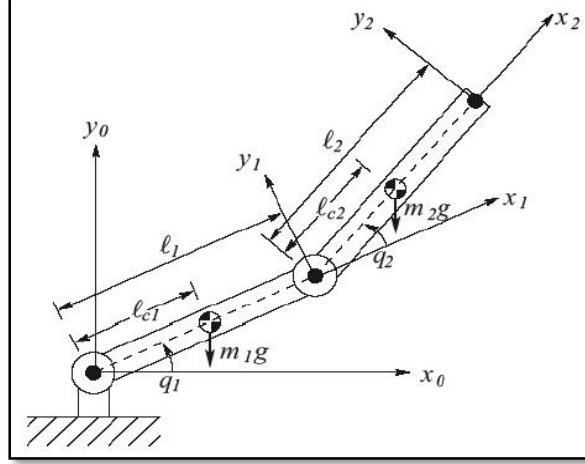


Figure 5.3 The two links manipulator [25].

$$D(q) = \sum_{i=1}^2 \{ m_i j_{vi}(q)^T j_{vi}(q) \} + \sum_{i=1}^2 \{ j_{wi}^T(q) R_i(q) I_i R_i^T(q) j_{wi}(q) \}$$

The above equation consists of two parts, translation and rotation. The translation part is:

$$\sum_{i=1}^2 \{ m_i j_{vi}(q)^T j_{vi}(q) \} = m_1 j_{v1}(q)^T j_{v1}(q) + m_2 j_{v2}(q)^T j_{v2}(q)$$

Where,

$$j_{v1}(q) = \begin{bmatrix} -l_{c1} \sin q_1 & 0 \\ l_{c1} \cos q_1 & 0 \\ 0 & 0 \end{bmatrix}$$

$$j_{v2}(q) = \begin{bmatrix} -l_1 \sin q_1 - l_{c2} \sin(q_1 + q_2) & -l_{c2} \sin(q_1 + q_2) \\ l_1 \cos q_1 + l_{c2} \cos(q_1 + q_2) & l_{c2} \cos(q_1 + q_2) \\ 0 & 0 \end{bmatrix}$$

$$\begin{aligned}
& m_1 j_{v1}(q)^T j_{v1}(q) + m_2 j_{v2}(q)^T j_{v2}(q) = \\
& m_1 \begin{bmatrix} -l_{c1} \sin q1 & 0 \\ l_{c1} \cos q1 & 0 \\ 0 & 0 \end{bmatrix}^T \begin{bmatrix} -l_{c1} \sin q1 & 0 \\ l_{c1} \cos q1 & 0 \\ 0 & 0 \end{bmatrix} + m_2 \\
& \quad \begin{bmatrix} -l_1 \sin q1 - l_{c2} \sin(q1 + q2) & -l_{c2} \sin(q1 + q2) \\ l_1 \cos q1 + l_{c2} \cos(q1 + q2) & l_{c2} \cos(q1 + q2) \\ 0 & 0 \end{bmatrix}^T \\
& \quad \begin{bmatrix} -l_1 \sin q1 - l_{c2} \sin(q1 + q2) & -l_{c2} \sin(q1 + q2) \\ l_1 \cos q1 + l_{c2} \cos(q1 + q2) & l_{c2} \cos(q1 + q2) \\ 0 & 0 \end{bmatrix} \\
& = m_1 \begin{bmatrix} l_{c1}^2 & 0 \\ 0 & 0 \end{bmatrix} + m_2 \begin{bmatrix} l_1^2 + l_{c2}^2 + 2 * l_1 * l_{c2} \cos q2 & l_{c2}^2 + l_1 * l_{c2} * \cos q2 \\ l_{c2}^2 + l_1 * l_{c2} * \cos q2 & l_{c2}^2 \end{bmatrix} \\
& = \begin{bmatrix} m_1 * l_{c1}^2 + m_2(l_1^2 + l_{c2}^2 + 2 * l_1 * l_{c2} \cos q2) & m_2(l_{c2}^2 + l_1 * l_{c2} * \cos q2) \\ m_2(l_{c2}^2 + l_1 * l_{c2} * \cos q2) & m_2 * l_{c2}^2 \end{bmatrix}
\end{aligned}$$

The rotation part of D (q) is given by:

$$\sum_{i=1}^2 \{ j_{wi}^T(q) R_i(q) I_i R_i^T(q) j_{wi}(q) \} = j_{w1}^T(q) R_1(q) I_1 R_1^T(q) j_{w1}(q) + j_{w2}^T(q) R_2(q) I_2 R_2^T(q) j_{w2}(q)$$

Where,

$$j_{w1} = \begin{bmatrix} 0 & 0 \\ 0 & 0 \\ 1 & 0 \end{bmatrix}, j_{w2} = \begin{bmatrix} 0 & 0 \\ 0 & 0 \\ 1 & 1 \end{bmatrix}, \text{ and from equation 5.4 we have } \Pi = R I R^T$$

$$j_{w1}^T(q) R_1(q) I_1 R_1^T(q) j_{w1}(q) + j_{w2}^T(q) R_2(q) I_2 R_2^T(q) = \begin{bmatrix} 0 & 0 & 1 \\ 0 & 0 & 0 \end{bmatrix} I_{zz}^1 \begin{bmatrix} 0 & 0 \\ 0 & 0 \\ 1 & 0 \end{bmatrix} +$$

$$\begin{bmatrix} 0 & 0 & 1 \\ 0 & 0 & 1 \end{bmatrix} I_{zz}^2 \begin{bmatrix} 0 & 0 \\ 0 & 0 \\ 1 & 1 \end{bmatrix}$$

$$= I_{zz}^1 \begin{bmatrix} 1 & 0 \\ 0 & 0 \end{bmatrix} + I_{zz}^2 \begin{bmatrix} 1 & 1 \\ 1 & 1 \end{bmatrix} = \begin{bmatrix} I_{zz}^1 + I_{zz}^2 & I_{zz}^2 \\ I_{zz}^2 & I_{zz}^2 \end{bmatrix}$$

D (q) =

$$\begin{bmatrix} m_1 * l_{c1}^2 + m_2(l_1^2 + l_{c2}^2 + 2 * l_1 * l_{c2} \cos q2) & m_2(l_{c2}^2 + l_1 * l_{c2} * \cos q2) \\ m_2(l_{c2}^2 + l_1 * l_{c2} * \cos q2) & m_2 * l_{c2}^2 \end{bmatrix} +$$

$$\begin{bmatrix} II_{zz}^1 + II_{zz}^2 & II_{zz}^2 \\ II_{zz}^2 & II_{zz}^2 \end{bmatrix}$$

$$D (q) = \begin{bmatrix} d_{11} & d_{12} \\ d_{21} & d_{22} \end{bmatrix}$$

$$d_{11} = m_1 * l_{c1}^2 + m_2(l_1^2 + l_{c2}^2 + 2 * l_1 * l_{c2} \cos q2) + II_{zz}^1 + II_{zz}^2$$

$$d_{12} = d_{21} = m_2(l_{c2}^2 + l_1 * l_{c2} * \cos q2) + II_{zz}^2$$

$$d_{22} = m_2 * l_{c2}^2 + II_{zz}^2$$

By applying the mass values and the length of each link to the D (q) matrix, the matrix elements will be as follow:

$$d_{11} = m_1 * l_{c1}^2 + m_2(l_1^2 + l_{c2}^2 + 2 * l_1 * l_{c2} \cos q2) + II_{zz}^1 + II_{zz}^2$$

$$d_{12} = d_{21} = m_2(l_{c2}^2 + l_1 * l_{c2} * \cos q2) + II_{zz}^2$$

$$d_{22} = m_2 * l_{c2}^2 + II_{zz}^2$$

Where,  $m_1 = 3.5$  g,  $l_1 = .035$  m,  $l_{c1} = 0.0175$  m,  $l_{c2} = .015$  m,  $m_2 = .00255$  g.

$$d_{11} = 2.137 * 10^{-4} + 2.7 * 10^{-6} * \cos q2 \quad (5.28)$$

$$d_{12} = d_{21} = 1.33 * 10^{-4} + 1.34 * 10^{-6} * \cos q2 \quad (5.29)$$

$$d_{22} = 1.33 * 10^{-4} \quad (5.30)$$

Now, calculating the D (q) matrix for the other fingers that have three links:

$$D (q) = \sum_{i=1}^3 \{m_i j_{vi}(q)^T j_{vi}(q)\} + \sum_{i=1}^3 \{j_{wi}^T(q) R_i(q) I_i R_i^T(q) j_{wi}(q)\}$$

First, by starting with the translation part:

$$\sum_{i=1}^3 \{m_i j_{vi}(q)^T j_{vi}(q)\} = m_1 j_{v1}(q)^T j_{v1}(q) + m_2 j_{v2}(q)^T j_{v2}(q) + m_3 j_{v3}(q)^T j_{v3}(q)$$

Where,

$$j_{v1}(q) = \begin{bmatrix} -l_{c1} \sin q1 & 0 & 0 \\ l_{c1} \cos q1 & 0 & 0 \\ 0 & 0 & 0 \end{bmatrix}$$

$$j_{v2}(q) = \begin{bmatrix} -l_1 \sin q1 - l_{c2} \sin(q1 + q2) & -l_{c2} \sin(q1 + q2) & 0 \\ l_1 \cos q1 + l_{c2} \cos(q1 + q2) & l_{c2} \cos(q1 + q2) & 0 \\ 0 & 0 & 0 \end{bmatrix}$$

$$j_{v3}(q) =$$

$$\begin{bmatrix} -l_1 \sin q1 - l_2 \sin(q1 + q2) - l_{c3} \sin(q1 + q2 + q3) & -l_2 \sin(q1 + q2) - l_{c3} \sin(q1 + q2 + q3) & -l_{c3} \sin(q1 + q2 + q3) \\ l_1 \cos q1 + l_2 \cos(q1 + q2) + l_{c3} \cos(q1 + q2 + q3) & l_2 \cos(q1 + q2) + l_{c3} \cos(q1 + q2 + q3) & l_{c3} \cos(q1 + q2 + q3) \\ 0 & 0 & 0 \end{bmatrix}$$

The rotation part is given by

$$= II_{ZZ}^1 \begin{bmatrix} 1 & 0 & 0 \\ 0 & 0 & 0 \\ 0 & 0 & 0 \end{bmatrix} + II_{ZZ}^2 \begin{bmatrix} 1 & 1 & 0 \\ 1 & 1 & 0 \\ 0 & 0 & 0 \end{bmatrix} + II_{ZZ}^3 \begin{bmatrix} 1 & 1 & 1 \\ 1 & 1 & 1 \\ 1 & 1 & 1 \end{bmatrix}$$

$$D(q) = \begin{bmatrix} d_{11} & d_{12} & d_{13} \\ d_{21} & d_{22} & d_{23} \\ d_{31} & d_{32} & d_{33} \end{bmatrix}$$

$$d_{11} = m_1 l_{c1}^2 + m_2 (l_1^2 + l_{c2}^2 + 2 l_1 l_{c2} \cos q_2) + m_3 ((l_1 + l_2)^2 + l_{c3}^2 + 2 (l_1 + l_2) l_{c3} \cos q_3) + II_{ZZ}^1 + II_{ZZ}^2 + II_{ZZ}^3$$

$$d_{12} = d_{21} = m_2 (l_{c2}^2 + 2 l_1 l_{c2} \cos q_2) + m_3 (l_2^2 + l_{c3}^2 + l_1 l_2 \cos q_2 + l_1 l_{c3} \cos(q_2 + q_3) + 2 l_2 l_{c3} \cos(q_3)) + II_{ZZ}^2 + II_{ZZ}^3$$

$$d_{13} = d_{31} = m_3 (l_{c3}^2 + l_1 l_{c3} \cos(q_2 + q_3) + l_2 l_{c3} \cos q_3) + II_{ZZ}^3$$

$$d_{22} = m_2 l_{c2}^2 + m_3 (l_{c3}^2 + l_2^2 + 2 l_2 l_{c3} \cos q_3) + II_{ZZ}^2 + II_{ZZ}^3$$

$$d_{23} = d_{32} = m_3 (l_{c3}^2 + l_2 l_{c3} \cos q_3) + II_{ZZ}^3$$

$$d_{33} = m_3 l_{c3}^2 + II_{ZZ}^3$$

Where,  $l_{ci}$  is the distance from the joint i-1 to the mass center of the link i.

Calculating the g (q) matrix:

The gravity matrix of the three links finger and thumb are given by:

$$\mathbf{g}(\mathbf{q}) = \left[ \frac{\partial P(\mathbf{q})}{\partial q_1} \quad \frac{\partial P(\mathbf{q})}{\partial q_2} \quad \frac{\partial P(\mathbf{q})}{\partial q_3} \right]^T \text{ for the three links fingers.}$$

$$\mathbf{g}(\mathbf{q}) = \left[ \frac{\partial P(\mathbf{q})}{\partial q_1} \quad \frac{\partial P(\mathbf{q})}{\partial q_2} \right]^T \text{ for the thumb:}$$

$$P = P_1 + P_2 + P_3 \quad (5.31)$$

$$P_1 = m_1 g l_{c1} \sin q_1 \quad (5.32)$$

$$P_2 = m_2 g (l_1 \sin q_1 + l_{c2} \sin(q_1 + q_2)) \quad (5.33)$$

$$P_3 = m_3 g (l_1 \sin q_1 + l_2 \sin(q_1 + q_2) + l_{c3} \sin (q_1 + q_2 + q_3)) \quad (5.34)$$

From equations 5.32, 5.33, and 5.34, the equation of P(q) for the three links fingers will be:

$$P(\mathbf{q}) = m_1 g l_{c1} \sin q_1 + m_2 g (l_1 \sin q_1 + l_{c2} \sin(q_1 + q_2)) + m_3 g (l_1 \sin q_1 + l_2 \sin(q_1 + q_2) + l_{c3} \sin (q_1 + q_2 + q_3))$$

And for the thumb will be:

$$P(\mathbf{q}) = m_1 g l_{c1} \sin q_1 + m_2 g (l_1 \sin q_1 + l_{c2} \sin(q_1 + q_2))$$

Now, we can calculate each element in g (q) matrix for the thumb:

$$\frac{\partial P(\mathbf{q})}{\partial q_1} = m_1 g l_{c1} \cos q_1 + m_2 g (l_1 \cos q_1 + l_{c2} \cos (q_1 + q_2))$$

$$\frac{\partial P(\mathbf{q})}{\partial q_2} = m_2 g l_{c2} \cos (q_1 + q_2)$$

$$\mathbf{g}(\mathbf{q}) = \begin{bmatrix} m_1 g l_{c1} \cos q_1 + m_2 g (l_1 \cos q_1 + l_{c2} \cos (q_1 + q_2)) \\ m_2 g l_{c2} \cos (q_1 + q_2) \end{bmatrix}$$

For the other three links fingers, we have:

$$\frac{\partial P(\mathbf{q})}{\partial q_1} = m_1 g l_{c1} \cos q_1 + m_2 g (l_1 \cos q_1 + l_{c2} \cos (q_1 + q_2)) + m_3 g (l_1 \cos q_1 + l_2 \cos (q_1 + q_2) + l_{c3} \cos (q_1 + q_2 + q_3))$$

$$\frac{\partial P(q)}{\partial q_2} = m_2 g l_{c2} \cos (q_1 + q_2) + m_3 g (l_2 \cos (q_1 + q_2) + l_{c3} \cos (q_1 + q_2 + q_3))$$

$$\frac{\partial P(q)}{\partial q_3} = m_3 g l_{c3} \cos (q_1 + q_2 + q_3)$$

$$g(q) =$$

$$\left[ \begin{array}{c} m_1 g l_{c1} \cos q_1 + m_2 g (l_1 \cos q_1 + l_{c2} \cos (q_1 + q_2)) + m_3 g (l_1 \cos q_1 + l_2 \cos (q_1 + q_2) + l_{c3} \cos (q_1 + q_2 + q_3)) \\ m_2 g l_{c2} \cos (q_1 + q_2) + m_3 g (l_2 \cos (q_1 + q_2) + l_{c3} \cos (q_1 + q_2 + q_3)) \\ m_3 g l_{c3} \cos (q_1 + q_2 + q_3) \end{array} \right]$$

Next, we will calculate the matrix C (q) as follow:

First, starting with the thumb C (q,  $\dot{q}$ ) = [C<sub>kj</sub>]:

$$\begin{aligned} C_{kj} &= \sum_{i=1}^2 c_{ijk}(q) \dot{q}_i \\ &= \sum_{i=1}^2 \frac{1}{2} \left\{ \frac{\partial d_{k,j}}{\partial q_i} + \frac{\partial d_{k,i}}{\partial q_j} - \frac{\partial d_{i,j}}{\partial q_k} \right\} \dot{q}_i \\ C_{11} &= \sum_{i=1}^2 c_{i11} \dot{q}_i = c_{111} \dot{q}_1 + c_{211} \dot{q}_2 \end{aligned} \quad (5.35)$$

$$C_{111} = \frac{1}{2} \left\{ \frac{\partial d_{11}}{\partial q_1} + \frac{\partial d_{11}}{\partial q_1} - \frac{\partial d_{11}}{\partial q_1} \right\} = 0 \quad (5.36)$$

$$C_{211} = \frac{1}{2} \left\{ \frac{\partial d_{11}}{\partial q_2} + \frac{\partial d_{12}}{\partial q_2} - \frac{\partial d_{21}}{\partial q_1} \right\} = -m_2 l_1 l_{c2} \sin q_2 \quad (5.37)$$

By substituting equations 5.35 and 5.36 in equation 5.37, we can find C<sub>11</sub>:

$$C_{11} = -m_2 l_1 l_{c2} \sin q_2 \dot{q}_2$$

Calculating C<sub>21</sub>:

$$C_{21} = \sum_{i=1}^2 c_{i12}(q) \dot{q}_i = c_{112} \dot{q}_1 + c_{212} \dot{q}_2 \quad (5.38)$$

$$C_{112} = \frac{1}{2} \left\{ \frac{\partial d_{21}}{\partial q_1} + \frac{\partial d_{21}}{\partial q_1} - \frac{\partial d_{11}}{\partial q_2} \right\} = m_2 l_1 l_{c2} \sin q_2 \quad (5.39)$$

$$C_{212} = \frac{1}{2} \left\{ \frac{\partial d_{21}}{\partial q_2} + \frac{\partial d_{22}}{\partial q_1} - \frac{\partial d_{21}}{\partial q_2} \right\} = 0 \quad (5.40)$$

From equations (5.38), (5.39), and (5.40), C<sub>12</sub> will be:

$$C_{21} = m_2 l_2 l_{c2} \sin q_2 \dot{q}_1$$

Calculating  $C_{12}$ :

$$C_{12} = \sum_{i=1}^2 c_{i21}(q) \dot{q}_i = c_{121} \dot{q}_1 + c_{221} \dot{q}_2 \quad (5.41)$$

$$C_{121} = \frac{1}{2} \left\{ \frac{\partial d_{12}}{\partial q_1} + \frac{\partial d_{11}}{\partial q_2} - \frac{\partial d_{12}}{\partial q_1} \right\} = -m_2 l_1 l_{c2} \sin q_2 \quad (5.42)$$

$$C_{221} = \frac{1}{2} \left\{ \frac{\partial d_{12}}{\partial q_2} + \frac{\partial d_{12}}{\partial q_2} - \frac{\partial d_{22}}{\partial q_1} \right\} = -m_2 l_1 l_{c2} \sin q_2 \quad (5.43)$$

$$\begin{aligned} C_{12} &= c_{121} \dot{q}_1 + c_{221} \dot{q}_2 \\ &= -m_2 l_1 l_{c2} \sin q_2 (\dot{q}_1 + \dot{q}_2) \end{aligned}$$

Calculating  $C_{22}$ :

$$C_{22} = \sum_{i=1}^2 c_{i22}(q) \dot{q}_i = c_{122} \dot{q}_1 + c_{222} \dot{q}_2 \quad (5.41)$$

$$C_{122} = \frac{1}{2} \left\{ \frac{\partial d_{22}}{\partial q_1} + \frac{\partial d_{21}}{\partial q_2} - \frac{\partial d_{12}}{\partial q_2} \right\} = 0 \quad (5.42)$$

$$C_{222} = \frac{1}{2} \left\{ \frac{\partial d_{22}}{\partial q_2} + \frac{\partial d_{22}}{\partial q_2} - \frac{\partial d_{22}}{\partial q_2} \right\} = 0 \quad (5.43)$$

$$\begin{aligned} C_{22} &= c_{122} \dot{q}_1 + c_{222} \dot{q}_2 \\ &= 0 \end{aligned}$$

The  $C(q, \dot{q})$  matrix of the thumb will be:

$$C(q, \dot{q}) = \begin{bmatrix} -m_2 l_1 l_{c2} \sin q_2 & \dot{q}_2 & -m_2 l_1 l_{c2} \sin q_2 (\dot{q}_1 + \dot{q}_2) \\ m_2 l_2 l_{c2} \sin q_2 & \dot{q}_1 & 0 \end{bmatrix}$$

Now, we will calculate  $C(q, \dot{q})$  for the three links fingers:

$$C(q, \dot{q}) = \sum_{i=1}^3 \frac{1}{2} \left\{ \frac{\partial d_{kj}}{\partial q_i} + \frac{\partial d_{ki}}{\partial q_j} - \frac{\partial d_{ij}}{\partial q_k} \right\} \dot{q}_i$$

$$C_{11} = \sum_{i=1}^3 c_{i11} \dot{q}_i = c_{111} \dot{q}_1 + c_{211} \dot{q}_2 + c_{311} \dot{q}_3$$

$$C_{111} = \frac{1}{2} \left\{ \frac{\partial d_{11}}{\partial q_1} + \frac{\partial d_{11}}{\partial q_1} - \frac{\partial d_{11}}{\partial q_1} \right\} = 0 \quad (5.44)$$

$$C_{211} = \frac{1}{2} \left\{ \frac{\partial d_{11}}{\partial q_2} + \frac{\partial d_{12}}{\partial q_1} - \frac{\partial d_{21}}{\partial q_1} \right\} = -m_2 l_1 l_{c2} \sin q_2 \quad (5.45)$$

$$C_{311} = \frac{1}{2} \left\{ \frac{\partial d_{11}}{\partial q_3} + \frac{\partial d_{13}}{\partial q_1} - \frac{\partial d_{31}}{\partial q_1} \right\} = -m_3 (l_1 + l_2) l_{c3} \sin q_3 \quad (5.46)$$

From equations (5.44), (5.45), and (5.46),  $C_{11}$  will be:

$$C_{11} = c_{111} \dot{q}_1 + c_{211} \dot{q}_2 + c_{311} \dot{q}_3 = -m_2 l_1 l_{c2} \sin q_2 \dot{q}_2 - m_3 (l_1 + l_2) l_{c3} \sin q_3 \dot{q}_3$$

Calculating  $C_{21}$ :

$$C_{21} = \sum_{i=1}^3 c_{i12}(q) \dot{q}_i = c_{112} \dot{q}_1 + c_{212} \dot{q}_2 + c_{312} \dot{q}_3$$

$$C_{112} = \frac{1}{2} \left\{ \frac{\partial d_{21}}{\partial q_1} + \frac{\partial d_{21}}{\partial q_1} - \frac{\partial d_{11}}{\partial q_2} \right\} = m_2 l_1 l_{c2} \sin q_2 \quad (5.47)$$

$$C_{212} = \frac{1}{2} \left\{ \frac{\partial d_{21}}{\partial q_2} + \frac{\partial d_{22}}{\partial q_1} - \frac{\partial d_{21}}{\partial q_2} \right\} = 0 \quad (5.48)$$

$$C_{312} = \frac{1}{2} \left\{ \frac{\partial d_{21}}{\partial q_3} + \frac{\partial d_{23}}{\partial q_1} - \frac{\partial d_{31}}{\partial q_2} \right\} = -l_2 l_{c3} \sin q_3 \quad (5.49)$$

From equations (5.47), (5.48), and (5.49),  $C_{12}$  will be:

$$C_{21} = c_{112} \dot{q}_1 + c_{212} \dot{q}_2 + c_{312} \dot{q}_3 = m_2 l_1 l_{c2} \sin q_2 \dot{q}_1 - l_2 l_{c3} \sin q_3 \dot{q}_3$$

Calculating  $C_{12}$ :

$$C_{12} = \sum_{i=1}^3 c_{i21}(q) \dot{q}_i = c_{121} \dot{q}_1 + c_{221} \dot{q}_2 + c_{321} \dot{q}_3$$

$$c_{121} = \frac{1}{2} \left\{ \frac{\partial d_{12}}{\partial q_1} + \frac{\partial d_{11}}{\partial q_2} - \frac{\partial d_{12}}{\partial q_1} \right\} = -m_2 l_1 l_{c2} \sin q_2$$

$$c_{221} = \frac{1}{2} \left\{ \frac{\partial d_{12}}{\partial q_2} + \frac{\partial d_{12}}{\partial q_2} - \frac{\partial d_{22}}{\partial q_1} \right\} = -2 m_2 l_1 l_{c2} \sin q_2 - m_3 l_1 l_2 \sin q_2 - m_3 l_1 l_{c3} \sin(q_2 + q_3)$$

$$c_{321} = \frac{1}{2} \left\{ \frac{\partial d_{12}}{\partial q_3} + \frac{\partial d_{13}}{\partial q_2} - \frac{\partial d_{32}}{\partial q_1} \right\} = -0.5 m_3 l_1 l_{c3} \sin(q_2 + q_3) - m_3 l_2 l_{c3} \sin q_3 -$$

$$0.5 m_3 l_1 l_{c3} \sin(q_2 + q_3)$$

$$C_{12} = c_{121} \dot{q}_1 + c_{221} \dot{q}_2 + c_{321} \dot{q}_3$$

$$= -m_2 l_1 l_{c2} \sin q_2 \dot{q}_1 - 2 m_2 l_1 l_{c2} \sin q_2 \dot{q}_2 - m_3 l_1 l_2 \sin q_2 \dot{q}_2 - m_3 l_1 l_{c3} \sin(q_2 + q_3) \dot{q}_2 - 0.5 m_3 l_1 l_{c3} \sin(q_2 + q_3) \dot{q}_3 - m_3 l_2 l_{c3} \sin q_3 \dot{q}_3 - 0.5 m_3 l_1 l_{c3} \sin(q_2 + q_3) \dot{q}_3$$



Calculating  $C_{22}$ :

$$C_{22} = \sum_{i=1}^3 c_{i22}(q)\dot{q}_i = c_{122} \dot{q}_1 + c_{222} \dot{q}_2 + c_{322} \dot{q}_3$$

$$C_{122} = \frac{1}{2} \left\{ \frac{\partial d_{22}}{\partial q_1} + \frac{\partial d_{21}}{\partial q_2} - \frac{\partial d_{12}}{\partial q_2} \right\} = 0$$

$$C_{222} = \frac{1}{2} \left\{ \frac{\partial d_{22}}{\partial q_2} + \frac{\partial d_{22}}{\partial q_2} - \frac{\partial d_{22}}{\partial q_2} \right\} = 0$$

$$C_{322} = \frac{1}{2} \left\{ \frac{\partial d_{22}}{\partial q_3} + \frac{\partial d_{23}}{\partial q_2} - \frac{\partial d_{32}}{\partial q_2} \right\} = -m_3 l_2 l_{c3} \sin q_3$$

$$C_{22} = c_{122} \dot{q}_1 + c_{222} \dot{q}_2 + c_{322} \dot{q}_3$$

$$= -m_3 l_2 l_{c3} \sin q_3 \dot{q}_3$$

Calculating  $C_{13}$ :

$$C_{31} = \sum_{i=1}^3 c_{i31}(q)\dot{q}_i = c_{131} \dot{q}_1 + c_{231} \dot{q}_2 + c_{331} \dot{q}_3$$

$$C_{131} = \frac{1}{2} \left\{ \frac{\partial d_{13}}{\partial q_1} + \frac{\partial d_{11}}{\partial q_3} - \frac{\partial d_{13}}{\partial q_1} \right\} = -m_3 (l_1 + l_2) l_{c3} \sin q_3$$

$$C_{231} = \frac{1}{2} \left\{ \frac{\partial d_{13}}{\partial q_2} + \frac{\partial d_{12}}{\partial q_3} - \frac{\partial d_{23}}{\partial q_1} \right\} = -m_3 l_1 l_{c3} \sin(q_2 + q_3) - m_3 l_2 l_{c3} \sin q_3$$

$$C_{331} = \frac{1}{2} \left\{ \frac{\partial d_{13}}{\partial q_3} + \frac{\partial d_{13}}{\partial q_3} - \frac{\partial d_{33}}{\partial q_1} \right\} = -m_3 l_1 l_{c3} \sin(q_2 + q_3) - m_3 l_2 l_{c3} \sin q_3$$

$$C_{13} = c_{131} \dot{q}_1 + c_{231} \dot{q}_2 + c_{331} \dot{q}_3$$

$$= -m_3 (l_1 + l_2) l_{c3} \sin q_3 \dot{q}_1 - (m_3 l_1 l_{c3} \sin(q_2 + q_3) + m_3 l_2 l_{c3} \sin q_3) \dot{q}_2$$

$$- (m_3 l_1 l_{c3} \sin(q_2 + q_3) + m_3 l_2 l_{c3} \sin q_3) \dot{q}_3$$

Calculating  $C_{31}$ :

$$C_{13} = \sum_{i=1}^3 c_{i13}(q)\dot{q}_i = c_{113} \dot{q}_1 + c_{213} \dot{q}_2 + c_{313} \dot{q}_3$$

$$C_{113} = \frac{1}{2} \left\{ \frac{\partial d_{31}}{\partial q_1} + \frac{\partial d_{31}}{\partial q_1} - \frac{\partial d_{11}}{\partial q_3} \right\} = m_3 (l_1 + l_2) l_{c3} \sin q_3$$

$$C_{213} = \frac{1}{2} \left\{ \frac{\partial d_{31}}{\partial q_2} + \frac{\partial d_{32}}{\partial q_1} - \frac{\partial d_{21}}{\partial q_3} \right\} = -0.5 m_3 l_1 l_{c3} \sin(q_2 + q_3) + 0.5 m_3 l_1 l_{c3} \sin(q_2 + q_3) +$$

$$m_3 l_2 l_{c3} \sin q_3$$

$$C_{313} = \frac{1}{2} \left\{ \frac{\partial d_{31}}{\partial q_3} + \frac{\partial d_{33}}{\partial q_1} - \frac{\partial d_{31}}{\partial q_3} \right\} = 0$$

$$C_{31} = c_{113} \dot{q}_1 + c_{213} \dot{q}_2 + c_{313} \dot{q}_3$$

$$= m_3 (l_1 + l_2) l_{c3} \sin q_3 \dot{q}_1 - (0.5 m_3 l_1 l_{c3} \sin(q_2 + q_3) - 0.5 m_3 l_1 l_{c3} \sin(q_2 + q_3) + m_3 l_2 l_{c3} \sin q_3) \dot{q}_2$$

Calculating  $C_{32}$ :

$$C_{32} = \sum_{i=1}^3 c_{i23}(q) \dot{q}_i = c_{123} \dot{q}_1 + c_{223} \dot{q}_2 + c_{323} \dot{q}_3$$

$$C_{123} = \frac{1}{2} \left\{ \frac{\partial d_{32}}{\partial q_1} + \frac{\partial d_{31}}{\partial q_2} - \frac{\partial d_{12}}{\partial q_3} \right\} = -0.5 m_3 l_1 l_{c3} \sin(q_2 + q_3) + 0.5 m_3 l_1 l_{c3} \sin(q_2 + q_3) +$$

$$m_3 l_2 l_{c3} \sin q_3$$

$$C_{223} = \frac{1}{2} \left\{ \frac{\partial d_{32}}{\partial q_2} + \frac{\partial d_{32}}{\partial q_2} - \frac{\partial d_{22}}{\partial q_3} \right\} = m_3 l_2 l_{c3} \sin q_3$$

$$C_{323} = \frac{1}{2} \left\{ \frac{\partial d_{32}}{\partial q_3} + \frac{\partial d_{33}}{\partial q_2} - \frac{\partial d_{32}}{\partial q_3} \right\} = 0$$

$$C_{32} = c_{123} \dot{q}_1 + c_{223} \dot{q}_2 + c_{323} \dot{q}_3$$

$$C_{32} = (-0.5 m_3 l_1 l_{c3} \sin(q_2 + q_3) + 0.5 m_3 l_1 l_{c3} \sin(q_2 + q_3) + m_3 l_2 l_{c3} \sin q_3) \dot{q}_1 + m_3 l_2 l_{c3} \sin q_3 \dot{q}_2$$

Calculating  $C_{23}$ :

$$C_{23} = \sum_{i=1}^3 c_{i32}(q) \dot{q}_i = c_{132} \dot{q}_1 + c_{232} \dot{q}_2 + c_{332} \dot{q}_3$$

$$C_{132} = \frac{1}{2} \left\{ \frac{\partial d_{23}}{\partial q_1} + \frac{\partial d_{21}}{\partial q_3} - \frac{\partial d_{13}}{\partial q_2} \right\} = 0.5 m_3 l_1 l_{c3} \sin(q_2 + q_3) + m_3 l_2 l_{c3} \sin q_3 +$$

$$0.5 m_3 l_1 l_{c3} \sin(q_2 + q_3)$$

$$C_{232} = \frac{1}{2} \left\{ \frac{\partial d_{23}}{\partial q_2} + \frac{\partial d_{22}}{\partial q_3} - \frac{\partial d_{23}}{\partial q_2} \right\} = -m_3 l_2 l_{c3} \sin q_3$$

$$C_{332} = \frac{1}{2} \left\{ \frac{\partial d_{23}}{\partial q_3} + \frac{\partial d_{23}}{\partial q_3} - \frac{\partial d_{33}}{\partial q_2} \right\} = -m_3 l_2 l_{c3} \sin q_3$$

$$C_{23} = c_{132} \dot{q}_1 + c_{232} \dot{q}_2 + c_{332} \dot{q}_3$$

$$= (0.5 m_3 l_1 l_{c3} \sin(q_2 + q_3) + m_3 l_2 l_{c3} \sin q_3 + 0.5 m_3 l_1 l_{c3} \sin(q_2 + q_3))$$

$$\dot{q}_1 - m_3 l_2 l_{c3} \sin q_3 \dot{q}_2 - m_3 l_2 l_{c3} \sin q_3 \dot{q}_3$$

Calculating  $C_{33}$ :

$$C_{33} = \sum_{i=1}^3 c_{i33}(q) \dot{q}_i = c_{133} \dot{q}_1 + c_{233} \dot{q}_2 + c_{333} \dot{q}_3$$

$$C_{133} = \frac{1}{2} \left\{ \frac{\partial d_{33}}{\partial q_1} + \frac{\partial d_{31}}{\partial q_3} - \frac{\partial d_{13}}{\partial q_3} \right\} = 0$$

$$C_{233} = \frac{1}{2} \left\{ \frac{\partial d_{33}}{\partial q_2} + \frac{\partial d_{32}}{\partial q_3} - \frac{\partial d_{23}}{\partial q_3} \right\} = 0$$

$$C_{333} = \frac{1}{2} \left\{ \frac{\partial d_{33}}{\partial q_3} + \frac{\partial d_{33}}{\partial q_3} - \frac{\partial d_{33}}{\partial q_3} \right\} = 0$$

$$C_{33} = c_{133} \dot{q}_1 + c_{233} \dot{q}_2 + c_{333} \dot{q}_3$$

$$C_{33} = 0$$

## **Chapter 6 : EMG Signal Processing**

### **6.1 Introduction**

This chapter discusses the mechanism of the muscle contractions and how to sense these activities. An explanation will be given for the way to process the signals that have been detected from the muscle to be readable by the controller, and finally, this chapter will show how to control the design and how to create an action dependent upon the incoming signal. There are three types of muscles in human bodies; skeletal muscles, which are connected to the skeleton and are responsible for body motions; smooth muscles, which are found in the walls of the human body's visceral organs except for the heart; and cardiac muscles, which are found in the heart's walls and are responsible for the heart's activities. This chapter focuses on the skeletal muscles which are responsible for human activities.

### **6.2 EMG and the Muscle Contraction**

Electromyography (EMG) is an experimental technique used to study and analyze the activity of the muscles by measuring the physiological variations in the muscle's fibers. The EMG technique can measure the muscle's activities, such as flexing and contracting, caused by an electrical signal that comes from neurons in the body which cause these physiological variations. There is a small functional unit called the motor unit, as shown in Figure 6.1 below, which is responsible for delivering the neuron signal to the muscle's fibers. When the electrical signal comes from the neuron to the muscle, an ionic change

will happen between the inside and outside of a muscle cell and a small potential difference will generate between muscle fibers. This potential will release Acetylcholine at the synaptic cleft. The synaptic cleft is the part of the neuron that translates the electrical signal into chemical action. This chemical action will affect the body like an ion pump of potassium and sodium ions which causes the depolarization and re-polarization processes.

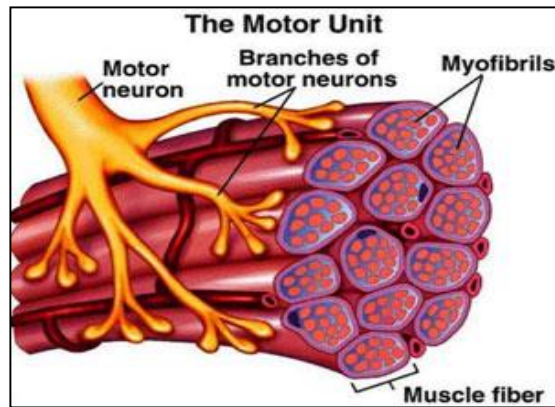


Figure 6.1 Motor unit [26].

The outside of the muscle cell, when the muscle is in a rest situation, is highly saturated with the positive ions of sodium (+Na), and the potassium ions (+K). They are concentrated inside the muscle cell [27] as shown in Figure 6.2 a. During the depolarization process, the ion sodium pump will open as the effect of the neuron electrical signal, and it will pump sodium ions to the inside of the muscle cell as shown in Figure 6.2 b. Because of the many positive sodium ions (+Na) that entered into the cell, the inside of the cell will become positive and the membrane potential will become +30m to +40mv in about one millisecond. At this point the sodium channels will close and sodium ions cannot enter the cell again. In the period of repolarization, as shown in Figure 6.2 c, the opposite operation will occur. Whereas, the potassium ions will move into the cell, and the sodium ions will

go out of the cell, and that will decrease the potential difference to be -80 mv. The high percentage of sodium ions inside the cell will close the sodium pump, and it will encourage the potassium pump to open and allow the potassium ions to go out of the muscle's cell.

In order to get the rest situation of the muscle, the ATP-ase gate (+K /+Na pump) will move three positive sodium ions (+Na) from the inside of the cell to the outside for each pair of potassium ions (+K), getting into the cell as shown in Figure 6.2 d. Both the depolarization and repolarization will form a wave which moves along the surface of the muscle's fibers. There are two ways to measure this wave, either by the needle EMG, using surgery or surface EMG using surface electrodes. With surface EMG there is a need to use three surface electrodes. The first electrode will connect on the middle of the muscle, the second one will be at the end of the muscle, and the third one will be connected close to the bone as a ground.

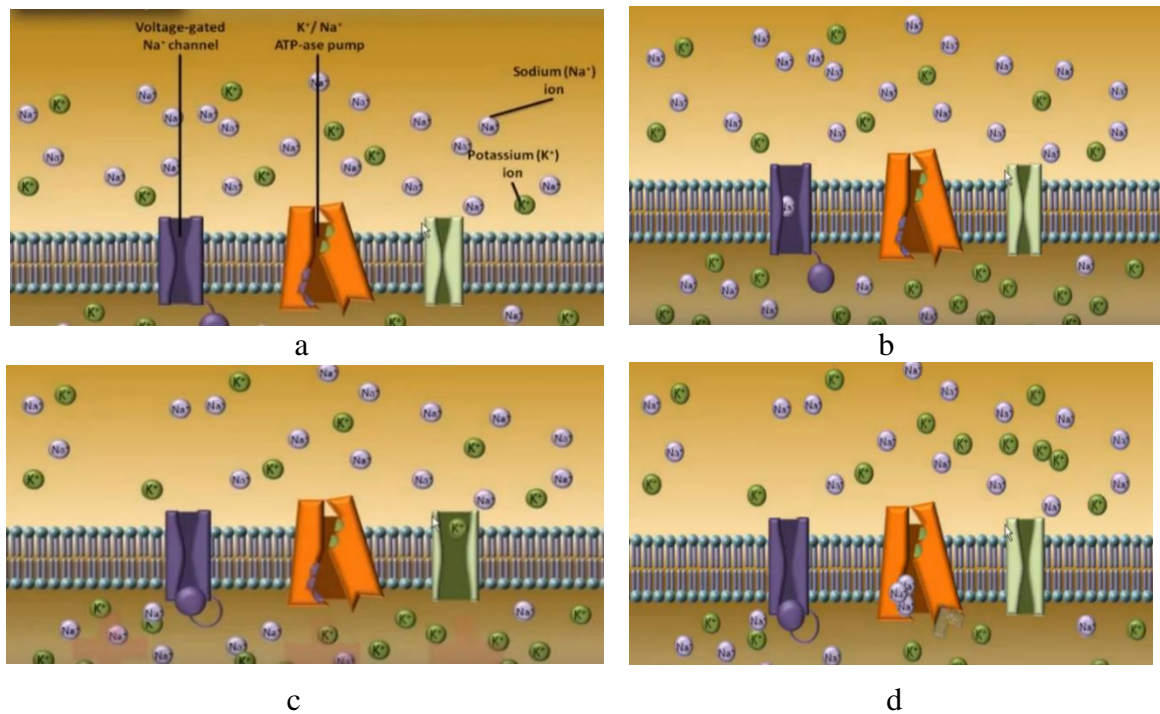


Figure 6.2 a, b, c, and d: Shows the mechanism of the muscle [28].

### 6.3 Surface EMG

Getting an EMG signal from the muscle is not an easy process, because this process needs to use effective ways to detect, decompose, and process the EMG signal. The EMG signal detects the current activity of muscles (contraction/relaxation) which is caused by electricity signals. This comes from the nerves that are connected to these muscles, and it can read from more than one muscle at the same time with a lot of noise signals. There are two ways in which to measure the EMG signal, either by the invasive EMG (needle EMG) as shown in Figure 6.3-a, which needs some surgical processes to connect the needle to the muscle in which we want to measure the activity.

The second method to measure the EMG signal is the non-invasive EMG or surface EMG as shown in Figure 6.3-b. This method needs to use electrodes on the skin that covers the muscle to measure its activity. After getting the EMG signal, this signal will pass through some stages beginning with differential amplifier, the low pass filter, the high pass filter, and the amplifier stage. Much research has been done to improve the EMG signal measurements, so that they will be more effective in many applications such as medical, sports, and human-machines devices. One of the biggest challenges facing how to improve the EMG signal acquisition, is how to remove the noise signals.



Figure 6.3 (a) Is invasive electrode [29], [30] and (b) is non-invasive electrode [31].

#### **6.4 Noise in the EMG Signal**

There are several types of noise that can affect the surface EMG detecting and processing operations. One of these noise is the motion artifact noise, which is either caused by a bad connection between the electrode and the skin, or because of the movement of the connections cables between the electrodes and the rest of the circuit. To avoid this kind of noise, the skin should be prepared well, and the amputee should be sure that the electrodes are fixed on the skin. Also, the cables between the electrodes and the rest of the circuit should be as short as possible. This is what is known as the active electrode.

Furthermore, there is ambient noise which is caused by electromagnetic radiations which come from the surrounding devices such as electrical power wires, radio waves, television, light bulbs... etc. This kind of noise can be limited by choosing appropriate kinds of filters. There are noises that result from the electronic components that have been used in detection or processing the EMG signal. Power line radiation (50 HZ or 60 HZ) has an effect on the measured EMG signal. Some of the designs use notch filters to remove these noise, but notch filters are not recommended with the EMG. The dominant energy of the EMG signal is limited between the 50 to 150 HZ range, and using notch filters to remove 50 to 60 HZ from the received signal will hide most of the important muscle activities. The last two types of noise can be reduced by twisting the cables that connect the electrodes to the circuit as shown in Figure 3.1b. By twisting the two cables into many small areas instead of one big area, the electromagnetic field that is generated by one area will cancel the electromagnetic field that formed in the next area, and the total electromagnetic field will decrease.



## 6.5 EMG Signal Detecting and Processing

With surface EMG, two electrodes should be used for each single muscle, and at least one electrode will be common between all muscles as shown in Figure 6.4 below. The first electrode (electrode one), should be connected to the middle of the muscle. Electrode two should be connected to the end of the muscle, and the last electrode will connect close to the bone as a ground (the ground could be common between many muscles). The reason for using two electrodes for the muscle is to remove some of the noise signals. The differential amplifier will be used to subtract the signal that comes from electrode two from the signal which comes from electrode one to enhance the overall signal. Let  $(S_1 + n)$  be the signal coming from electrode one.  $(S_2 + n)$  is the signal coming from electrode two, where  $n$  represents some of the similar noise that each signal contains. After doing the differentiation the final signal will be:

Final signal

$$= (S_1 + n) - (S_2 + n) \quad (6.1)$$

$$= S_1 - S_2 \quad (6.2)$$

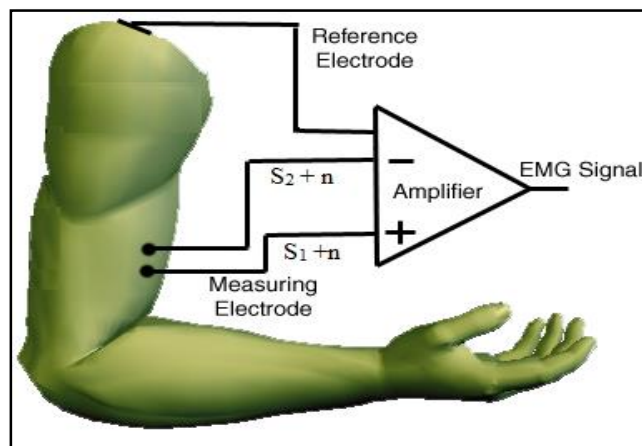


Figure 6.4 The differential amp for two electrode signals [32].

From the above equation, it is clear that any common signal between the two electrodes will be removed, and the difference between the two signals will be amplified in the next step. Some of the signals which come from “unwanted muscle”, the muscle that is laying close to the muscle being measured for activity, will be considered as a common signal, and that signal will be removed or reduced.

Four things should be observed carefully during the detecting and processing of the EMG signal. The input impedance between the skin and the electrode can vary from several thousand ohms to several mega ohms. The input impedance for the differential amplifier should be as large as possible to prevent the distortion and attenuation of the detecting signal. The use of an instrumentational amplifier instead of an operation amplifier is very important for this project because it has high input impedance and low output impedance. The preparation of the skin should emphasize that the skin needs to be clean and covered with gel to increase the electricity conduction. The electrode should be connected well to the skin and the cable between the electrode and the rest of the circuit should not be long. Finally, the correct components should be chosen in order to improve performance of the prosthetic hand.

## **6.6 Common-mode Rejection Ratio CMRR.**

The ideal differentiation amplifier is expected to amplify the difference between the two inputs  $V_2$  and  $V_1$  with approximately infinite gain. A common-mode voltage will result due to factors such as asymmetry in the circuit, output impedance of the tail current

source, and changes with frequency due to the tail current sources shunt capacitance. The common mode voltage of the amplifier depends on its design and what the user needs.

The common-mode voltage  $V_{cm}$  is the average of the two input voltage.

$$V_{cm} = \frac{V_1 + V_2}{2} \quad (6.3)$$

The common-mode gain  $A_{cm}$  is given by

$$A_{cm} = \frac{V_o}{V_{cm}} \quad (6.4)$$

Where  $V_o$  is the output voltage of the amplifier.

What is the common-mode rejection ratio CMRR? It is the ratio of differential gain to common mode gain. The CMRR is the ability of the device to reject the common mode signals. It is one of the very important properties in the operational amplifier, and there are many applications need the CMRR to be a very high.

$$CMRR = 20 \text{ Log} \left( \frac{A_d}{A_{cm}} \right) \quad (6.5)$$

$$V_o = A_d * (V_1 - V_2) + A_{cm} * \left( \frac{V_1 + V_2}{2} \right) \quad (6.6)$$

Where,  $A_d$  is the differential gain and  $A_{cm}$  is common-mode gain.

### **6.7 Instrumentational Amplifier.**

The differentiation operation is the first step after getting a signal from the electrodes. In this state, the signal of electrode two will be subtracted from the signal of electrode one to eliminate the noise to enhance the electrode's signal. The detecting voltages by electrodes are very small, sometimes in micro volts. The differentiation stage should have some requirements to deal with this small amount of voltages, such as high

input impedance, low output impedance, and high common mode rejection ratio (CMRR). These requirements cannot be satisfied by using an operation amplifier as a differentiation amplifier because it does not have all these properties. The best way is to use an instrumentational amplifier which can reject the common voltage between its two inputs. An instrumentational amplifier is a combination of three operation amplifiers, combined together in a way that gives very useful properties. The circuit diagram of the instrumentational amplifier is shown in the Figure 6.5 below:

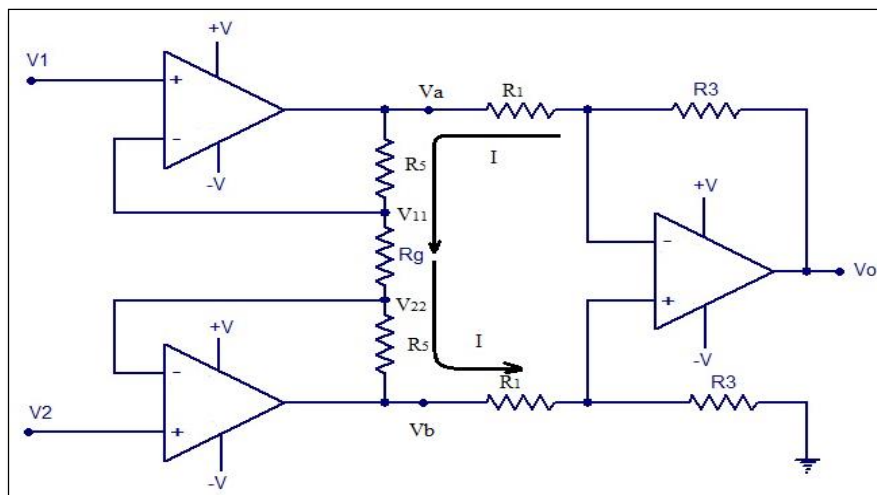


Figure 6.5 The entire circuit of the instrumentation amplifier.

Where,  $R_1$ ,  $R_3$ , and  $R_5$  are built-in resistors,  $R_g$  (gain resistor) is a built-out resistor, and this resistor can control the gain of the instrumentation amplifier. The first two op-amp amplifiers of the instrumentation amplifier work as buffers (voltage followers) to eliminate some noise from the signal, and they have high input impedance. The third op-amp amplifier is differentiation amplifier, and it has low output impedance. The gain of the third op-amp amplifier can be calculated from the following equations:

Let the voltage at the intersection point between  $R_5$  and  $R_g$  from the upper is  $V_{11}$ , and the intersection point between  $R_5$  and  $R_g$  from the lower is  $V_{22}$ .

$$V_O = - \left( \frac{R_3}{R_1} \right) V_a + V_b \left( \frac{R_3}{R_1 + R_3} \right) \left( 1 + \frac{R_3}{R_1} \right) \quad (6.7)$$

$$V_O = - \left( \frac{R_3}{R_1} \right) V_a + V_b \frac{R_3}{R_1}$$

$$V_O = \frac{R_3}{R_1} (V_b - V_a) \quad (6.8)$$

Because of the high input impedance in both op-amplifiers, there is no current that passes through the terminals (the positive terminal and the negative terminal).

Therefore,

$$V_1 = V_{11} \quad \text{and} \quad V_2 = V_{22}$$

$$V_a - V_1 = I * R_5 \quad (6.9)$$

$$V_1 - V_2 = I * R_g \quad (6.10)$$

$$V_2 - V_b = I * R_5 \quad (6.11)$$

By rearranging equation (6.10),

$$I = \frac{V_1 - V_2}{R_g}$$

By substituting I in equation (6.9) we will get:

$$V_a - V_1 = \frac{V_1 - V_2}{R_g} * R_5$$

$$V_a = V_1 \left( 1 + \frac{R_5}{R_g} \right) - V_2 * \frac{R_5}{R_g} \quad (6.12)$$

By substitute I in equation (6.11) we will get:

$$V_2 - V_b = \frac{V_1 - V_2}{R_g} * R_5$$

$$V_b = \left( 1 + \frac{R_5}{R_g} \right) V_2 - V_1 * \frac{R_5}{R_g} \quad (6.13)$$

By substituting equations (6.12) and (6.13) in equation (6.8), the output voltage will be:

$$V_O = \frac{R_3}{R_1} \left[ \left( V_2 \left( 1 + \frac{R_5}{R_g} \right) - V_1 * \frac{R_5}{g} \right) - \left( V_1 \left( 1 + \frac{R_5}{R_g} \right) - V_2 * \frac{R_5}{R_g} \right) \right]$$

$$V_O = \frac{R_3}{R_1} \left[ V_2 \left( 1 + 2 * \frac{R_5}{R_g} \right) - V_1 \left( 1 + 2 * \frac{R_5}{R_g} \right) \right] \quad (6.14)$$

It is clear that the output voltage depends on the value of  $R_g$ , and the gain can be controlled by changing the value of  $R_g$ .

### 6.8 AD620 Instrumentational Amplifier.

In this project, the AD620 instrumentational amplifier was chosen to be used in the differentiation stage, because it has some properties that make it perfect for the EMG data acquisition. It's gain can be set from 1 to 10,000 by changing only one resistance  $R_g$  [33], which is connected between pin one and pin eight as shown in Figure 6.6. Here, the gain (G) is given in data sheet as the following formula:

$$G = 1 + \frac{49.4 \text{ k}\Omega}{R_g} \quad (6.15)$$

In our design we chose  $R_g$  equal to  $500\Omega$  therefore the gain will be:

$$G = 1 + \frac{49.4 \text{ k}\Omega}{500\Omega} = 99.8 \approx 100$$

The second advantage of the AD620 INA comes from its ability to work with a very wide range of power supply ( $\pm 2.3 \text{ v}$  to  $\pm 18 \text{ v}$ ). Furthermore, it has a 100 db common-mode rejection ratio, and that makes it a very good instrumentational amplifier for the EMG purpose.

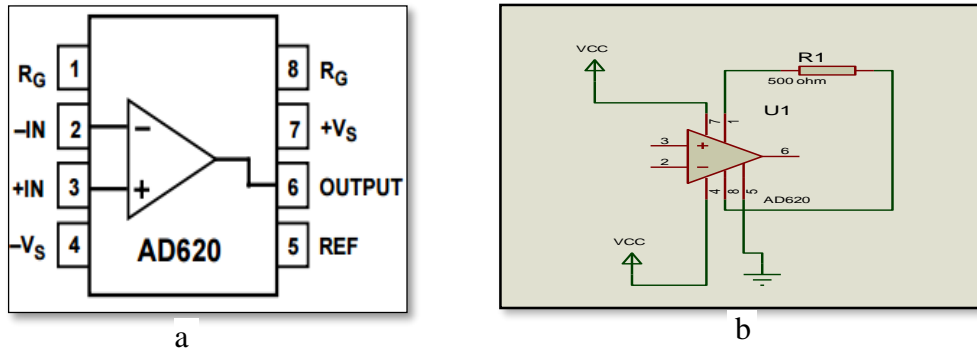


Figure 6.6 (a) Is the pinout of AD620 and (b) Is the circuit diagram of AD620.

This instrumentational amplifier has a low cost of about \$1.6, high accuracy, and low noise. The design in this project depends on two +9 v batteries as a power supply. This INA with its small design size and low power, and low input bias current will be perfect for the EMG acquisition process.

From the figures above, it is clear that the AD620 has eight pins. Pin number one and pin number eight will connect to each other by a 500Ω gain resistor to set the gain of the AD620 to be 100. Pin number two and pin number three will be input pins for the signals that come from electrode one and electrode two.

Pin number four and pin number seven will be the pins for -9v and +9v power voltage of the AD620 respectively. The reference pin (pin number five) will be connected to the ground of the circuit such as the ground electrode. The output pin (pin number 6) will connect to the next step in the rest of the circuit.

## 6.9 Pre-Amplifier Stage.

After getting a signal from the instrumentational amplifier, this signal should pass through a low pass filter then high pass filter. There is a problem with this step because this signal is a very small to be filtered. Therefore, this signal should be large enough to pass through these filters, but not so large that it has noise, and these noise should not be amplified. In the second stage of signal processing, the getting signal will amplify by a factor of 10 by using the LM324 operation amplifier. There are several reasons for choosing this amplifier. One of these reasons is the low price that this device has. Also, it can be operated with a wide range of voltage supply from  $\pm 3.5$  to  $\pm 18$  v. Furthermore, it has a low-current drain and four operational amplifiers inside, as shown if Figure 6.7 below, that make it equal to use four of the LM741 operational amplify

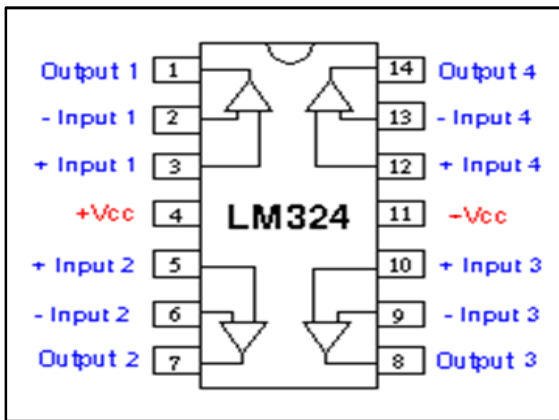


Figure 6.7 The LM324 operation amplifier.

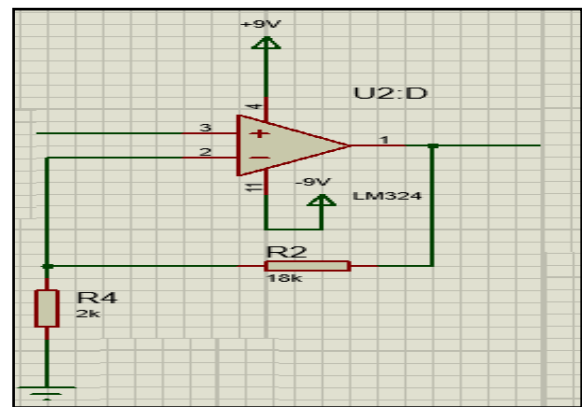


Figure 6.8 The LM324 schematic.

In this step, two resistors will be used to set the amplifier gain. The first resistor is 18 k $\Omega$ , which connects between the negative input and the output, and the other is 2k $\Omega$ , which connects the negative input to the ground as shown in Figure 6.8 above:



## 6.10 Filtering Stages

The electronic filter is one of the most popular electronic devices used in many applications of daily life such as communication, audio application, signal processing... etc. In general, the filters are used to remove unwanted signals during signal processing. There are several kinds of filters that can be divided depending on the purpose for their use. It could be divided according to what type of signal should be processed, which is either a digital signal or an analog signal. Also, these two types can be divided into many kinds according to which range of frequencies need to be filtered. For example, the 1k HZ low pass filter will allow the signal with maximum frequency of 1k HZ to pass and prevents any signal with higher frequency from passing.

A band pass filter allows the signal with frequency ranged between two cut-off frequencies to pass, and it prevents any other signals from going out. There is a high pass filter which is used to pass the signal that has a frequency higher than the cut-off frequency.

A stop-band filter works opposite to the working of the band-pass filter which prevents the signal from passing. This signal has a frequency range between two cut-off frequencies. Furthermore, the filters have been divided into many types depending on the response such as pole responses or poles and zero responses. Inverse Chebyshev and elliptic filters are required zeros in frequency response to give us the sharp cut off, but these filters will be more complicated when they are the passive filter.

For this project, the unity gain 2-poles (second order), low pass active filter with cut-off frequency of 400 HZ circuit will be used. This low pass filter will be followed by the high pass filter which has the same specifications, with a 30 HZ cut-off frequency. The

passive filter is cheaper than the active filter, but the active filter will be used in this design for three reasons. First, the active filter gives low output impedance, and that will be helpful to drive the next stage. Second, with the active filter it is easy to apply gain to the circuit, in this way the overall circuit will be smaller. With the active filter, the inductor will not be used. In low frequencies the inductor will have a large size. This is a nice small filter design for low frequency, for which there is no need for a big size inductor.

To explain how the filter works, a simple filter as shown in Figure 6.9 below will be taken as an example:

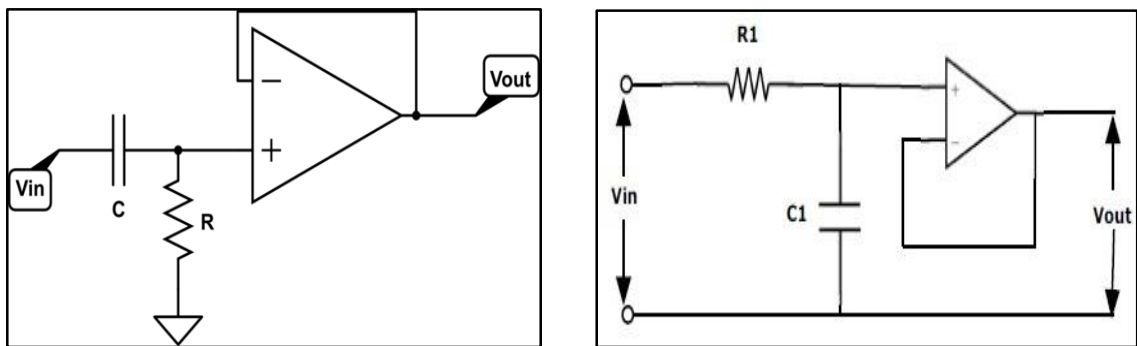


Figure 6.9 Left is high pass filter, right is low pass filter.

When the input voltage ( $V_{in}$ ) has low frequency for the high pass filter in Figure 6.9 a, the time will be very long at the capacitor. The capacitor will have enough time to be fully charged and to become an open circuit, and no current will pass through the circuit. When the input voltage ( $V_{in}$ ) has high frequency, the capacitor will not have enough time to be fully charged. It will become a short circuit and all the current will pass to the output. The opposite thing will happen with the low-pass filter in Figure 6.9. At low frequency input voltage, the capacitor will be an open circuit and the current will pass through the

resistor R1 to the output. On the other side, when the input voltage has high frequency, the capacitor will become a short circuit and no current will pass to the output.

### **6.10.1 Sallen-Key Filter**

There are many different filters such as Chebyshev, Sallen-key, Butterworth, inverse Chebyshev, and elliptic. Each one of these filters has some properties which help the designer to choose which filter is best for the application and for the performance requirements. One of the most important properties in second order filters, is the quality factor of the filter (Q). This is the measure of the peaking value of the filter (it tells the magnitude of the filter at the pole frequency). Many applications required a quality factor to be high. To satisfy a high quality factor it is necessary to use a positive feedback amplifier such as the Sallen-key filter. The reason for choosing the Sallen-key filter is because it is a simple way to get the two poles active filter with few components, and is a simple circuit diagram. Also, it has very large input impedance and very small output impedance

### **6.10.2 Transfer Function Calculation of the Sallen-key Filter**

This section will discuss how to calculate the transfer function analysis of generic unity-gain of the Sallen-key filter shown in Figure 6.10 below under the assumption that the operation amplifier is ideal.

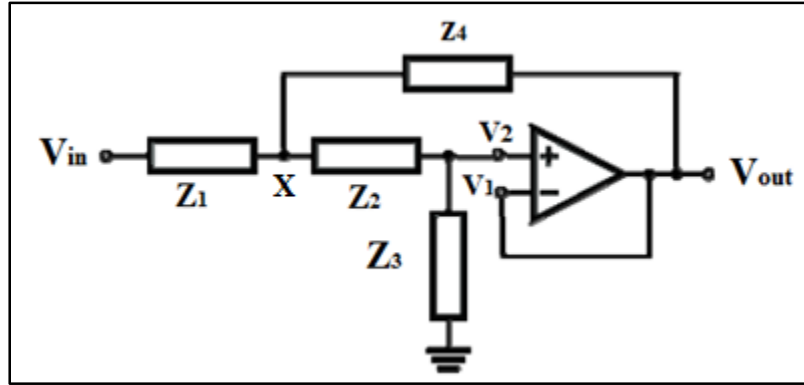


Figure 6.10 The generic unity-gain Sallen-key filter.

Because of the high input impedance of the operation amplifier, no current will pass through.

Therefore,

$$V1=V2=Vout \quad (6.16)$$

By applying Kirchoff's current law (KCL) at the Vx node,

$$\frac{V_{in}-V_x}{z_1} = \frac{V_x-V_{out}}{z_4} + \frac{V_x-V_2}{z_2} \quad (6.17)$$

By substituting equation 6.16 in equation 6.17,

$$\frac{V_{in}-V_x}{z_1} = \frac{V_x-V_{out}}{z_4} + \frac{V_x-V_{out}}{z_2} \quad (6.18)$$

Using KCL at node V2

$$\frac{V_x-V_{out}}{z_2} = \frac{V_{out}}{z_3}$$

By arranging the above equation:

$$V_x = V_{out} \left( \frac{z_2}{z_3} + 1 \right) \quad (6.19)$$

Substituting equation 6.19 in equation 6.18 to determine the transfer function:

$$\frac{V_{in} - V_{out} \left( \frac{Z_2}{Z_3} + 1 \right)}{Z_1} = \frac{V_{out} \left( \frac{Z_2}{Z_3} + 1 \right) - V_{out}}{Z_4} + \frac{V_{out} \left( \frac{Z_2}{Z_3} + 1 \right) - V_{out}}{Z_2}$$

$$\frac{V_{out}}{V_{in}} = \frac{Z_3 Z_4}{Z_1 Z_2 + Z_4 (Z_1 + Z_2) + Z_3 Z_4} \quad (6.20)$$

### 6.10.3 Low-pass and High-pass Filter Sallen-Key

A low pass and a high pass filter are very common filters in many electronic applications such as signal processing. Consider a low pass Sallen-Key filter as shown in Figure 6.11 below with a cut-off frequency of (400). This stage is responsible for removing unwanted signals with frequencies less than 400 HZ. To do that, it is necessary to calculate the components in Figure 6.11 that gives this signal. At low frequencies, C1 and C2 will be open circuits, and the signal will buffer to the output. At high frequencies, the two capacitors will act as short circuits, and no signal will appear at the output. Near to the cut-off frequency the capacitor C2 will provide a positive feedback which enhances the quality factor of the signal (Q).

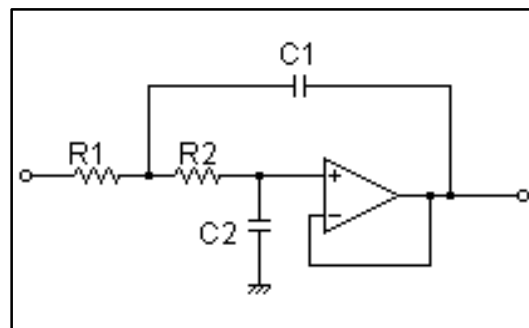


Figure 6.11 The low pass filter Sallen-key.

By comparing Figure 6.10 and Figure 6.11 we will get:

$$Z_1 = R_1, Z_2 = R_2, Z_3 = \frac{1}{sC_2}, \text{ and } Z_4 = \frac{1}{sC_1}$$

By substituting these components in equation 6.20, the transfer function will be:

$$\frac{V_{out}}{V_{in}} = \frac{\frac{1}{sC_2} * \frac{1}{sC_1}}{R_1 R_2 + \frac{1}{sC_1} (R_1 + R_2) + \frac{1}{sC_2} * \frac{1}{sC_1}} = \frac{1}{s^2 R_1 R_2 C_1 C_2 + s C_2 (R_1 + R_2) + 1} \quad (6.21)$$

Let,

$$s = j * 2 * \pi * f$$

$$f_c = \frac{1}{2 * \pi * \sqrt{(R_1 R_2 C_1 C_2)}} \quad (6.22)$$

$$Q = \frac{\sqrt{(R_1 R_2 C_1 C_2)}}{R_1 C_1 + R_2 C_1} \quad (6.23)$$

By choosing  $R_1 = R_2 = 4 \text{ k}\Omega$ ,  $C_1 = 200 \text{ nf}$ , and  $C_2 = 100 \text{ nF}$ , the cut-off frequency and the quality factor

Will be:

$$f_c \approx 300 \text{ Hz}, Q = 0.67 \text{ for } c_1 = 200 \text{ nf}$$

And

$$f_c \approx 440 \text{ Hz}, Q = 0.311 \text{ for } c_1 = 820 \text{ nf}$$

The high pass Sallen-key filter in Figure 6.12 is the final step in this filtering stage. This filter is used to pass a signal with frequency greater than 30 Hz. This stage will be done by choosing the appropriate components to calculate the transfer function, cut-off frequency, and the quality of the filter.

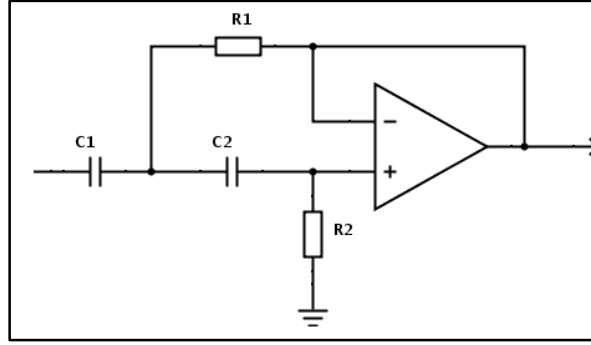


Figure 6.12 The high pass filter Sallen-key.

By comparing Figure 6.12 and Figure 6.10

$$Z_1 = \frac{1}{sC_1}, Z_2 = \frac{1}{sC_2}, Z_3 = R_2, \text{ and } Z_4 = R_1$$

By substituting these components in equation 6.20, the transfer function will be:

$$\frac{V_{out}}{V_{in}} = \frac{R_1 R_2}{\frac{1}{sC_1} * \frac{1}{sC_2} + R_1 \left( \frac{1}{sC_1} + \frac{1}{sC_2} \right) + R_1 * R_2} = \frac{s^2 C_1 C_2}{s^2 C_1 C_2 + \frac{1}{R_2} \left( \frac{1}{sC_1} + \frac{1}{sC_2} \right) + \frac{1}{R_1 R_2}} \quad (6.24)$$

Let,

$$S = j * 2 * \pi * f$$

$$f_c = \frac{1}{2 * \pi * \sqrt{(R_1 R_2 C_1 C_2)}} \quad (6.25)$$

$$Q = \frac{\sqrt{(R_1 R_2 C_1 C_2)}}{R_2 (C_2 + C_1)} \quad (6.26)$$

By choosing  $R_1 = 180 \text{ k}\Omega$ ,  $R_2 = 180 \text{ k}\Omega$ ,  $C_1 = 103 \text{ nF}$ ,  $C_2 = 8 \text{ nF}$ , the cut-off frequency and the quality factor will be:

$$f_c = 30.8 \text{ Hz}, Q = 0.26$$

### 6.11 Amplifying Stage

After filtering stages, the signal became more readable and contains very few noise. The only problem with this signal is that this signal is too small to be readable by the controller to make a decision. This step will try to amplify the detecting EMG signal many

times to become between 1.5v to 6.5v depending on the muscle signal, and how many muscle fibers are activated at this moment. To do that, the LM324 operation amplifier is used as a non-inverting amplifier to amplify the signal 210 times, by using two resistors. The resistor R2 (180kΩ) is connected between the output pin and negative terminal pin (inverting input pin). This resistor is considered as negative feedback, which keeps the input voltage to the Op-Amp at approximately zero. The second resistor is R1 (860Ω), and is connected between the inverting input pin and the ground, see Figure 6.13.

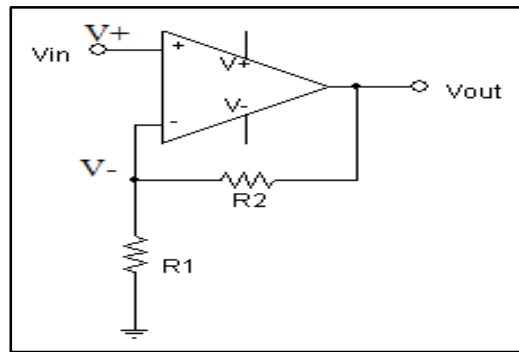


Figure 6.13 The operation amplifier.

$$V_{out} = A_{VOL} (V_{+} - V_{-}) \quad (6.27)$$

Where,  $A_{VOL}$  is the open-loop voltage gain of the LM324 Op-Amp is equal to 50.

We then have:

$$V_{+} = V_{in} \quad (6.28)$$

$$V_{-} = V_{out} * \frac{R_1}{R_1 + R_2} \quad (6.29)$$

From 6.27, 6.28, and 6.29 we get:

$$V_{out} = A_{VOL} \left( V_{in} - V_{out} * \frac{R_1}{R_1 + R_2} \right)$$



$$\frac{V_{out}}{V_{in}} = A_v = \frac{1}{\frac{1}{A_{VOL}} + \frac{R_1}{R_1 + R_2}}$$

Where,  $A_v$  is the voltage gain, and  $\frac{1}{A_{VOL}} \approx 0$ , because  $A_{VOL}$  is very big. Then, the above

equation will be:

$$\frac{V_{out}}{V_{in}} = A_v = 1 + \frac{180k\Omega}{860\Omega} \approx 210$$

## **Chapter 7 : Prosthetic Hand Control**

### **7.1 Introduction**

This chapter will discuss the control part of the design, the feedback coming from each finger, and the fingers' movement simulation. After detecting the signal from the arm's muscles and processing this signal to be readable by the Arduino UNO, which is the controller used in this project, the Arduino will take control of the fingers, depending on the incoming signal. The Arduino controls five servo motors. Each one of these motors actuates one finger. Each finger has one force sensor connected to the fingertip to sense if something touched the finger. If something did touch the finger, the sensor will send a signal to turn on and turn off the transistor switch. That transistor will turn on or turn off the vibration motor, which is connected to the amputee's arm, which makes him respond to this touching sense. A Simulink will be designed for the hand's movements by using a V-rep program.

### **7.2 Hardware Connection**

Chapter six mentioned that the final signal will be an analog signal coming from each finger's muscle. There is a need for a controller unit with at least five analog input pins. Each finger needs to actuate by a servo motor. The controller should have five more output pins as shown in Figure 7.1 below. Arduino UNO has been chosen to be our controller in this project because of four properties.

The Arduino has fourteen input/output digital pins which give the user the opportunity to deal with many devices at the same time. This low-cost controller has very simple software and the ability to show the data to the user on the screen as numbers or as a drawing. In addition, if anything goes wrong with any part of this controller, it is easy to replace this part without replacing the entire controller.

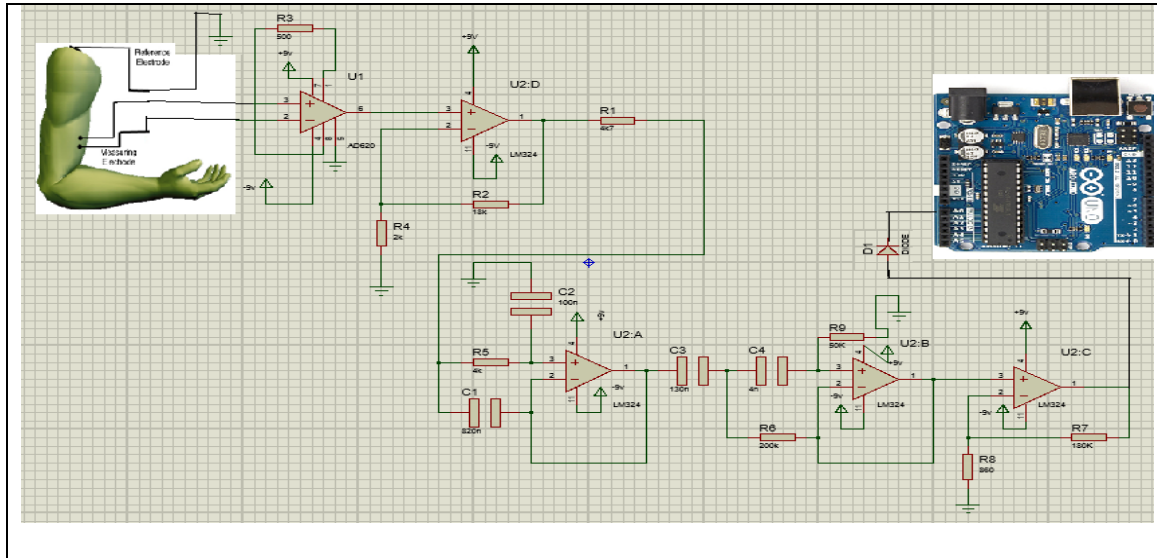


Figure 7.1 The diagram of the circuit.

### 7.3 Muscle Training and Signal Reading

During the connection of the electrodes to the skin, several important steps should be followed. It is important to use gel to give the best impedance to the skin and the best EMG signal as mentioned before. There is a need to prepare the skin and remove anything that could affect the quality of the signal [34], such as hair or dead skin cells. Choosing small-size electrodes will help avoid reading from more than one muscle's fibers. Applying the electrodes parallel to the muscle fibers will give the best reading. Once these steps have been completed, and the signals are being sent, the signal should be calibrating.

Calibration means that the controller will read the signal for each finger's muscle and save this reading to use as a reference when dealing with the program. Each finger's signal will have a value ranging between the small amounts, which represent the action resulting from a small amount of muscle fibers activated at this moment, and the largest signal reading, which is the result of the activation of all the muscle fibers. This signal is not coming just from the muscle activity that is being measured, but there is a small signal coming from another muscle lying close to the muscle being measured. During the calibration, the programmer tried to read the signal from each finger in a different situation, and movements such as a strong open, strong closed, open with different angles, and closing one or more fingers with a slow motion, etc.

In the training process, the amputee will try to move each finger's muscle to record muscle signals. These readings will be put into the program to make this program suitable for this particular amputee. Each person has different sized muscles, and he/she can produce different values for their EMG signals. The signals coming from one amputee may be different from others, and the designer should test these signals for each person who is being fitted.

#### **7.4 Programming the Arduino**

The Arduino program will have two parts; dealing with the EMG signals and controlling servo motors. The five signals that came to the analog input pins of the Arduino from pin A0 to A4 will be read. Whereas, pinky finger, ring finger, middle finger, index finger, and the thumb are connected to A0, A1, A2, A3, and A4 respectively. These signals

as shown in Figure 8.17 are not regular signals, and they go up and down with different peak values. The program has many ways to read these signals. The programmer can sample the signal and take the average of the summation. The program will take 75 samples and calculate the average of these samples to make a calibration. The calibration is important because the detectable signal is coming from more than one muscle. The incoming signal will be compared to the number which represents the signal strength that should have been received from training that muscle.

During the using of this prosthetic hand, the Arduino will continually check each analog pin if there is a signal or not, and to know how many fingers are activated in each single moment. In case there is a signal on one pin, and this signal is lying in the range of data that we got from the training, the Arduino will turn on the motor that corresponds to this muscle's signal. For example, if we suppose that the training of the pinky finger's signal during contraction was ranged between  $= 1.25 \text{ V} \sim 2.0 \text{ V}$ . This range will be saved in the Arduino program to use it for comparing with the data that comes from A0 when the amputee uses this prosthetic. The Arduino will continually check if the signal on pin A0 is lying in the range of  $1.25 \text{ V} \sim 2 \text{ V}$ . If yes, that's means the pinky's muscle is in contraction, and the Arduino will control the motor that should actuate the pinky finger. When the signal goes down this value, that means the muscle became in rest again. Therefore, the Arduino will control the servo motor to open the pinky finger.

The same thing will happen if there is more than one finger activated at the same time. The Arduino will not turn on the motor of any finger unless the signal of that finger

reaches the range of data that has been recorded in the training. And the signal will not be in that range of data unless the muscle was in contraction at that moment.

After reading the finger's incoming signal, the Arduino will start the next step, controlling the servo motors that actuates this finger. The controller will turn on the motor with 0 - 180 degrees to close or open the finger when there is a contraction signal, or the muscle will rest.

### **7.5 Simulink Model of the Hand's Design**

The Simulink is important to demonstrate how the design works. The Simulink portion of this design will show some of the prosthetic hand's movements and how each finger can move. A V-rep program has been used to design and control the Simulink of this prosthetic hand because of the flexibility that this program has. With V-rep, it is possible to find forward kinematic, inverse kinematic, to add sensors (software and hardware), and to connect the design with outside environments. This program gives the user two options for design and two options for control. For design, there are many built-in designs that the user can choose for his/her project. The user can also build his/her design from basic components, such as cylinders, joints to create movement, cuboid, etc. For control, the user has to choose to either control the joints (the parts which are responsible for movement) by changing the joint properties or by writing a program to make control.

## 7.6 Design Details

Building the fingers is not an easy process. The fingers need to use more than six geometric shapes to build one finger link, and it is important to change some of the properties. A revolute joint has been used to connect each of the two links and to give the design the dynamic movement. All these links have the same dimensions as the prosthetic hand that has been created.

Each link consists of two sides and one bottom. The sides consist of two thin cylinders connected by a rectangle. The bottom consists of one rectangle. The two links are connected with each other by a revolute joint passing through the cylinders of both links. By rotating that joint, the links will move and the finger will have movement.

To make all joints and links work in a regular mechanism. It is necessary to make each part as an orphan to the previous one, beginning from the fingertip and ending with the palm. The palm will be the parent of all the fingers. The first link of each finger will be the parent to the rest of the joints and links in that finger. The final shape of the link and finger is shown below in Figure 7.2.

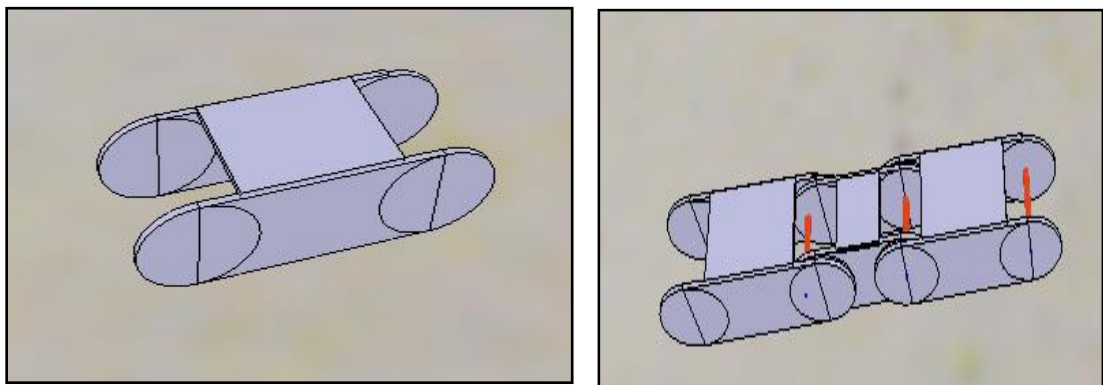


Figure 7.2 Shows the design of link and finger in V-rep program.

To control the finger's movement, a short program has been written for each revolute joint in which this code controls the amount and speed of the joint's movement. This simulation will show the movements of closing and opening the five fingers at a slow speed.

## **7.7 Feedback Signal**

The feedback signal makes the design more significant and more useful for amputees. It is a good thing for amputees to have an artificial hand helping them do their daily life's activities, but it better for them if they can feel what they touch. This property can be achieved by connecting a force sensor (as shown in Figure 3.3) in each fingertip. In this step, a 2N2222 NPN transistor will be used as a switch [35] to allow the current to pass to the vibration motor shown in Figure 7.3. The force sensor will connect to the base of the transistor, while the emitter will connect to the motor, and the collector will connect to the power supply and the other wire of the vibration motor. When there is no force on the force sensor its resistor will be very large (open circuit), and no current will pass through to turn on the transistor. When there is a force on the force sensor, the resistor of this sensor will decrease by increasing the applying force. Decreasing the force sensor's resistor value means that the current will pass through the transistor's base. Passing current greater than  $I_{sat}$  (saturation current) through the base means the collector will connect to the emitter. More current pass will allow the increase of the speed of the vibration motor. The speed of the vibration will represent how much pressure there is between each finger and the object.



When the vibration is high, that means the finger presses strong on the object and the opposite is true.

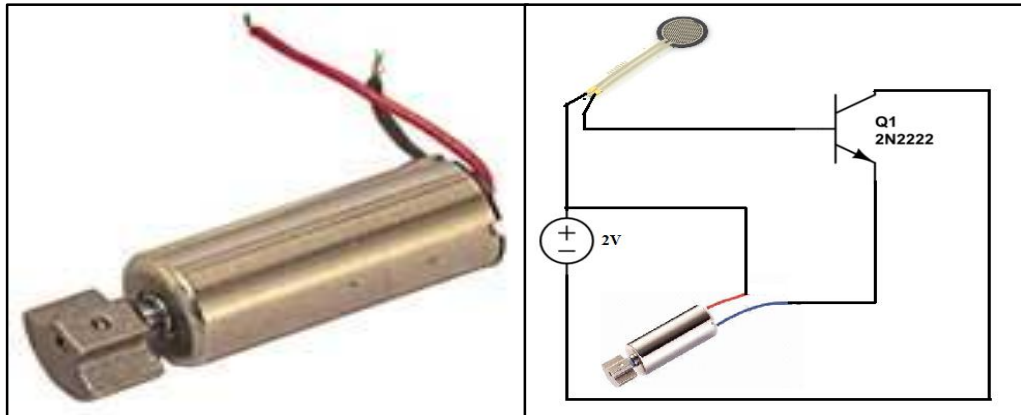


Figure 7.3 Left is the vibration motor, right is the feedback circuit.

## **Chapter 8 : Results**

The prototype prosthetic hand, shown in Figure 3.4, has been tested for each finger separately. The test included several parts. First, the movements of each finger were tested while imitating a human hand's movements. Second, the force was measured for each finger during the grasping process. Third, the EMG signals were determined for each finger. Furthermore, the feedback signal from each finger was tested as was the ability to control the vibration motor. Fifth, the total cost and weight of the prosthetic hand was presented for all components and materials.

The following results have been found:

### **8.1 Hand Results**

Where,  $\theta_1$  is ranged between 0 to 90 degrees,  $\theta_2$  is ranged between 0 to 80 degrees, and  $\theta_3$  is ranged between 0 to 60 degrees. By considering the fact that there is a tie wrap used to close and open the finger,  $\theta_3$  will change at the end of the closing or opening movements. During the closing and opening operations, the joint's angles will change between minimum and maximum values to satisfy the grasp requirements. During the joint rotations a maximum  $x$  can satisfy when all joints have 0 degree and the maximum  $y$  will be a little bit less than the length when the first joint angle was at 90 degrees and the other joints at 0 degrees.

Using equation 4.25, the fingertip x and y coordinates with respect to the finger's base are the first two elements in the last column. The coordinate's equations for each finger can be found as follows:

For the pinky finger:

$$X = 2.5 * C\theta_{123} + 2 * C\theta_{12} + 2.5 * C\theta_1$$

$$Y = 2.5 * S\theta_{123} + 2 * S\theta_{12} + 2.5 * S\theta_1$$

For the ring finger:

$$X = 2.5 * C\theta_{123} + 2 * C\theta_{12} + 3.5 * C\theta_1$$

$$Y = 2.5 * S\theta_{123} + 2 * S\theta_{12} + 3.5 * S\theta_1$$

For the middle finger:

$$X = 3.5 * C\theta_{123} + 2 * C\theta_{12} + 3.5 * C\theta_1$$

$$Y = 3.5 * S\theta_{123} + 2 * S\theta_{12} + 3.5 * S\theta_1$$

For the index finger:

$$X = 2.5 * C\theta_{123} + 2 * C\theta_{12} + 3.5 * C\theta_1$$

$$Y = 2.5 * S\theta_{123} + 2 * S\theta_{12} + 3.5 * S\theta_1$$

For the thumb:

$$X = 3.3 * C\theta_{12} + 3.5 * C\theta_1$$

$$Y = 3.3 * S\theta_{12} + 3.5 * S\theta_1$$

The results that shown in the following table come from applying three different joint variables to the above equations. The pictures will explain some of the positions for each fingertip during closing process.

Finger	Movement #	$\theta_1$	$\theta_2$	$\theta_3$	X	Y	Force N
pinky	1	0	0	0	7	0	9.81
	2	90	80	60	-3.57	.93	6.86
	3	45	40	30	.88	6	12.7
Ring	1	0	0	0	8	0	11.5
	2	90	80	60	-3.57	1.9	10
	3	45	40	30	1.6	6.7	13.2
Middle	1	0	0	0	9	0	11.5
	2	90	80	60	-4.2	1.16	9.81
	3	45	40	30	1.17	7.64	14.7
Index	1	0	0	0	8	0	11
	2	90	80	60	-3.57	1.9	9.5
	3	45	40	30	1.6	6.7	13
Thumb	1	90	0		0	6.8	15.7
	2	160	25		-6.57	0.9	13.7
	3	135	15		-5.3	4.1	17.65

Table 8.1 Shows the x and y coordinates and the force of the fingertip for different angles



Figure 8.1 The movements of middle finger.



Figure 8.2 The movements of index finger.



Figure 8.3 The movements of pinky finger.



Figure 8.4 The movements of ring finger.

From table 8.1 it is clear that the maximum x coordinate for pinky, ring, middle, index, and thumb are 7, 8, 9, 8, -6.57 respectively. The minus sign means that the coordinate lies opposite to the direction of the axis of the base. The table shows the results for only three different angles for each joint. Figures 8.1 ~8.4 show the space that each finger can move in during closing and opening operations.



Figure 8.5 Show the hand when holding a tennis ball in different situations.

From above table and figures, it is clear that the fingers can move in enough space to cover almost the same as the human's movements. Where, the structure of the fingers is flexible, that's means the finger's joints can move all at the same time, or just one or two joints can move together to hold different shapes of objects. This structure will create the ability to grasp different objects as shown in the figures below:



Figure 8.6 Precision open.



Figure 8.7 Tripod grip.

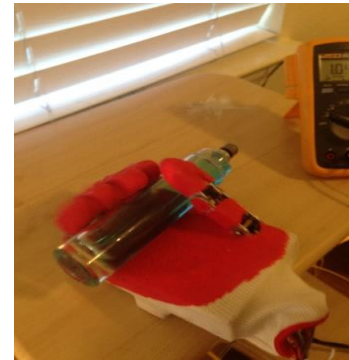


Figure 8.8 Hook grip.



Figure 8.9 Mouse grip.



Figure 8.10 Relaxed grip.



Figure 8.11 Power grip.

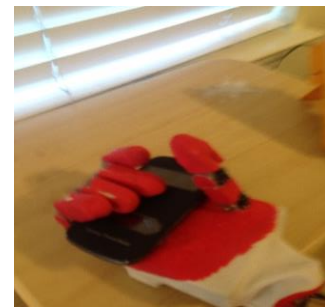


Figure 8.12 Show different gripping patterns.

## 8.2 Signal Results

The second part of this chapter will discuss the signal results. First, it will show the EMG signal detected from the electrodes without any filters or treatment (except amplifying). Then, this section of chapter will show the effect of filters and amplifiers on this signal. Finally, it will show the final signal for each finger.

When the electrode detects the EMG signal, this signal will be very small and has a lot of noise as shown in Figures 8.13 and 8.14 below:



Figure 8.13 Signal when the muscle at contraction.

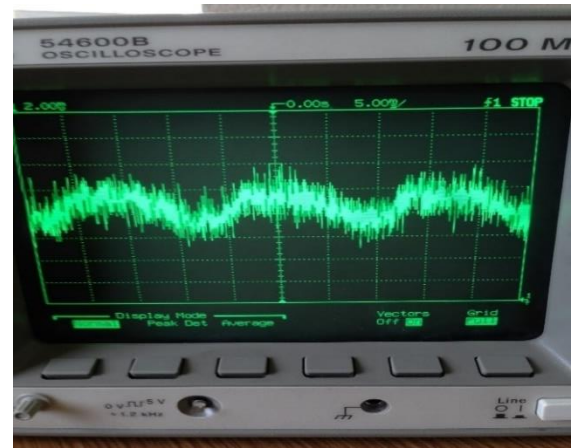


Figure 8.14 Signal when the muscle at rest.

Whereas, the signal in pictures 8.13 and 8.14 is measured from pin 6 at AD620 (instrumentational amplifier) that means this signal is amplified by about 100 times. Then, the signal will pass through pre-amplifier stage, low pass filter, high pass filter, and amplifier stage. The final signal of the circuit is shown in Figures 8.15 ~ 8.18 below.





Figure 8.15 Two short contractions.

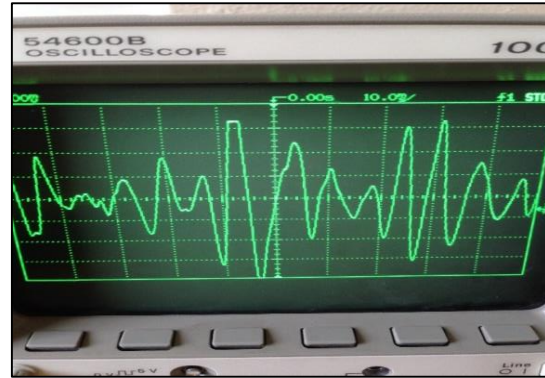


Figure 8.16 Muscle at contraction.

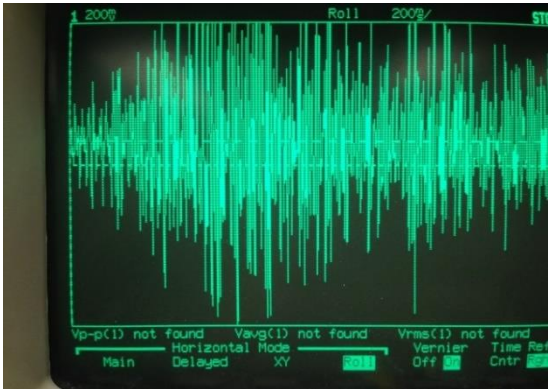


Figure 8.17 Long contraction.

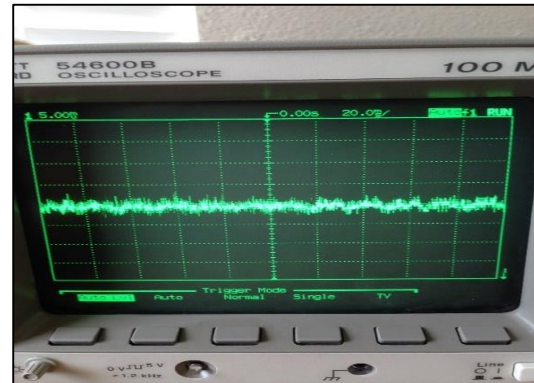


Figure 8.18 Muscle at rest.

From Figures 8.15~8.18 we can note that the signal has positive and negative values. The problem now is that we should remove the negative values to be readable by the Arduino. To do that, a diode will be used to remove the negative part of the signal as shown in Figures 8.19.

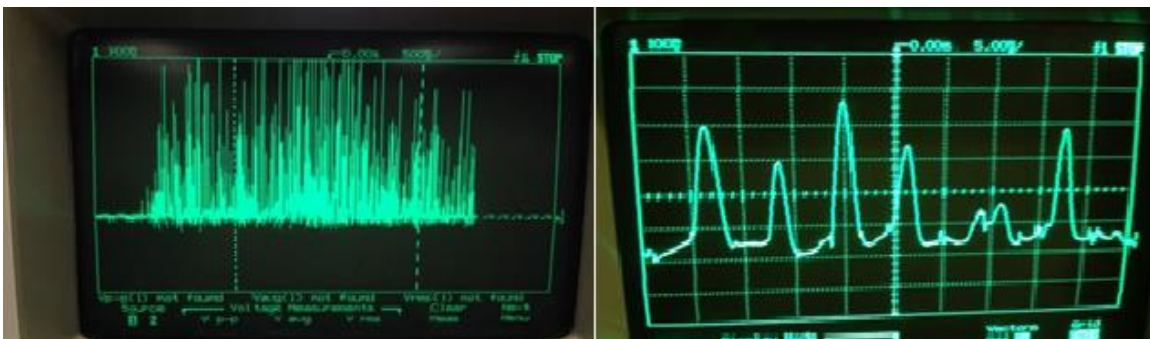


Figure 8.19 Signal after cutting the negative part.



When the Arduino receives this signal, it will sample this signal, and it will take the average of samples. In the second part of this section, the signal of each finger will be presented in pictures to show the amount and the frequency of this signal at contraction and rest.



Figure 8.20 EMG signal of pinky finger.

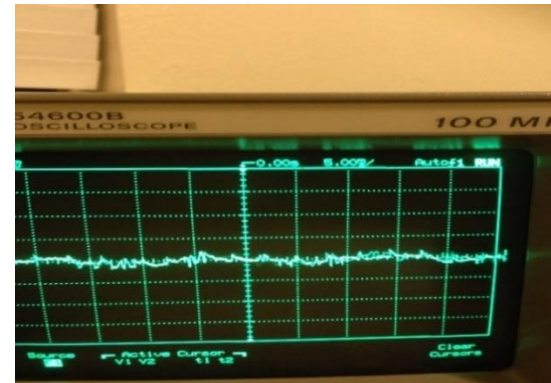


Figure 8.21 EMG signal of ring finger.



Figure 8.22 EMG signal for middle finger.



Figure 8.23 EMG signal of the index finger.



Figure 8.24 EMG of thumb.

Finally, the next two tables show the price and weight of the hand's design, the EMG circuit, and the feedback circuit.

Component	Quantity	Price for one (\$)	Weight (g)	The price of all (\$)	The weight of all (g)
Design's structure	1	20	147.3	20	147.3
Rubber glove	1	1		1	
Others (wires, glue...)		1		1	
Screw	48	0.1	0.3	4.8	14.4
Nut	26	0.04	0.3	1.04	7.8
Copper cylinder	10	.088	1.2	0.88	12
Force sensor	5	1.75	0.1	8.725	0.5
Servo motor	5	1.528	9	7.64	45
Total				45.085	227

Table 8.2: Shows the weight and price of the hand.

Component	Quantity	Price for one \$	Price for all \$
Arduino	1	3.46	3.46
LM324N	1	0.324	0.324
AD620	1	1.576	1.576

Resistors	10	0.02	0.2
820nf Capacitor	1	0.56	0.56
100nf Capacitor	2	0.01	0.02
33nf Capacitor	1	0.09	0.09
4nf Capacitor	1	0.3	0.3
Diode	1	0.04	0.04
2N2222 Transistor	1	0.02	0.02
Electrodes cable	1.5	1.55	2.325
Electrodes	3	0.1578	0.47
Vibration motor	5	0.66	3.3
Solder	1	1.6	1.6
Pcp board	0.5	0.144	0.072
Total			14.267

Table 8.3: Shows the price of each element and the total price of the EMG detecting circuit and feedback circuit.

## **Chapter 9 : Conclusion and Future Work**

### **9.1 Conclusion**

This thesis project processes the design of a prosthetic hand controlled by the surface EMG signal. This cost-effective hand has 14 degree of freedom, and is made from aluminum sheet to be light and strong. The hand has five fingers, and each finger has three links except the thumb which has two links. Each finger is actuated separately by using servomotor which is controlled by Arduino. The Arduino controls the angle of the servomotor and the servomotor will pull a tie wrap to open or close the finger.

This prosthetic hand is controlled by the surface EMG signal which comes from the rest of the amputee's arm. The surface EMG signal should pass through many steps to be readable by the Arduino. The first step is detecting the EMG signal from the muscle by using three electrodes. Electrode one is connected to the top of the muscle, electrode two is connected to the end of muscle, and the third electrode is a reference electrode which is connected to the bone.

The reference electrode could be common between many muscles. That means if there is a circuit to test five muscles, it will need eleven electrodes. One will be common between all muscles and two electrodes for each muscle. After detecting a signal from the muscle, the next step will be to subtract the signal of electrode two from the signal of electrode one to remove the common noise. Then the signal should amplify several times to be large enough to pass through the next step.

In this pre-amplifying step, the signal will amplify for several times because it has noise and we don't want to amplify these noise. The next step is the filtering step where the signal should pass through the low pass filter then high pass filter to extract the EMG signal and remove almost all noise. The final step in EMG signal processing is the amplifying step where the signal will be amplified to be big enough to read by the Arduino to make control for the hand's fingers.

After designing the hand and getting the EMG signal, the project focused on getting a feedback signal from each finger. The feedback signal is the signal that tells the amputees if there is any object that is touching any finger. To do that, there is a force sensor connected to each fingertip which senses if there is any force applied on the finger. The way that the force sensor tells the amputee about this force, is by turning on the vibration motor which is connected to the amputee's arm, the speed of the vibration motor related with the amount of the force that is applied to the fingertip. The design of the hand has been simulated by using the v-rep program. This design has good functions that make it very good and useful for amputees. It is affordable, has light weight, easy to fix, good finger control, and very good EMG detecting. I hope this project will make good difference in many amputees' lives.

## **9.2 Future Work and Recommendations**

After successfully designing and testing this project there is some recommendations for future work on this project. First of all, the feedback sensing ability should be improved. As mentioned before, each finger has a force sensor attached to the fingertip that can sense

if there is something in touch with the finger. To improve the ability of sensing it is very important to increase the ability of the hand to sense in any part of the hand or fingers not just in fingertip. To do that that, I recommended creating an artificial skin which covers all hand and has a good sensing ability and good friction to catch the object.

On the other hand, this design can tell the amputee if the object touches the finger hardly or softly. But it cannot tell the amputee more properties about this object such as the temperature, if it is soft or not, if it is big or small, the shape of this object ...etc. Some of these properties are very important for blind people. To make this project very useful for blind people it is important to activate some feedback which tells the amputee about these properties.

## References

- [1] Jessica Badger, “Meet the real-life bionic woman: Earlsfield fitness fanatic proud owner of hand built with F1 technology,” 2015.
- [2] M. Seo, D. Yoon, J. Kim, and Y. Choi, “EMG-based Prosthetic Hand Control System Inspired by Missing-Hand Movement,” no. Urai, pp. 290–291, 2015.
- [3] Department of Physics and University of Illinois at Urbana-Champaign, “Q & A: Twisted Wires,” 2007.
- [4] S. K. Choudhary, D. Chakraborty, N. M. Kakoty, and S. M. Hazarika, “Development of cost effective EMG controlled three fingered robotic hand,” Proc. 2012 3rd Int. Conf. Comput. Commun. Technol. ICCCT 2012, pp. 104–109, 2012.
- [5] P. Geethanjali and K. K. Ray, “A Low-Cost Real-Time Research Platform for EMG Pattern Recognition-Based Prosthetic Hand,” IEEE/ASME Trans. Mechatronics, vol. 20, no. 4, pp. 1948–1955, 2014.
- [6] X. Jing, X. Yong, Y. Jiang, H. Yokoi, and R. Kato, “A low-degree of freedom EMG prosthetic hand with nails and springs to improve grasp ability,” Proc. - 2014 7th Int. Conf. Biomed. Eng. Informatics, BMEI 2014, no. 25249025, pp. 562–567, 2015.
- [7] A. L. Crawford and A. Perez-Gracia, “Design of a Robotic Hand With a Biologically-Inspired Parallel Actuation System for Prosthetic Applications,” Vol. 2 34th Annu. Mech. Robot. Conf. Parts A B, vol. 2, no. PARTS A AND B, pp. 29–36, 2010.



- [8] C. Scott, G. Sen Gupta, and L. Tang, "Sensing and processing of bio-metric signals for use in low cost bio-robotic systems," 2014 IEEE Sensors Appl. Symp. SAS 2014 - Proc., pp. 283–288, 2014.
- [9] V. Kumar and E. Todorov, "A low-cost and modular, 20-DOF anthropomorphic robotic hand: design, actuation and modeling," 2013 13th IEEE-RAS Int. Conf. Humanoid Robot., pp. 368–375, 2013.
- [10] N. Federico, "Metrological Issues Concerning Low Cost EMG- Controlled Prosthetic Hand," pp. 3–8, 2012.
- [11] Y. Jiang, S. Sakoda, S. Hoshigawa, H. Ye, Y. Yabuki, T. Nakamura, M. Ishihara, T. Takagi, S. Takayama, and H. Yokoi, "Development and Evaluation of Simplified EMG Prosthetic Hands," 2014.
- [12] H. Ye, S. Sakoda, Y. Jiang, and S. Morishita, "Pinch - Force - Magnification Mechanism of Low Degree of Freedom EMG Prosthetic Hand for Children," pp. 2466–2469, 2015.
- [13] D. Van Der Riet, R. Stopforth, and G. Bright, "Control Considerations of the Low Cost Prosthetic Touch Hand," pp. 225–232, 2015.
- [14] S.-Y. Jung, S. Kang, M. Lee, and I. Moon, "~ " ~ ~ I," pp. 83–86, 2007.
- [15] J. K. Jacqueline Louise Finch,lyn Harvey Heath,Ann Rosalie David, "Biomechanical Assessment of Two Artificial Big Toe Restorations From Ancient Egypt and Their Significance to the History of Prosthetics," 2012.
- [16] Robert H.Meier, "History of Arm Amputation, Prosthetic Restoration, and Arm Amputation Rehabilitation."

- [17] ISAAC PERRY CLEMENTS, “How Prosthetic Limbs Work.”
- [18] M. R. Al-Mulla, F. Sepulveda, and M. Colley, “A review of non-invasive techniques to detect and predict localised muscle fatigue,” *Sensors*, vol. 11, no. 4, pp. 3545–3594, 2011.
- [19] RYAN CLINGMAN, “EVALUATION OF A NOVEL MYOELECTRIC TRAINING DEVICE,” University of Virginia, 2010.
- [20] C. J. De Luca, “SURFACE ELECTROMYOGRAPHY: DETECTION AND RECORDING.”
- [21] “3-lead Muscle / Electromyography Sensor for Microcontroller Applications MyoWare™ Muscle Sensor (AT-04-001) DATASHEET.”
- [22] Texas Instruments, “LMx24-N, LM2902-N Low-Power, Quad-Operational Amplifiers,” 2015.
- [23] “Force Sensitive Resistor (FSR).”
- [24] Kjell Magne Fauske, “Example: Annotated manipulator,” 2006.
- [25] M. W. Spong, S. Hutchinson, and V. M., “Robot Modeling and Control,” *Control*, vol. 141, no. 1, p. 419, 2006.
- [26] M. Zahak, “Signal Acquisition Using Surface EMG and Circuit Design Considerations for Robotic Prosthesis,” in *Computational Intelligence in Electromyography Analysis - A Perspective on Current Applications and Future Challenges*, InTech, 2012.
- [27] “Neuromuscular Junction Lecture Notes,” 2011.
- [28] Algonquin Academic, “Action Potential Generation in Skeletal Muscle,” 2013.

[Online]. Available: <https://www.youtube.com/watch?v=WvV510gUlco>.

[Accessed: 25-Jul-2016].

- [29] Erica Jacques, “What is an EMG, and How Does it Work?,” 2014.
- [30] “Lifelines Neuro-diagnostic.”
- [31] “What is EMG (Electromyography) and how does it work?,” 2015.
- [32] Dr. Rich Vogel, “Overview of EMG,” 2016.
- [33] A. Devices, “Low Cost Low Power Instrumentation Amplifier AD620.”
- [34] P. Konrad, “The abc of emg,” *A Pract. Introd. to Kinesiol. ...*, no. April, pp. 1–60, 2005.
- [35] V. B. Kitovski, “Electronic devices and circuit theory, 6th edition, R. Boylestad and L. Nashelsky, Prentice Hall International Inc., 1996, 950 pp. A4 (paperback),” *Microelectronics J.*, vol. 29, no. 8, p. 574, 1998.
- [36] S. N.kale, “Fundamental of Robotic Manipulator,” 2013.
- [37] “Kinematics (Advanced Methods in Computer Graphics) Part 1.”
- [38] Winifred Warren, “Introduction to Concepts in Robotics In this lecture, you will learn: -Robot classification -Links and Joints -Redundant manipulator - Workspace.,” 2015.